Aus dem Bereich Physiologie
Theoretische Medizin und Biowissenschaften
der Medizinischen Fakultät
der Universität des Saarlandes, Homburg (Saar)

The role of Trpc channels

in the hormonal regulation of reproduction

Dissertation zur Erlangung des Grades eines Doktors der Naturwissenschaften

der medizinischen Fakultät

der UNIVERSITÄT DES SAARLANDES

2019

Vorgelegt von Thomas Blum (M.sc.)

geb. am: 01.09.1988 in Ludwigshafen am Rhein

Tag der Promotion: 16.06.2020

Dekan: Prof. Dr. M. D. Menger

Berichterstatter: Prof. Dr. T. Leinders-Zufall
Prof. Dr. U. Boehm
Prof. Dr. J. Engel

"If you want to assert a truth, first make sure it's not just an opinion that you desperately want to be true."

Neil deGrasse Tyson, 2013

Index

List of figures

Abstract

The hypothalamus is the control center of the endocrine system and it comprises of various nuclei that can regulate reproduction. Of the two main reproductive pathways, the classical hypothalamic-pituitary-gonadal (HPG) axis relies on gonadotropin-releasing hormone (GnRH) and the lactotroph axis depends on dopamine and prolactin. Little information is available regarding the physiological function of hypothalamic neurons and how they influence reproduction.

GnRH – the so called master molecule of reproduction – is an important regulator of gonadotropin secretion from the anterior pituitary. GnRH acts via its receptor (GnRHR) not only in the pituitary but also in neurons of the hypothalamus. A mouse model in which GnRHR neurons were genetically-tagged using a green fluorescent protein (GFP) enabled me to show that indeed these neurons respond to GnRH, inducing a depolarization and increased action potential activity. I could show that an inward current was underlying this GnRH-induced depolarization in GnRHR neurons. Canonical transient receptor potential (Trpc) channels have been postulated to be involved in regulation of hormonal and homeostatic signals in the hypothalamus and subsequent reproduction. Especially Trpc5 was suggested to be linked to GnRHR activation in juvenile gonadotrops.

In order to investigate whether the absence of Trpc channels – in particular Trpc5 – could influence the regulation of both reproductive pathways several mutant mouse lines were used. Only the loss of single members of the Trpc1, c4 and c5 subfamily caused a reduction of fertility in mice, whereas deletion Trpc5 showed the highest impact on reproductive capabilities. Trpc5-deficiency causes hypoprolactinemia in both female and male mice. In female mice the hypoprolactinemia co-occurs with oligoovulation and prolonged estrous cycle length. The HPG axis in these female mice is unbalanced causing decreased serum levels of follicle-stimulating hormone (FSH) and a slight mistiming of luteinizing hormone (LH) surges. Olfactory cues as well as copulatory stimuli of wildtype male mice were able to improve the hypoprolactinemic condition of Trpc5-deficient females in a preliminary set of experiments. In male mice reduced prolactin levels are connected with poor sperm motility (asthenozoospermia) and increased sperm count, whereas the HPG axis seems to be unaffected.

In an attempt to determine the cause of hypoprolactinemia and resulting subfertility in female mice, dopaminergic neurons of the arcuate hypothalamic nucleus (ARC) were investigated at the cellular level. Dopaminergic neurons of the hypothalamus – especially of the ARC – maintain the regulation of prolactin release from lactotroph cells of the anterior pituitary and could be shown to be Trpc5 positive. One key feature of these neurons is their spontaneous infraslow rhythmic oscillatory burst activity. Trpc5 is crucial to maintain the spontaneous infraslow rhythmic oscillatory burst activity in dopaminergic ARC neurons. My data indicates

that Trpc5 positively affects the onset of a burst, the burst duration and the voltage conducted during a burst. This suggests that Trpc5 is a limiting factor for burst frequency and the interval between bursts. Therefore, loss of Trpc5 increases the overall activity of dopaminergic ARC neurons, which in turn should increase the amount of dopamine released into the median eminence, subsequently suppressing prolactin secretion and inducing hypoprolactinemia.

Besides the general role of Trpc5 in the upkeep of membrane oscillations, Trpc5 is an essential component of the prolactin feedback loop. Prolactin stimulation of dopaminergic ARC neurons causes the phosphorylation of signal transducer and activator of transcription (STAT) 5 as well as an increase in electrical activity. Loss of Trpc5 abolishes the electrical component of the prolactin feedback loop but not the phosphorylation of STAT5. Therefore Trpc5-deficient dopaminergic ARC neurons lose their ability to fully respond to prolactin stimulation and to participate conventionally in the short loop feedback.

This thesis provides conclusive evidence for the influence of Trpc5 in dopaminergic neurons of the arcuate nucleus upon prolactin regulation in the pituitary gland. Moreover, Trpc5 channelopathies as a cause for prolactin dysregulation or other dysfunctions or disease will be an interesting topic for further fundamental research on Trpc channels.

Zusammenfassung

Der Hypothalamus ist das Kontrollzentrum des endokrinen Systems und besteht aus verschiedenen Kernen, die die Fortpflanzung regulieren können. Von den beiden regulatorischen Achsen der Fortpflanzung ist die klassische Hypothalamus-Hypophysen-Gonaden-Achse (HPG-Achse) auf das Gonadoliberin (engl.: gonadotropin-releasing hormone; GnRH) und die laktotrope Achse auf Dopamin und Prolaktin angewiesen. Über die physiologische Funktion von hypothalamischen Neuronen und deren Einfluss auf die Reproduktion ist bisher nur wenig bekannt.

GnRH, das sogenannte Mastermolekül der Reproduktion, ist ein bedeutender regulatorischer Faktor für die Freisetzung der Gonadotropine aus der Hypophyse. GnRH wirkt über seinen Rezeptor (GnRHR) nicht nur in der Hypophyse, sondern auch an Neuronen des Hypothalamus. Ein Mausmodell, in dem GnRHR-Neurone unter Verwendung eines grün fluoreszierenden Proteins (GFP) genetisch markiert wurden, ermöglichte mir den Nachweis, dass diese Neurone tatsächlich auf GnRH reagieren und eine Depolarisation sowie eine Erhöhung der Aktionspotentialfrequenz auslösen. Ich konnte zeigen, dass ein Einwärtsstrom der GnRH-induzierten Depolarisation in GnRHR-Neuronen zugrunde liegt. Es wurde postuliert, dass kanonische Rezeptor-Potential-Kanäle (Trpc-Kanäle) an der Regulation hormoneller und homöostasischer Signale im Hypothalamus und dadurch an der Reproduktion beteiligt sind. Insbesondere wurde Trpc5 mit der GnRHR-Aktivierung in juvenilen Gonadotropen in Verbindung gebracht.
Um zu untersuchen, ob das Fehlen von Trpc-Kanälen, insbesondere Trpc5, die Regulation beider Reproduktionswege beeinflussen könnte, wurden mehrere mutierte Mauslinien verwendet. Der Verlust von Trpc1, c4 oder c5 führte zu einer Verringerung der Fertilität bei Mäusen. Ein Mangel an Trpc5 zeigte den größten Einfluss auf die Fortpflanzungsfähigkeit, wohingegen das Ausschalten mehrerer Trpc-Kanäle nicht zu einer verminderten Fruchtbarkeit führte. Trpc5-Mangel verursacht Hypoprolaktinämie bei weiblichen und männlichen Mäusen. Bei weiblichen Mäusen tritt die Hypoprolaktinämie gleichzeitig mit einer Oligoovulation und einem verlängerten Östruszyklus auf. Die HPG-Achse bei diesen weiblichen Mäusen ist unausgewogen, was zu einem verminderten Serumspiegel des follikelstimulierenden Hormons (FSH) und eine Variabilität des Anstiegs des luteinisierenden Hormons (LH) führt. Olfaktorische sowie kopulatorische Stimuli von männlichen Wildtyp-Mäusen konnten die Hypoprolaktinämie von Trpc5-defizienten weiblichen Tieren in einer vorläufigen Reihe von Experimenten lindern. Bei männlichen Mäusen ist ein reduzierter Prolaktinspiegel mit einer schlechten Spermienmotilität (Asthenozoospermie) und einer erhöhten Spermienzahl verbunden, wohingegen die HPG-Achse bei Männern nicht beeinflusst zu sein scheint.

In einem Versuch, die Ursache der Hypoprolaktinämie und die daraus resultierende Subfertilität bei weiblichen Mäusen zu bestimmen, wurden dopaminerge Neurone des hypothalamischen Nucleus arcuatus (ARC) auf zellulärer Ebene untersucht. Dopaminerge Neurone des Hypothalamus, insbesondere des ARC, regulieren die Freisetzung von Prolaktin durch laktotrope Zellen der Adenohypophyse. Es konnte gezeigt werden, dass diese dopaminergen Neurone Trpc5 exprimieren. Ein Schlüsselmerkmal dieser Neurone ist ihre spontane, niederfrequente, oszillierende Burst-Aktivität. Trpc5 ist essenziell, um diese niederfrequenten Oszillationen in dopaminergen ARC Neuronen aufrecht zu erhalten. Meine Ergebnisse zeigen, dass Trpc5 einen positiven Einfluss auf die initiale Phase, die Dauer und die geleitete Spannung eines Burst nimmt. Dies legt nahe, dass Trpc5 ein limitierender Faktor der Burst-Frequenz und des Intervalls zwischen den Bursts darstellt. Ein Verlust von Trpc5 würde deshalb eine erhöhte Aktivität der dopaminergen ARC Neurone, dadurch eine erhöhte Freisetzung von Dopamine in die Eminentia mediana, eine Unterdrückung der Prolaktinsekretion und somit eine Hypoprolaktinämie verursachen.

Neben der allgemeinen Funktion von Trpc5 in der Aufrechterhaltung von Membranoszillationen ist Trpc5 ein wesentlicher Bestandteil der Prolaktin-Rückkopplungsschleife. Eine Stimulation von dopaminergen ARC Neuronen mit Prolaktin bewirkt die Phosphorylierung von Signaltransduktor und Aktivator der Transkription (STAT) 5, sowie eine Erhöhung der elektrischen Aktivität. Ein Knockout von Trpc5 hebt die elektrische Komponente der Prolaktin-Rückkopplungsschleife, jedoch nicht die Phosphorylierung von STAT5, auf. Hierdurch verlieren Trpc5-defiziente dopaminerge ARC Neurone ihre Fähigkeit, vollständig und adäquat auf eine Prolaktin-Stimulation zu reagieren und somit ihre Rolle in der Rückkopplungsschleife zu übernehmen.

Diese Arbeit liefert schlüssige Beweise dafür, dass Trpc5 in dopaminergen Neuronen des ARC die Prolaktinregulation in der Hypophyse direkt beeinflusst und dass Trpc5-Kanalopathien, als Ursache für Prolaktindysregulation, andere Funktionsstörungen oder Krankheiten, spannende Themen für die weitere Grundlagenforschung an Trpc-Kanälen sein werden.

Abbreviations

ACH	Autocorrelation histograms
aCSF	Artificial cerebrospinal fluid
ACTH	Adrenocorticotropic hormone, adrenocorticotropin
ANOVA	Analysis of variance
aPit	Anterior pituitary
ARC	Arcuate nucleus
AVPV	Anteroventral periventricular nucleus
BDNF	Brain-derived neurotrophic factor
CAG	CMV-IE enhancer/chicken-βactin/rabbit beta-globulin hybrid promotor
CAGS	Chicken β-actin promoter and cytomegalovirus enhancer
CMV	Cytomegalovirus
CNS	Central nervous system
D	Diestrus
D2R	Dopamine receptor subtype 2
DA	Dopamine
DAG	Diacylglycerol
dm	dorsomedial
DMSO	Dimethyl sulfoxide
E	Estrus
EGTA	Ethylene glycol-bis(2-aminoethylether)-N,N,N`,N`-tetraacetic acid
ERα	Estrogen receptor α
FSH	Follicle stimulation hormone
GFP	Green fluorescent protein
GH	Growth hormone, somatotropin
GnRH	Gonadotropin releasing hormone
GnRHR	Gonadotropin releasing hormone receptor
GPCR	G-protein-coupled receptor
GRIC	GnRHR-internal ribosome entry site-Cre
GTP	Guanosine triphosphate
HPG	Hypothalamic-pituitary-gonadal axis
IC	Artificial intracellular solution
IP_3	Inositol-1,4,5-trisphosphate
IR-DIC	Infrared-optimized differential interference contrast

IRES	Internal ribosome entry site
ISI	Interspike interval
IVC	Individually ventilated cages
JAK	Janus kinase
LH	Luteinizing hormone
LPC	Lysoposphatidylcholine
M	Metestrus
MPO	Medial preoptic area
NDS	Normal donkey serum
P	Proestrus
PBS	Phosphate buffered saline
PCOS	Polycystic ovary syndrome
Pe	Periventricular nucleus
PFA	Paraformaldehyde
PHDA	Periventricular hypophyseal dopamine neuron
PIP_2	Phosphatidylinositol-4,5-bisphosphate
PIP_3	Phosphatidylinositol-3,4,5-trisphosphate
PKC	Protein kinase C
PLC	Phospholipase C
POA	Preoptic area
POCT	Point-of-care testing
PRL	Prolactin
pSTAT5	Phosphorylated signaltransducer and activator of transcription 5
PSTH	Peristimulus time histogram
PTFE	Polyfluoroethylene
RI	Rhythmicity index
S1P	Sphingosine-1-phosphate
SA	Splice acceptor
SD	Standard deviation
SDS	Dodecylsulfate Na-salt
SEM	Standard error of the mean
STAT	Signal transducer and activator of transcription
Th	Tyrosine hydroxylase
THDA	Tuberohypophyseal dopamine neurons
TIDA	Tuberoinfundibular dopamine neuron
TM	Transmembrane domain

Trp	Transient receptor potential
Trpc	Transient receptor potential, canonical
TSH	Thyroid-stimulating hormone, thyrotropin
TTX	Tetrodotoxin
VGCC	Voltage gated calcium channel
VNO	Vomeronasal organ
WPRE	Woodchuck hepatitis virus post-transcriptional regulatory element

1. Introduction

Olfactory and pheromonal cues detected in the nose and the involved neuronal processing play a key role in many social and reproductive behaviors. It is commonly accepted that socially-relevant cues detected in the accessory olfactory system (vomeronasal organ, VNO) are first relayed to the accessory olfactory bulb and from there via the amygdala to the hypothalamus, where the electrical signals are transformed into an endocrine response to modulate the behavioral output. The hypothalamus is the control center of the endocrine system and it comprises various nuclei, which are known to regulate reproduction, body homeostasis, stress, defensive and aggressive behavior. Transient receptor potential (Trp) channels – especially the canonical Trp channels – arise as important key components at multiple stages of these neural circuits.

1.1 Regulatory elements of reproductive homeostasis

Reproduction relies on the neuroendocrine control of several hormones secreted from the pituitary gland. These hormones are controlled by neuroendocrine cells of the hypothalamus, which release their specific modulatory hormones into the hypothalamo-hypophyseal portal vessel system. Reproductive hormones show cyclic alterations during the reproductive cycle in female mice. These hormonal changes are associated with adjustments in the female tract and sexual responsiveness. The duration of the estrous cycle is approximately 4-5 days and it can be divided into four distinct phases: metestrus, diestrus, proestrus and estrus (Fig. 1). The estrous cycle can also be split into the luteal and the follicular phase. The luteal phase comprises metestrus and diestrus, whereas the ovulatory phase comprises proestrus and estrus. The follicular phase is marked by maturation of follicles in the ovaries during proestrus. Prior to ovulation, several hormones need to rise. In the early aspect of proestrus, blood levels of estrogen rise, causing gonadotropin-releasing hormone (GnRH), which is released in a pulsatile manner to increase its frequency and amplitude, causing the ovulatory surge of luteinizing hormone (LH) and follicle-stimulating hormone (FSH). In estrus, ovulation occurs, marking the phase of receptivity in mice (Miller and Takahashi, 2013). The luteal phase is defined by the transformation of follicles into the corpus luteum. Progesterone is secreted by the corpus luteum and is required to prepare the endometrium for nidation and maintenance of an early pregnancy. In the absence of pregnancy, the corpus luteum will stop progesterone secretion and regress over time (Bachelot and Binart, 2005). The late luteal phase is characterized by a slow increase in estrogen, which becomes more pronounced in the following phase of proestrus (Butcher et al., 1974; Sisk et al., 2001; Goldman et al., 2007; Caligioni, 2009).

Vaginal cytology is a powerful tool to assess the different phases of the estrous cycle in mice. In metestrus, a mixture of cell types is present. These are in large parts leucocytes, but also nucleated epithelial and/or cornified epithelial cells. In most cases, diestrus shows only leucocytes present in vaginal smears, with hardly any other cell types. With rising levels of estrogen in proestrus, nucleated epithelial cells are the dominating cell type in the vaginal cytology of female mice. There is also a tendency for them to form clusters or strands. In estrus, the vaginal smear shows a predominance of cornified epithelial cells, often forming needle-like shapes or round with jagged irregular edges (Goldman et al., 2007; Caligioni, 2009).

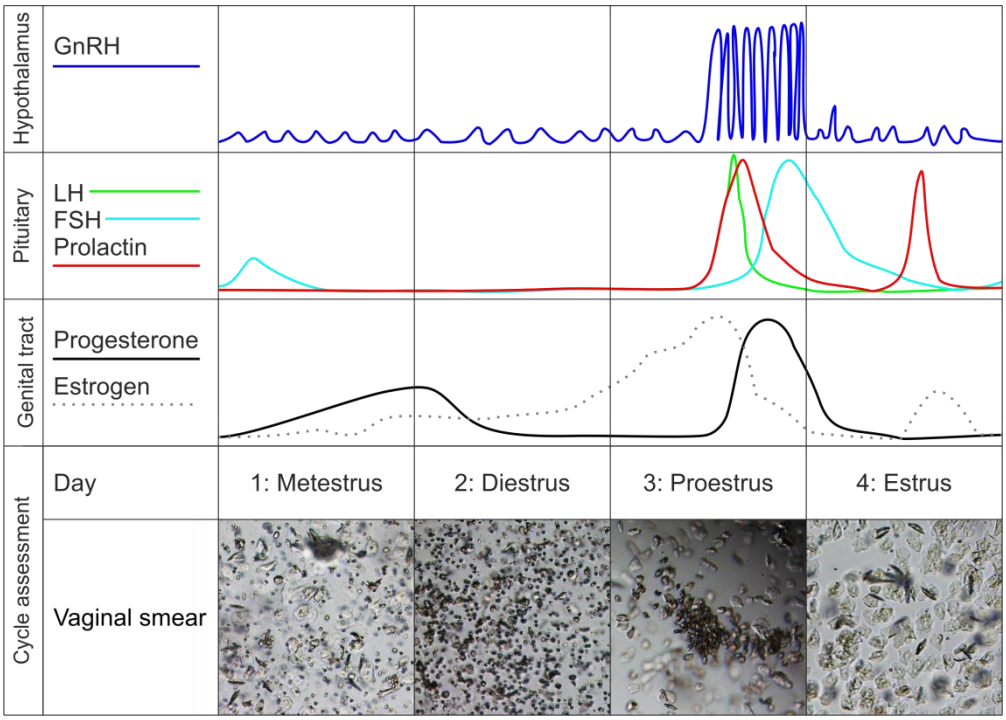

Figure 1: Hormonal changes of a female mouse during the reproductive cycle.
The reproductive (estrous) cycle of a female mouse takes 4-5 days in general, and can be divided into four different stages: metestrus, diestrus, proestrus and estrus. These different stages can be monitored by vaginal smears and cytological assessment. The reproductive hormones, gonadotropin-releasing hormone (GnRH), luteinizing hormone (LH), follicle-stimulating hormone (FSH), prolactin, progesterone and estrogen show fluctuations during the estrous cycle, showing a pronounced increase during the later phase of proestrus, when ovulation occurs. Hormonal data combines data from laboratories evaluating hormonal levels in either blood samples or brain microdialysis (Butcher et al., 1974; Sisk et al., 2001).

1.1.1 The classical reproductive axis: Tracking the master molecule of reproduction

In order to ensure a proper reproductive function, mammalian species rely upon the correct and well-timed secretion of gonadotropin-releasing hormone (GnRH) from GnRH neurons located in the medial preoptic area (MPO) of the hypothalamus (Fig 2). These neurons extend their axons to the external zone of the median eminence and release GnRH into the hypothalamo-hypophyseal portal vessel system (Fink and Jamieson, 1976; Sarkar et al., 1976; Clarke and Cummins, 1982; Clarke, 1987; Gore, 2002). GnRH is released in a pulsatile manner, increasing in amplitude and frequency prior to ovulation (Sisk et al., 2001; Gore, 2002).

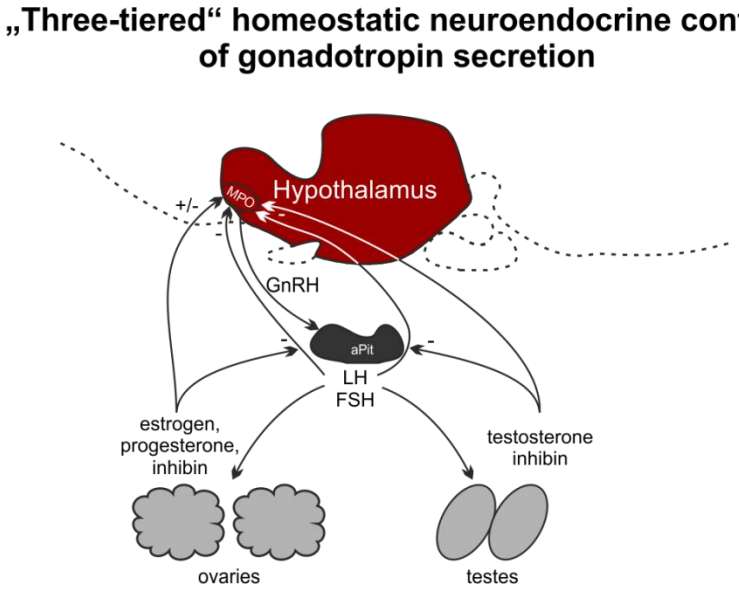

Figure 2: Hypothalamic-pituitary-gonadal (HPG) axis in mice.
GnRH neurons located in the medial preoptic area (MPO) in the hypothalamus produce and release gonadotropin-releasing hormone (GnRH) into the hypophyseal portal vessel system. At the anterior pituitary (aPit), GnRH stimulates gonadotrope cells to produce and secrete the two gonadotropins, luteinizing hormone (LH) and follicle-stimulating hormone (FSH). The gonadotropins in turn act on the gonads in both genders to control steroidogenesis and reproductive function, and give feedback to the hypothalamus. These sex steroids give feedback to both gonadotrope cells in the pituitary gland and GnRH neurons of the hypothalamus to guarantee the homeostatic control of gonadotropin secretion.

GnRH is transported by the portal system to the anterior pituitary (aPit, Fig 2). In order to maintain reproductive success, GnRH needs to bind to its receptor – which is present in gonadotrope cells – to stimulate the release of the gonadotropins LH and FSH. These circulating hormones then act upon the gonads to stimulate sex steroid hormone production and secretion. LH and FSH also provide negative feedback to GnRH neurons in the MPO. In females, the gonadotropins stimulate the release of estrogen and progesterone and regulate oocyte maturation and ovulation (Gore, 2002). Estrogen and progesterone provide mainly negative feedback to both hypothalamus and pituitary, whereupon estrogen during proestrus switches to a positive feedback on GnRH neurons, enabling the increased GnRH release and subsequent surge of LH (Fig. 3, Clarke et al., 2012; Radovick et al., 2012). During the

luteal phase, GnRH and LH are released in low pulses. In this case, estrogen can act on ERα-positive kisspeptin neurons in the arcuate nucleus (ARC), thus inhibiting their activity. Prior to ovulation, estrogen strongly increases, surpassing a threshold level and causing activation of ERα-positive subsets of kisspeptin neurons in the ARC, the anteroventral periventricular nucleus (AVPV), and the preoptic area (POA). These neurons then release kisspeptin onto GnRH neurons, increasing their activity and permitting a LH surge and thereby ovulation (Liu et al., 2008; Piet et al., 2013; Ronnekleiv and Kelly, 2013; Ronnekleiv et al., 2015).

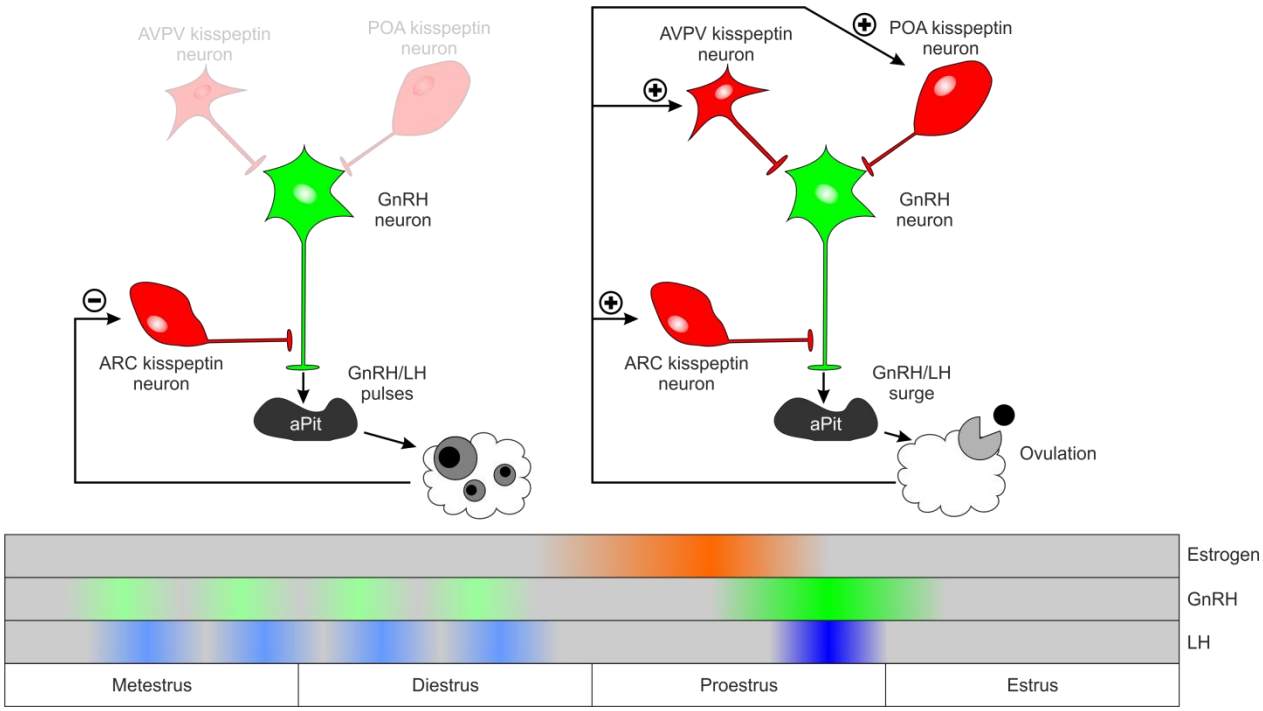

Figure 3: Switch of estrogen feedback prior to ovulation.
During the reproductive cycle the negative feedback needs to be lifted to enable a rise in GnRH which causes a LH surge. During metestrus and diestrus GnRH and LH are released in a pulsatory manner. Estrogen released from the ovaries inhibits ERα-positive kisspeptin neurons in the arcuate nucleus (ARC), causing the reduced secretion of GnRH. At the end of diestrus, estrogen levels begin to rise. During proestrus estrogen levels strongly rise, increasing over a threshold level, which is thought to be necessary to shift estrogen to a positive feedback. This estrogen surge stimulates ERα-positive kisspeptin neurons in multiple areas of the hypothalamus, namely the ARC, the anteroventral periventricular nucleus (AVPV) and the preoptic area (POA). The hereby released kisspeptin stimulates GnRH neurons and increases the release of GnRH causing a surge of LH and thereby ovulation. (Adapted from (Clarke et al., 2012)).

In males GnRH, LH and FSH behave similarly but have different effects at the gonadal level. FSH stimulates Sertoli cells, which are required for spermatogenesis in addition to testosterone, which is secreted from Leydig cells upon LH stimulation. Negative feedback is provided by both LH/FSH and testosterone (Kong et al., 2014).

1.1.2 The lactotroph axis: Dopaminergic suppression of prolactin secretion

Besides GnRH and the gonadotropins – which are part of the classic HPG axis – the reproductive hormone prolactin has circulating concentrations that increase prior to ovulation. Prolactin secretion is controlled by an unusual neuroendocrine axis, the lactotroph axis. Prolactin is mainly synthesized by lactotroph cells in the anterior pituitary (aPit) and performs a large variety of important biological functions in the whole body, reportedly having about 300 different actions (Larsen and Grattan, 2012; Grattan and Le Tissier, 2015). Prolactin is best known for its role in lactation.

Similar to the hormones of the classic HPG axis, prolactin also shows cyclic alterations in accordance with the estrous cycle, generating a prolactin surge in late proestrus. In rodents, prolactin is needed to maintain the corpus luteum and thereby progesterone secretion (Grattan and Le Tissier, 2015). In addition to preparing the ovaries and reproductive tract for a pregnancy, prolactin is also involved in adaptive responses of body homeostasis to enable successful reproduction.

The luteal phase in rodents is extremely short due to the lack of prolactin to maintain the corpus luteum. If mating occurs, the corpus luteum is preserved (Neill and Reichert, 1971). There is evidence that mating or a copulomimetic stimulus induces twice daily surges of prolactin (Butcher et al., 1972; Smith and Neill, 1976; Egli et al., 2010; Larsen and Grattan, 2010; Le Tissier et al., 2015). Prolactin surges continue until day 10 if the mating is fertile, followed by pregnancy (Smith and Neill, 1976). These surges coincide with reduced activity of dopaminergic neurons of the hypothalamus (Lerant et al., 1996; Andrews et al., 2001). Prolactin surges cease due to the action of placental lactogens providing feedback to both the hypothalamus and pituitary (Tonkowicz et al., 1983; Tonkowicz and Voogt, 1983b, a; Gorospe and Freeman, 1985; Arbogast et al., 1992; Tomogane et al., 1992; Tomogane et al., 1993; Le Tissier et al., 2015). Towards the end of a pregnancy, prolactin levels rise to induce mammogenesis (Bern and Nicoll, 1968; Freeman et al., 2000; Larsen and Grattan, 2012; Le Tissier et al., 2015). Prolactin not only affects the growth and development of the mammary gland, but it is also vital for milk synthesis (lactogenesis) and the upkeep of milk secretion (galactopoiesis, Nelson and Gaunt, 1936; Lyons, 1942; Cowie et al., 1969). Prolactin triggers the uptake of amino acids, the generation of milk proteins, glucose uptake and the production of milk sugar and milk fats (Barber et al., 1992; Anderson et al., 2014).
Increased levels of prolactin also have the ability to suppress fertility. Hyperprolactinemia – either pathophysiological or caused by pregnancy or lactation – suppresses LH pulse frequency and magnitude as well as GnRH secretion into the portal blood system (Grattan et al., 2007), although it also acts directly on gonadotrope cells, thus reducing LH secretion and GnRH sensitivity (Cheung, 1983; Tortonese et al., 1998).

In contrast to females, the function of prolactin in males is not widely studied, as complete infertility in knockout models is restricted to females (Horseman et al., 1997; Ormandy et al., 1997). It is known that hyperprolactinemia in males results in a loss of libido and infertility (De Rosa et al., 2003), most likely due to the suppression of GnRH secretion. There are also hints that prolactin is important in testis function, as its receptor has been found in testis and there on Leydig cells, promoting increased LH-receptor expression and increased androgen production (Purvis et al., 1979), and on Sertoli cells, improving FSH binding (Guillaumot et al., 1996). These results could not be confirmed using prolactin and prolactin receptor knockouts, showing normal plasma testosterone concentrations, arguing that LH responses are unaltered and prolactin signaling is expendable for the male testicular function (Binart et al., 2003). As prolactin in males has not revealed any key functions to date, the modulatory influence of prolactin on male fertility and possibly on paternal behavior has already been described (Schradin and Anzenberger, 1999).

Another important general function of prolactin is its role in the neuroendocrine control of prolactin secretion (Fig. 4). Prolactin is an uncommon pituitary hormone, as its release is spontaneous and predominantly inhibited by the hypothalamus (Freeman et al., 2000; Ben-Jonathan and Hnasko, 2001). The presence of an prolactin-inhibitory factor released by the hypothalamus could be confirmed in mouse models of median eminence lesions (Arimura et al., 1972) or interrupted pituitary stalk (Kanematsu and Sawyer, 1973). The recognition of dopamine as the prolactin-inhibitory factor has been strongly debated because hypothalamic hormones have been described as peptide hormones. Known for its neurotransmitter function, dopamine started to be recognized as the prolactin-inhibiting factor after dopaminergic terminals were found in the median eminence (Fuxe, 1963) and the inhibitory effect of dopamine and dopaminergic agonists was shown (MacLeod et al., 1970). It took almost another decade to demonstrate the presence of dopamine receptor (subtype 2, D2R) on the prolactin-producing lactrotroph cells of the pituitary gland (Mansour et al., 1990).

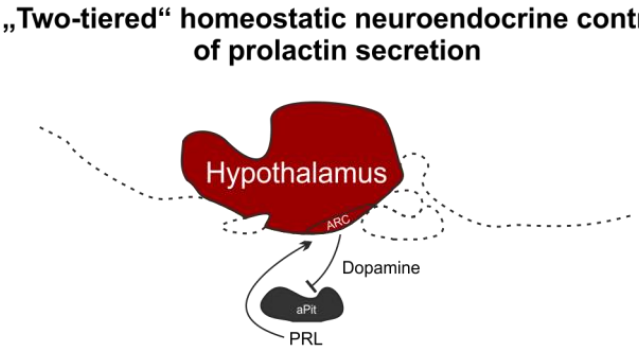

Figure 4: Lactotroph axis in mice.
Dopaminergic neurons of the arcuate nucleus (ARC) of the hypothalamus produce and release dopamine into the hypothalamo-hypophyseal portal vessel system at the level of the median eminence. Dopamine can thereby influence the secretory activity of lactotroph cells in the anterior pituitary (aPit). These cells spontaneously secrete prolactin (PRL). Upon binding of dopamine to the D2 receptor on lactotroph cells this prolactin release is subdued. Prolactin itself provides a short-feedback loop, stimulating dopaminergic neurons in the ARC to control its own secretion.

The neuroendocrine dopamine neurons can be divided into three sub-populations: the tuberoinfundibular dopaminergic (TIDA) neurons, located in the dorsomedial arcuate nucleus (ARC) and terminating in the external zone of the median eminence; the tuberohypophyseal dopaminergic (THDA) neurons, located in the rostral ARC and projecting in the hypthalamo-hypophyseal tract to the intermediate and neural lobe of the pituitary gland; and the periventricular hypophyseal dopaminergic (PHDA) neurons of the more rostral part of the periventricular nucleus (Pe), which only project to the intermediate lobe of the pituitary (Fuxe, 1963; Bjorklund et al., 1973; Holzbauer and Racke, 1985; Goudreau et al., 1992). TIDA neurons have been shown to oscillate (Lyons et al., 2012) and release dopamine in a pulsatile fashion (Romano et al., 2013). During the luteal phase, dopaminergic (DA) neurons release high amounts of dopamine into the hypothalamo-hypophyseal portal system, suppressing prolactin release from lactotroph cells via activation of D2R (Fig. 5 A). In order to enable prolactin function prior to ovulation and in early pregnancy, dopamine release needs to decline to lift the inhibition of spontaneous prolactin secretion from lactotroph cells (Fig. 5 B).

These dopaminergic neurons of the hypothalamus and the lactotroph cells of the anterior pituitary form a short feedback loop to regulate prolactin secretion (Fig. 5 C). Upon binding of prolactin to the prolactin receptor expressed on hypothalamic dopamine neurons, prolactin induces transductional and electrical changes (Lerant and Freeman, 1998; Grattan, 2001; Kokay and Grattan, 2005; Lyons et al., 2012; Lyons and Broberger, 2014). In a transcriptional pathway, prolactin induces TH gene expression and protein phosphorylation, increasing dopamine synthesis (Arbogast and Voogt, 1991; Ma et al., 2005a). This pathway is dependent on the JAK-STAT pathway and the prolactin receptors (Grattan et al., 2001;

Lerant et al., 2001; Kokay and Grattan, 2005; Ma et al., 2005b). Prolactin has a swift impact on the electrical activity of TIDA neurons, which is directly associated with increased dopamine release at the median eminence (Brown et al., 2012; Lyons et al., 2012; Romano et al., 2013). This pathway is likely independent from JAK-STAT. Prolactin can induce a change in membrane potential, which has been suggested to be due to a low voltage and a high voltage component. The 2-APB sensitive low voltage mixed cationic current is speculated to be a Trp-like current. The high voltage component is most likely a L-type voltage-gated calcium channel (VGCC), shifting BK-type K^+ channel voltage dependence to more hyperpolarizing potentials and thereby inhibiting the K^+ current and broadening action potentials (Lyons et al., 2012). Taken together, these two pathways increase the dopamine output at the median eminence and thereby downregulate prolactin secretion in the pituitary (Fig 5 C). This highly sensitive and elaborate multi-stage control of prolactin secretion highlights the complexity of regulating this hormonal axis.

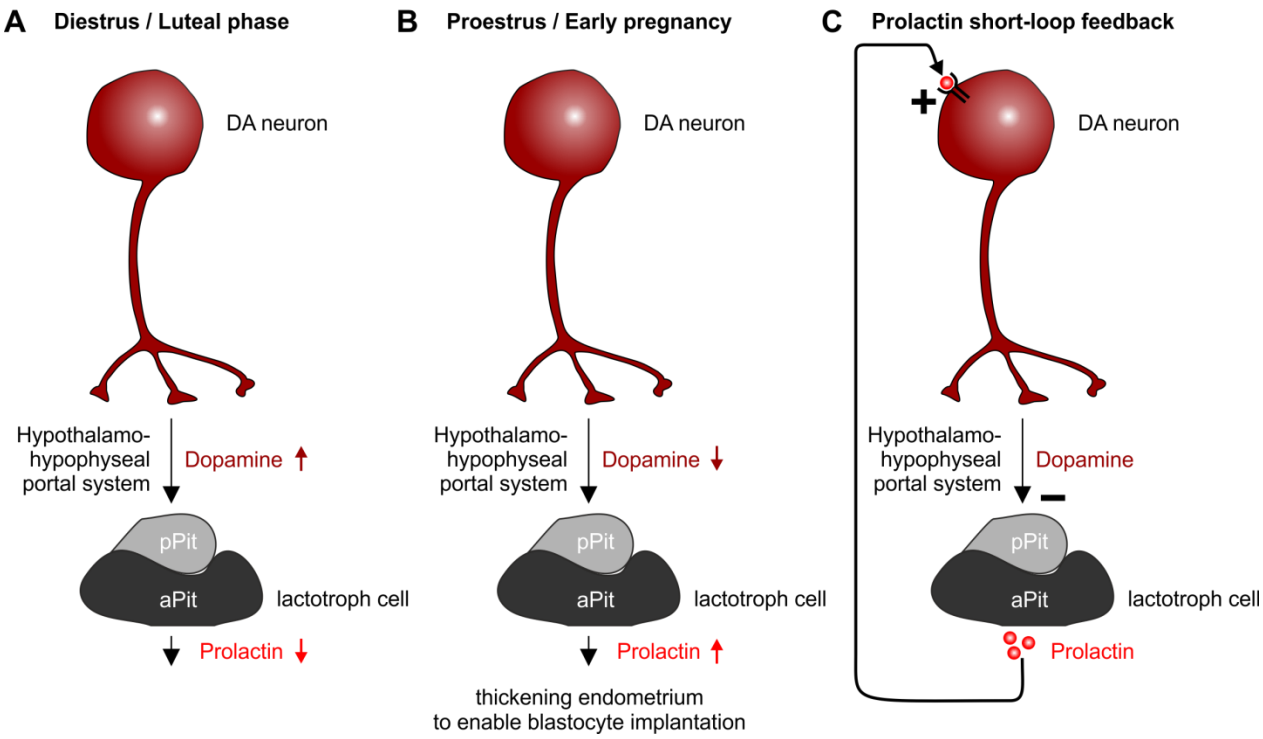

Figure 5: Correlation of dopamine and prolactin levels during different reproductive stages of a female mouse.
(A) During the luteal phase (diestrus) of the reproductive cycle, dopamine (DA) neurons need to release high levels of dopamine into the hypothalamo-hypophseal portal system to suppress prolactin secretion of lactotroph cells in the anterior pituitary (aPit). (B) In the ovulatory period of the estrous cycle and during early phases of pregnancy, dopamine levels decrease, enabling the lactotroph cells to release prolactin, which is necessary to stimulate a pathway to thicken the uterine wall for implantation and to for maintain an early pregnancy. (C) In contrast to other hormonal axes, prolactin secretion needs to be inhibited by its hypothalamic regulatory factor dopamine. Prolactin itself provides feedback onto hypothalamic dopamine neurons to increase dopamine release and thereby reduce its own secretion.

1.2 Canonical transient receptor potential (Trpc) channels and their influence on murine reproduction in the brain and pituitary.

Canonical transient receptor potential (Trpc) channels are a sub-family of Trp channels, which have the closest homology to the first-described Trp channels in *Drosophila* (Venkatachalam and Montell, 2007). The mammalian Trpc sub-family comprises seven members. In humans, only six of them are expressed, because here Trpc2 is a pseudogene. Trpc channels share at least 30% sequence homology with each other or *Drosophila* Trp channels. Based on sequence analogy, Trpcs can be divided into four sub-groups: Trpc1, Trpc2, Trpc4/c5, Trpc3/c6/c7 (Clapham et al., 2001; Montell et al., 2002; Fowler et al., 2007; Wu et al., 2010). Trpc proteins form tetrameric, non-selective, calcium permeable cation channels (Clapham et al., 2001). Trpc2 does not interact with known Trpc proteins aside from itself, while Trpc1 is able to form heteromeric channels with the Trpc4/c5 subgroup, and other Trpc subunits form heteromeric channels within their sub-group (Trpc4/c5 or Trpc3/c6/c7, Strubing et al., 2001; Hofmann et al., 2002; Plant and Schaefer, 2003; Strubing et al., 2003; Trebak et al., 2003; Berg et al., 2007; Broker-Lai et al., 2017). Trpc channels can be found throughout the central nervous system (CNS), although they have also been reported in the periphery, e.g. the olfactory system.

In the olfactory system, the processing of chemosignals relies on Trpc channels at various levels (Munger et al., 2009; Zufall, 2014). Of capital importance is Trpc2, a Trpc channel highly expressed in neurons of the vomeronasal organ (VNO, Liman et al., 1999; Leypold et al., 2002; Stowers et al., 2002). Loss of Trpc2 in mice causes changes in male-male and maternal aggression of mutant males (Leypold et al., 2002; Stowers et al., 2002), whereas mutant females show reduced female-specific behavior, such as maternal aggression and lactating behavior, as well as an increase in male behavior (Kimchi et al., 2007). Other Trp channels have been found in the olfactory system as well as the brain, which could affect the reported behavior. The expression pattern of Trp channels in the brain is poorly characterized due to the lack of validated antibodies for several Trp family members. In the rodent brain, all Trpc channel sub-types are expressed in different quantities (Fowler et al., 2007). Trpc4 (41%) and its closest homologue Trpc5 (24%) seem to be the highest expressed sub-types of Trpc channels in the brain, whereby both have been highly expressed in the hippocampus, cerebellum, cortex, amygdala and hypothalamus (Fowler et al., 2007; Riccio et al., 2009). In human brain areas, mRNA of all Trpc family members could be found (Riccio et al., 2002). The human orthologue for Trpc2 is an exception, being a pseudogene due to an early stop codon (Wes et al., 1995; Vannier et al., 1999). In contrast to the rodent brain, Trpc5 is the most brain-specific and strongly-expressed Trpc member in humans (Riccio et al., 2002). The highest expression of Trpc5 in the human brain has been

found in the amygdala, cerebellum, cortex, hippocampus and hypothalamus, which is similar to the expression patterns of Trpc5 in the rodent brain (Fowler et al., 2007).
The hypothalamus is a small yet important brain region, connecting sensory tissues with the effector tissues. The hypothalamus comprises several nuclei with a variety of functions known to influence reproduction, aggression, defensive behavior, metabolism and stress. Interestingly, various Trpc channel combinations appear to exist in the hypothalamic nuclei, suggesting that these channels could influence the homeostasis of the organism (Kelly et al., 2018).

Taken together, regulation of the endocrine system arises at the level of the hypothalamus. Hypothalamic nuclei regulate both hormonal axes controlling reproduction, namely the classical HPG axis and the lactrotroph axis.

In the classical HPG axis, GnRH neurons of the hypothalamus stimulate the release of gonadotropins from gonadotope cells of the pituitary gland, which subsequently trigger the release of sex hormones from the gonads. Hypothalamic GnRH neurons have been found to express multiple members of the Trpc channel family, namely Trpc4, Trpc1 and Trpc5 (in descending level of expression, (Zhang et al., 2008; Bosch et al., 2013; Zhang et al., 2013a; Zhang et al., 2013b)). Activity of GnRH neurons is modulated by kisspeptin (Liu et al., 2008; Piet et al., 2013; Ronnekleiv and Kelly, 2013; Ronnekleiv et al., 2015). Dependent on the estrous cycle stage and estrogen levels, kisspeptin is able to increase GnRH neuron activity (Fig. 3). This excitation of GnRH neurons has been shown to be dependent on Trpc1, Trpc4 and Trpc5 channels (Zhang et al., 2008; Bosch et al., 2013; Zhang et al., 2013a; Zhang et al., 2013b). Trpc5 is also recognized as a key component of excitatory regulation of kisspeptin neurons, which are located in the arcuate nucleus (Qiu et al., 2014; Kelly et al., 2018). Suppression of the classical HPG axis arises from the second reproductive axis, the lactotroph axis (Grattan and Le Tissier, 2015). Prolactin – which is permanently secreted by lactotroph cells of the anterior pituitary – can reduce both the frequency and amplitude of LH release (Cohen-Becker et al., 1986). Prolactin can activate its receptor located on a sub-population of hypothalamic GnRH neurons, directly reducing GnRH secretion into the portal blood system and thereby reducing serum LH levels (Weber et al., 1983; Grattan et al., 2007). Moreover, it can also act on gonadotrophs in the anterior pituitary, thus reducing LH secretion (Cheung, 1983; Tortonese et al., 1998). In humans, therapeutic use of GnRH can overcome hyperprolactinemia-induced infertility, suggesting that reduced GnRH secretion is the cause. As the sub-population of GnRH neurons expressing prolactin receptor is quite small (approximately 13% (Grattan et al., 2007)), indirect effects of prolactin on afferent neurons (e.g. kisspeptin neurons) could be the reason (Kokay et al., 2011; Brown et al., 2019).

In order to regulate the permanent secretion of prolactin from the pituitary, dopaminergic neurons of the hypothalamus secrete dopamine into the hypothalamo-hypophyseal portal system, which suppresses prolactin release (Fuxe, 1963; MacLeod et al., 1970; Mansour et al., 1990). Prolactin provides feedback to these dopaminergic neurons, increasing the synthesis and release of dopamine (Arbogast and Voogt, 1991; Ma et al., 2005a; Brown et al., 2012; Lyons et al., 2012; Romano et al., 2013). Here, pharmacological evidence has emerged indicating a Trpc-like current upon prolactin stimulation of dopaminergic neurons located in the arcuate nucleus of the hypothalamus (Lyons et al., 2012; Lyons and Broberger, 2014).

Trpc channels not only influence reproduction in the brain. Regulation of endocrine events at the level of the anterior pituitary is also thought to be dependent on Trpc channels, detected as mRNA or suggested using broad spectrum Trpc antagonists (Tomic et al., 2011; Kucka et al., 2012; Beck et al., 2017).

In gonadotrope cells, the secretory cells of the pituitary that are linked to the HPG axis – Trpc channel mRNA – could be shown in both male and female tissues. Trpc5 has been found to play an important role in juvenile gonadotrope cells of the anterior pituitary, albeit not being highly abundant in adult females. In juvenile gonadotropes, activation of Trpc5 using Englerin A (Trpc5 activator, (Akbulut et al., 2015)) has shown a robust increase in intracellular calcium. In addition, experiments with knockout mice have shown Trpc5 to be downstream of GnRHR activation (Beck et al., 2017; Gotz et al., 2017).

Lactotroph cells of the anterior pituitary – as part of the lactotroph axis and responsible for the secretion of prolactin – have also been shown to utilize Trpc channel activity. As lactotroph cells are spontaneously active, applications of broad spectrum blockers for Trpc channels cause reduced prolactin secretion. RT-PCR analysis of Trpc mRNA in a mixed population of anterior pituitary cells showed the presence of Trpc1/c4/c5/c6, with Trpc1 being the most abundant. Further experiments using Gd^{3+} – which is known to have a bimodal effect on Trpc channels – have been performed. Gd^{3+} enhances Trpc4/c5 channel currents but blocks the channel activity of Trpc1/c3/c6/c7. In lactotroph cells, the application of Gd^{3+} causes hyperpolarization and thereby inhibits prolactin release, suggesting Trpc1 and/or Trpc6 to be important in mediating prolactin release (Tomic et al., 2011; Kucka et al., 2012).
In the last decade, multiple roles for Trpc channels in the chemosensation of hypothalamic neurons have emerged. The variety of function ranges from thermoregulation, energy or body fluid homeostasis and arousal to reproduction (summarized in (Kelly et al., 2018). More putative functions for Trpc channels in hormonal regulation have been proposed based on pharmacological evidence (Williams et al., 2011; Lyons et al., 2012; Zhang and van den Pol, 2012), which still need to be addressed using appropriate mutant models. Trpc channels

have a wide impact on hormonal homeostatic processes and reproduction. This influence – especially of Trpc5 – is apparent at multiple levels of the complex regulation of murine reproduction.

1.3 Trpc5: a complex ion channel

Trpc5 subunits comprise six transmembrane domains (TM), forming a pore region between TM5 and TM6 (Okada et al., 1998; Philipp et al., 1998), with both N and C terminus intracellularly. Trpc5 channels are formed by the assembly of four sub-units, which is possible as a homomeric channel as well as a heteromeric channel including Trpc1 and/or Trpc4 sub-units (Strubing et al., 2001; Hofmann et al., 2002; Strubing et al., 2003). Trpc channels are non-selective cation channels permeable for both calcium and sodium ions and therefore candidates to increase cellular excitability (Owsianik et al., 2006). Trpc channels are thought to be receptor operated channels and classically downstream of G-protein-coupled receptors (GPCR, Clapham, 2003). Trpc5 channels are highly regulated and appear to be gated using diverse opening mechanisms. It is clearly shown that Trpc5 is activated by G protein-coupled receptors, which downstream induce phospholipase C activation (Schaefer et al., 2000; Venkatachalam et al., 2003; Zeng et al., 2004; Qiu et al., 2010; Qiu et al., 2014; Storch et al., 2017; Kelly et al., 2018; Qiu et al., 2018). PLC activity conveys phosphatidylinositol-4,5-bisphosphate (PIP_2) into diacylglycerol (DAG) and inositol-1,4,5-trisphosphate (IP_3). The direct activation mechanism of Trpc5 channels subsequent to PLC activation is still highly discussed. Several labs state that DAG itself does not activate Trpc5 channels (Hofmann et al., 1999; Strubing et al., 2003; Venkatachalam et al., 2003; Qiu et al., 2010), while others claim that Trpc5 or Trpc channels in general are all activated by DAG (Lee et al., 2003; Storch et al., 2017; Mederos et al., 2018). Activation of Trpc5 by DAG depends on the preceding PIP_2 depletion. Removal of PIP_2 detaches Na^+/H^+ exchanger regulatory factor (NHERF) from the C terminus of Trpc, thus rendering Trpc5 DAG-sensitive (Mederos et al., 2018). The involvement of the second PIP_2 cleavage product IP_3 and its receptor is still controversial (Schaefer et al., 2000; Kanki et al., 2001; Strubing et al., 2001; Venkatachalam et al., 2003; Xu et al., 2005).

In heterologous expression systems, Trpc5 channels are also activated by intracellular infusion of guanosine triphosphate (GTP)-γ-S, indicating that GTP bound G proteins can activate Trpc5 (Schaefer et al., 2000; Zhu et al., 2005; Jeon et al., 2012). Upon channel opening, calcium ions can permeate through the Trpc5 channel. It has also been indicated as a modulator or even activator of Trpc5 channels in expression systems. Calcium seems to be a regulator of Trpc5 activity at both the extracellular and intracellular side. Trpc5 displays a strong dependence on internal calcium, which is able to trigger channel opening when increased to 100 nM or more (Schaefer et al., 2000; Zeng et al., 2004). On the other hand,

Trpc5 is also dependent on extracellular calcium availability, not only in its role as a calcium permeable channel but also given that a strong increase in extracellular calcium leads to channel opening (Okada et al., 1998; Schaefer et al., 2000; Zeng et al., 2004). Alternatively, some reports suggest that Trpc5 is a sensor for membrane lipid composition, where altered amounts of specific lipids affect Trpc5 function, e.g. increased concentrations of lysophosphatidylcholine (LPC) and/or sphingosine 1-phosphate (S1P) activate Trpc5. On the other hand, PIP_2 depletion seems to stimulate channel activity (Beech, 2007a; Trebak et al., 2009; Beech, 2012), which can be e.g. be caused by PLC activation or the activation of PI3-kinase, converting PIP_2 into phosphatidylinositol-3,4,5-trisphosphate (PIP_3). Not only membrane lipids but also physical factors like membrane stretch induce Trpc5 channel opening (Gomis et al., 2008; Jemal et al., 2014), suggesting that the lipid environment of Trpc5 channels seems to be important for channel function.

As Trpc5 is able to form heteromeric tetramers with Trpc1 and/or Trpc4, the complexity of channel regulation is further complicated in heteromeric channels (Strubing et al., 2001; Beech, 2012). At least the GPCR mediated channel activation is maintained in heteromeric channels (Strubing et al., 2001; Hofmann et al., 2002; Strubing et al., 2003). It seems that Trpc4 or Trpc5 determine the channel gating of heteromeric channels, whereas the opening mechanism of homomeric Trpc1 channels remains unknown (Clapham et al., 2001; Strubing et al., 2001; Nesin and Tsiokas, 2014).

The opening mechanism for Trpc5 is still not completely decided, although the link to different receptor types (e.g. GPCRs, tyrosine kinase receptors, cytokine receptors) or second messengers (e.g. PLC, PIP_2, PIP_3, DAG, IP_3) is well accepted. The use of multiple ways leading to channel opening might be an advantage of Trpc5 in fulfillment of its numerous cell-type dependent functions.

1.4 Olfactory influence on reproductive physiology

Olfactory and pheromonal cues detected in the nose are processed in the brain and based on this recognition they play a key role in many reproductive behaviors. Female physiological responses to chemosignals can be either benefiting or impeding. The presence of male cues in the juvenile phase of female mice benefits an earlier initiation of puberty, which is named the Vandenbergh effect (Vandenbergh, 1969). Quite similar to the Vandenbergh effect is the Whitten effect, whereby male cues are able to promote ovulation in anovulatory females (Whitten et al., 1968). Moreover, the housing of several females in close proximity induces the McClintock effect, namely the synchronization of their estrous cycle (McClintock, 1984). On the other hand, among group-housed juvenile females lacking male cues, puberty is delayed, thus highlighting that social odors are vital in modulating puberty onset (Colby and Vandenberg, 1974). The Lee-Boot effect is again analogous, where group-housed females suppress their estrous cyclicity, causing pseudopregnancy (Van Der Lee and Boot, 1955). Another impending effect on reproduction can be found when exposing newly-pregnant female mice to unfamiliar males, causing pregnancy failure (Bruce, 1959, 1969). This is called the Bruce effect. Here, the chemosignals of unfamiliar males increase the dopamine release of the hypothalamus, causing a decline in prolactin levels. This eliminates the stabilizing effects of prolactin onto corpora lutea, leading to a lack of progesterone and subsequent nidation failure (Bellringer et al., 1980; Rosser et al., 1989; Brennan, 2009). Physiological responses to chemosignals influencing reproductive actions in male mice are poorly understood, although there are several hints that olfactory cues also bear the capability to delay puberty onset (Jemiolo and Novotny, 1994). Chemosignals of female origin hold the potential to elevate LH levels and thereby androgens in post-pubertal male mice (Macrides et al., 1975; Schulz et al., 2009). This is in agreement with findings that female odors can have a positive influence on spermatogenesis (Koyama and Kamimura, 2000).

It is thus clear that olfactory cues can influence reproductive physiology in both benefiting and hindering ways. The decision between benefit and handicap is due to a complex composition of the internal status of the mouse and environmental information.

1.5 Aims

The hypothalamus is the control center of the endocrine system and it comprises various nuclei that can regulate reproduction. Of the two main reproductive pathways, the classical HPG axis relies on gonadotropin-releasing hormone (GnRH) and the lactotroph axis depends on dopamine and prolactin. During my thesis project, I have examined both reproductive pathways with a focus on the regulation of hypothalamic neurons during the reproductive cycle. Little information is available regarding the physiological function of hypothalamic neurons and how they influence reproduction. In chapter 4.1, I investigated whether GnRH directly excites hypothalamic neurons and if GnRH induces an inward current. In the following chapters, I more closely examined the effect of different Trpc mutations on reproduction. I focused on reproductive capabilities and hormonal alterations (see chapter 4.2) as well as the altered activity of hypothalamic neurons involved in the hormonal regulation of prolactin homeostasis (see chapter 4.3). Trpc channels start to stand out as key members of hormonal regulation at the level of the hypothalamus and therefore they are important targets for understanding hormonal feedbacks and possible candidates as therapeutic targets.

The following aims and objectives were addressed:

(1) To investigate the role of hypothalamic neurons involved in reproduction, my first aim was directed to verify whether genetically-tagged GnRH receptor (GnRHR) neurons that express GFP (Wen et al., 2011) express a functional GnRHR. The objective was to determine whether these neurons respond to GnRH with a depolarization and an increase in their action potential activity. In a next step, I examined whether the GnRH-induced increase in membrane potential was due to the activation of a depolarizing current or the inhibition of a hyperpolarizing current.

(2) A new concept emerged that Trp channels could be involved in the regulation of various homeostatic physiological functions including reproductive functions. Trpc channels – especially Trpc5 – are highly expressed in the hypothalamus (Fowler et al., 2007; Kelly et al., 2018). Thus, my second aim was to determine whether Trpc5 channels are involved in the regulation of the lactotroph reproductive axis and if the absence of Trpc5 channels could influence the reproductive outcome of a pregnancy. The following objectives were addressed using various Trpc5-deficient mouse strains:

a. Examine the reproductive capability of wildtype versus Trpc5-deficient mice and any changes in pituitary hormonal levels to assess a hormonal imbalance induced by the loss of Trpc5. In particular, I determined the levels of prolactin that would give information regarding the functionality of the lactotroph axis.
b. Assess both male and female reproductive deficits by examining the sperm of male mice and the estrous cycle length, ovulatory events and the gonadotropin release of female mice.
c. Determine whether olfactory cues can rescue a Trpc5-deficiency-induced subfertility in female mice, as predicted by reports indicating that forced mating may reduce reproductive deficits due to olfactory cues enhancing reproductive function in recipient female mice (Whitten et al., 1968; Oboti et al., 2014)
d. Investigate the action potential activity of dopaminergic neurons in the hypothalamic arcuate nucleus to determine the cause of the reproductive deficit.
e. Examine whether the short feedback loop is affected in Trpc5-deficient dopaminergic neurons and if this is due to the phosphorylation of the signal transducer and activator of transcription 5 (STAT5), which is activated due to prolactin receptor activation in arcuate dopaminergic neurons.

2. Materials

2.1 Chemicals and enzymes

Adenosine 5`-triphosphate magnesium salt (Mg-ATP)	Sigma
Agar-Agar	Carl Roth GmbH & Co. KG
N,N-Bis(2-hydroxyethyl)-2-aminoethanesulfonic acid (BES)	Sigma
Bicuculine methocloride	Abcam
Calciumchlorid dihydrate for analysis	Grüssing GmbH
CGP 52432	Abcam
CNQX disodium salt	Abcam
Dako Fluorescent Mounting Medium	Dako
D-AP5	Abcam
Dimethyl sulfoxide (DMSO)	Fisher Scientific Inc.
Dodecylsulfate Na-salt (SDS)	Serva
Ethylene glycol-bis(2-aminoethylether)-N,N,N`,N`-tetraacetic acid (EGTA)	Sigma
D(+)-Glucose monohydrate for microbiology	Merck
Glycinem ACS reagent, ≥98.5%	Sigma-Aldrich
Gonadotropin releasing hormone (GnRH), Luteinizing Hormone releasing Hormone, L7134	Sigma-Aldrich
Guanosine 5-triphosphate sodium salt hydrate ≥95% (HPLC)	Sigma
HEPES	Sigma
Hydrochloric acid (HCl)	Merck
Hydrogen peroxide, for analysis, 35 wt. % solution in water, stabilized	Acros Organics
Isoflurane	Baxter International Inc.
Isopropanol	Fisher Chemical
Lucifer yellow CH dipotassium salt	Sigma
LY 341495 sodium salt	Abcam
Magnesium sulfate ($MgSO_4$) anhydrous	Grüssing GmbH
Methanesulfonatic acid	Sigma-Aldrich
Neurobiotin (RRID: AB_2313575)	Vector Labs
N-methyl-D-glucamine 99.0-100.5%	Sigma
Paraformaldehyde (PFA) BioChemica	AppliChem
Phosphate buffered saline (PBS) tablets	Sigma

Potassium chloride (KCl) 99,5% for analysis	Grüssing GmbH
Potassium hydroxide (KOH)	Grüssing GmbH
Prolactin, murine recombinant	Sigma
(+)-Sodium L-ascorbate BioXtra ≥99.0% (NT)	Sigma
Sodium chloride AnalR NORMAPUR	VWR Chemicals
Sodium dihydrogen phosphate monohydrate p.A.	AppliChem
Sodium hydrogen carbonate suitable for biopharmaceutical production	Merck
Sodium hydroxide (NaOH)	Grüssing GmbH
Sodium hypochloride 12% (Bleach)	Carl Roth GmbH & Co. KG
Sodium pyruvate Reagent Plus ≥99%	Sigma-Aldrich
Thiourea puriss. P.a., ACS reagent, ≥99.0%	Sigma-Aldrich
Triton X-100	Sigma-Aldrich
Tetrodotoxin (TTX) citrate	Biotrend

2.2 Antibodies and Serum

2.2.1 Primary antibodies

Rabbit-anti-TH	1:1000	RRID: AB_297840	Abcam
Mouse-anti-TH	1:1000	RRID: AB_1624244	Immunostar Acris
Rabbit-anti-pSTAT5	1:200	RRID: AB_2302702	Cell Signaling

2.2.2 Secondary antibodies

Goat-anti-rabbit Alexa488	1:500	RRID: AB_2576217	Invitrogen
Donkey-anti-mouse Alexa 647	1:1000	RRID: AB_162542	Invitrogen
Donkey-anti-rabbit Alexa 555	1:1000	RRID: AB_162543	Invitrogen
Streptavidin-Alexa 633	1:400	RRID: AB_2313500	Thermo Fisher

2.2.3 Serum

Normal donkey serum (NDS)	Vector Labs

2.3 MILLIPLEX Kits

MILLIPLEX MAP Mouse Pituitary Magnetic Bead Panel 7-plex: ACTH, BDNF, FSH, GH, PRL, TSH, LH	Merck
MILLIPLEX MAP Mouse Pituitary Magnetic Bead Panel 6-plex: ACTH, FSH, GH, PRL, TSH, LH	Merck
MILLIPLEX MAP Mouse Pituitary Magnetic Bead Panel 5-plex: ACTH, FSH, GH, PRL, TSH	Merck
MAGPIX Calibration Kit	Merck
MAGPIX Performance Verification Kit	Merck

2.4 Solutions and Buffers

Artificial cerebrospinal fluid (oxygenated with 95% O_2 / 5% CO_2, aCSF):
120 mM NaCl, 25 mM $NaHCO_3$, 5 mM KCl, 5 mM BES, 1 mM $MgSO_4$, 1 mM $CaCl_2$, 10 mM Glucose, pH 7.3, 300 mOsm/l

NMDG-substituted incubation solution (oxygenated with 95% O_2 / 5% CO_2):
93 mM NMDG, 84 mM HCl, 2.5 mM KCl, 1.2 mM NaH_2PO_4, 30 mM $NaHCO_3$, 20 mM HEPES, 5 mM Na-ascorbate, 2 mM thiourea, 3 mM Na-pyruvate, 10 mM $MgSO_4$, 0.5 mM $CaCl_2$, pH 7.3, 300 mOsm/l

Synaptic blocker solution (current clamp, oxygenated with 95% O_2 / 5% CO_2):
120 mM NaCl, 25 mM $NaHCO_3$, 5 mM KCl, 5 mM BES, 1 mM $MgSO_4$, 1 mM $CaCl_2$, 10 mM Glucose, 10 µM CNQX disodium salt, 50 µM D-AP5, 10 µM LY 341495 sodium salt, 10 µM bicuculine methochloride, 1 µM CGP 52432, pH 7.3, 300 mOsm/l

Synaptic blocker + Tetrodotoxin blocking solution (voltage clamp, oxygenated with 95% O_2 / 5% CO_2):
120 mM NaCl, 25 mM $NaHCO_3$, 5 mM KCl, 5 mM BES, 1 mM $MgSO_4$, 1 mM $CaCl_2$, 10 mM Glucose, 10 µM CNQX disodium salt, 50 µM D-AP5, 10 µM LY 341495 sodium salt, 10 µM bicuculine methochloride, 1 µM CGP 52432, 1 µM TTX citrate, pH 7.3, 300 mOsm/l

GnRH stimulation solution (current clamp, oxygenated with 95% O_2 / 5% CO_2):
120 mM NaCl, 25 mM $NaHCO_3$, 5 mM KCl, 5 mM BES, 1 mM $MgSO_4$, 1 mM $CaCl_2$, 10 mM Glucose, 10 µM CNQX disodium salt, 50 µM D-AP5, 10 µM LY 341495 sodium salt, 10 µM bicuculine methochloride, 1 µM CGP 52432, 10 nM GnRH, pH 7.3, 300 mOsm/l

GnRH stimulation solution (voltage clamp, oxygenated with 95% O_2 / 5% CO_2):

120 mM NaCl, 25 mM $NaHCO_3$, 5 mM KCl, 5 mM BES, 1 mM $MgSO_4$, 1 mM $CaCl_2$, 10 mM Glucose, 10 µM CNQX disodium salt, 50 µM D-AP5, 10 µM LY 341495 sodium salt, 10 µM bicuculine methochloride, 1 µM CGP 52432, 1 µM TTX citrate, 10 nM GnRH, pH 7.3, 300 mOsm/l

Prolactin stimulation solution (oxygenated with 95% O_2 / 5% CO_2):
120 mM NaCl, 25 mM $NaHCO_3$, 5 mM KCl, 5 mM BES, 1 mM $MgSO_4$, 1 mM $CaCl_2$, 10 mM Glucose, 500 nM prolactin, pH 7.3, 300 mOsm/l

Artificial intracellular solution (IC):
11.8 mM KCl, 133.2 mM KOH, 1 mM EGTA, 0.1 mM $CaCl_2$, 130 mM methanesulfonic acid, 1 mM Mg-ATP, 1 mM Na-GTP, 10 mM HEPES, pH 7.2, 280 mOsm/l

Antigen-retrieval solutions:

1% NaOH, 1% H_2O_2 in PBS

0.3% glycine in PBS

0.03% SDS in PBS

Phosphate buffered saline (PBS):
137 mM NaCl, 2.7 mM KCl, 10 mM phosphate buffer, pH 7.4 at 25 °C

4% Paraformaldehyde in PBS:
40 g paraformaldehyde in 1 l PBS, pH 7.4

Blocking solution for immunohistochemistry:
PBS, 4% NDS (for pSTAT5 3% NDS), 0.3% Triton X-100

2.5 Consumables

24-well Cell Culture Plates	Greiner Bio-one
4-well Cell Culture Plates Nunclon™ Delta Surface	Thermo Scientific
Aluminium Universal Coverfilm	Ratiolab GmbH
Capillary Glass, 8250, Filament, 1.50/0.86, 75 mm or 150 mm	Science Products GmbH
Cellstar Tubes 15 ml, 50 ml	Greiner Bio-one
Cover glas 24 x 40 mm	Carl Roth
Cover glas 24 x 50 mm	VWR International
Disposable Pasteur Pipettes	Chase Instruments
Disposable Spatulas	VWR International
Glassware, made of Borsilicate 3.3	VWR International
Heat-shrinking tube	DSG-Canusa GmbH
Infusion Set with micro adjustment	Becton Dickinson AG
MAGPIX Drive Fluid	Merck
Microscope slides superfrost	VWR International
Minivette® POCT	Sarstedt AG
Quality Pipette Tips 10 µl, 200 µl, 1000 µl	Sarstedt AG
Reagent Reservoirs	VWR International
Safe Seal Tips Professional 10 µl, 200 µl, 200 µl XL, 1000 µl	Biozyme Scientific GmbH
Safe-seal micro tube 0.5 ml, 1.5 ml, 2.0 ml	Sarstedt AG
Single Edge Carbon Steel Razorblade	Electron Microscopy Sciences
Stainless Steel Double Edge Razorblade	DORCO
Sterile Syringe 1 ml Omnifix®-F	Braun
Sterile Syringe 5 ml, 10 ml, 50 ml, 60 ml Luer-Lock	Becton Dickinson AG
Super glue, Loctite 401	Henkel AG
Syringe Filters 13mm w/0.2 µm PTFE Membrane	VWR International
Transfer pipette 6 ml	Sarstedt AG
Weighing Paper	Fischer Scientific

2.6 Equipment

Patch-Clamp Set Up:

Audio Monitor AM10, Grass Technologies	Astro-Med GmbH
Digital CCD Camera ORCA-R^2	Hamamatsu Photonics
Digital Storage Oscilloscope VC-6523	Hitachi Ltd.
EPC 9 Patch Clamp Amplifier	HEKA Elektronik GmbH
Imaging Station cell^R	Olympus GmbH
Improved Neubauer chamber (0.1 mm deep)	Hauser Scientific
LN insert for bathchamber, type 1 small rhombus black Teflon coated	Luigs & Neumann Feinmechanik und Elektrotechnik GmbH
LN insert for bathchamber, type 1 small rhombus ceramic	Luigs & Neumann Feinmechanik und Elektrotechnik GmbH
Low-pass Bessel Filter (LPF-8)	Warner Instruments LLC
Modular Syringe Holder 10 ml, 60 ml	Warner Instruments
Perfusion Mini Manifold, 8 to 1 ports	Warner Instruments
Platinum-iridium harp, spun with nylon threads	Own construction
Stopcocks with Luer Connections	Cole-Parmer
Upright Microscope Olympus BX-51WI	Olympus GmbH
Filter Cubes:	
GFP: Excitation (nm): 470/40, Emission (nm): 525/50	
tdTomato: Excitation (nm): 560/55, Emission (nm): 645/75	
Objective:	
UPlanFl 10x/0.30	
XLUMPlanFL N 20x/1.00 W	
Vibration Isolation Table VH3036W-OPT	Newport Corporation
Vibration Vacuum Pump SP302SA-V	Schwarzer Precision GmbH & Co. KG
Workstation Bathchamber:	Luigs & Neumann Feinmechanik und Elektrotechnik GmbH
2 Micromanipulators Mini 25	
Shifting Table 380FM-2P	
Platform LN Bridge 500	
Remote Control Keypad SM-7	
Control Box SM-7	

MAGPIX Multiplex Set Up:

MAGPIX System	Merck
Multi-Channel Ultra High-Performance Pipettors (8x 5-50 µl, 12x 20-200 µl)	VWR International
Ultra High-Performance Single Channel Pipettors (0.5-10 µl, 2-20 µl, 20-200 µl, 100-1000 µl)	VWR International
Ultrasonic Cleaner	EMAG Technologies
Vibration Plate Shaker Vibramax 100	Heidolph
Vortex Genie 2	Scientific Industries

Immunohistochemical area:

Shaker Promax 2020 Reciprocating	Heidolph
Single Channel Pipettes (0.1-2.0 µl, 0.5-10 µl, 10-100 µl, 100-1000 µl)	VWR International
Vortex Genie 2	Scientific Industries

Tissue collection and acute slicing:

Cooling Device CU 65	Microm
Double spatulas, spoon shape	Binder GmbH
Medical Forceps, Dumont 7b	Fine Science Tools
Noyes Curved Spring Scissors 14 mm Blade	Fine Science Tools
Surgical Scissors Sharp-Blunt 47 mm Blade	Fine Science Tools
Vibrating-Blade Microtome HM 650V	Zeiss
Water Bath TW20	JULABO Labortechnik

LSM880:

Images were obtained using a Zeiss LSM 880 confocal microscope including a 32-channel GaAsP-PMT and 2-channel PMT QUASAR detector. Pictures were taken using equal settings, assembled and only slightest adjusting for brightness.

General:

Analytical Plus balance AP250D	OHAUS
Incubator CB60 supplied with 5% CO_2 and 23.7% O_2 at 37° C	Binder
Filter Funnel with Clamp DS0315	Thermo Fisher Scientific
Magnet stirrer, Thermolyne Cimarec 2	Thermo Fisher Scientific
Microforge MF-830	Narishige International
Microwave Midea MWGED 9025 E	Midea Europe
Osmometer OM-815	Vogel GmbH & Co. KG
pH Meter PHM240	Radiometer Analytical
Precision Balance 572	Kern & Sohn GmbH
Single Channel Pipettes (0.5-10 µl, 10-100 µl, 20-200 µl, 100-1000 µl)	VWR International
Tube clamps Rotilabo®	Carl Roth
Ultrapure Water System Direct-Q 5	EMD Millipore
Vacuum pump Air Admiral® diaphragm	Cole-Parmer
Vertical Glass Microelectrode Puller PP-830	Narishige International
Vortex Genie 2	Scientific Industries

2.7 Software

CorelDraw	Corel Corporation
IGOR Pro	WaveMetrix
ImageJ	Wayne Rasband, NIH
Microsoft Excel	Microsoft Corporation
Neuroexplorer	Nex Technologies
Origin Pro	OriginLab Corporation
Patchmaster	HEKA Elekronik GmbH
xcellence rt	Olympus GmbH

2.8 Animals

Animal care and experimental procedures were reviewed and approved with the guidelines and ethical regulations established by the animal welfare committee of Saarland University and in compliance with the German Protection of Animals Act and the Regulation for the protection of animals used for scientific purposes (2010/63/EU). Mice were kept under standard light/dark cycle (12/12) with food and water *ad libitum* in individually ventilated cages (IVC, Tecniplast). All mice used were 6-15 weeks old.

Mice in breeding:

GnRHR-internal ribosome entry site-Cre (GRIC)

Gonadotropin releasing hormone receptor (GnRHR) is a G protein coupled receptor specifically expressed by gonadotropes in the anterior pituitary and by a subset of neurons in the brain, e.g. in the hypothalamus. In gonadotropes GnRH triggers the secretion of gonadotropins, LH and FSH. This mouse line has an integrated IRES-Cre cassette behind the exon 3 of the *GnRHR* gene (Wen et al., 2008). This mouse strain was kindly provided by Prof. Dr. U. Boehm (PZMS, Homburg, Saarland University, Germany).

ROSA26-CAGS-tauGFP (eR26-τGFP)

This reporter mouse line has a chicken β-actin promoter and CMV enhancer (CAGS), a *loxP*-flanked strong transcriptional stop signal (triple SV40 polyadenylation sequence), and a τGFP (Wen et al., 2011). Cre recombinase activity will delete the stop signal enabling the transcription of τGFP. This mouse strain was kindly provided by Prof. Dr. U. Boehm (PZMS, Homburg, Saarland University, Germany).

GRIC/eR26-τGFP

GRIC and eR26-τGFP mice were crossbred to visualize GnRHR cells both in the pituitary gland (gonadotropes) as well as in several brain regions, e.g. in the hypothalamus (Wen et al., 2011).

Th-Cre

Tyrosine hydroxylase (TH) is a rate-limiting enzyme in the biosynthesis of catecholamines which catalyzes the conversion of tyrosine to L-DOPA. Therefore, it is suitable as a marker for dopaminergic neurons. B6.Cg-*7630403G23Rik*$^{Tg(Th\text{-}cre)1Tmd}$/J (JR# 008601, The Jackson Laboratory) mice carry a construct of a 9.0 kb fragment of the rat TH promoter, a synthetic intron, cDNA of Cre recombinase and a SV40 polyadenylation sequence, that was inserted into chromosome 9 causing a 624 kbp deletion in the *7630403G23Rik* locus (Savitt et al., 2005). The resulting mouse line expresses Cre recombinase under the control of the rat TH promotor enabling the conditional mutation in catecholaminergic cells.

R26-tdTomato

The Rosa26 (*Gt(ROSA)26Sor*) locus is a commonly used locus for the generation of Cre-reporter mice. In the B6.Cg-*Gt(ROSA)26Sor*$^{tm14(CAG-tdTomato)Hze}$/J (JR# 007914, The Jackson Laboratory) mouse line a construct containing a CMV-IE enhancer/chicken beta-actin/rabbit beta-globin hybrid promotor (CAG), a *FRT* site, a *loxP*-flanked STOP cassette, the sequence of tdTomato, a woodchuck hepatitis virus post-transcriptional regulatory element (WPRE) and a polyA signal was included between the exon 1 and 2 of the Rosa26 locus (Madisen et al., 2010). When Cre recombinase is active the STOP cassette will be deleted and tdTomato expressed.

Th-tdTomato

To visualize of dopaminergic neurons in the arcuate nucleus of the hypothalamus the aforementioned mouse lines, Th-Cre and R26-tdTomato, were crossed to obtain the mouse line referred to as Th-tdTomato. In this mouse line the STOP cassette of the R26-tdTomato is deleted in catecholaminergic cells due to Cre recombinase resulting in robust tdTomato expression.

Trpc5^{L3F1}

The canonical transient receptor potential (Trpc) channel Trpc5 is part of the Trpc subfamily of non-selective, calcium-permeable and receptor operated cation channels. This mouse line carries a construct containing a *loxP*-flanked Exon 4 of the *Trpc5* gene, a splice acceptor (SA)-IRES-GFP cassette, a FRT sequence, and a third *loxP* site, the so-called *Trpc5*^{L3F1} allel (Xue et al., 2011). These mice were kindly provided by Prof. Dr. M. Freichel (University of Heidelberg), Prof. Dr. V. Flockerzi and Dr. P. Weissgerber (Saarland University).

Trpc5-E4$^{-/-}$

Trpc5$^{-/-}$ mice, kindly provided by Prof. Dr. M. Freichel (University of Heidelberg), Prof. Dr. V. Flockerzi and Dr. P. Weissgerber (Saarland University), are a result of crossbreeding Trpc5^{L3F1} with the CMV-Cre deleter mouse strain. Here, the Exon 4, the IRES-GFP cassette, and the FRT sequence were removed to obtain mice with a *Trpc5* null allel (Xue et al., 2011). This mouse line will be referred to as Trpc5-E4$^{-/-}$.

Trpc5-E5$^{-/-}$

The Trpc5$^{tm1.1Lbj}$/Mmjax (JR# 024535, MMRCC Stock No: 37349-JAX, The Jackson Laboratory) mouse line was obtained by mating Sox2-Cre mice with mice that carry a *Trpc5* gene alongside a *loxP*-flanked Exon 5 resulting in Trpc5 knockout mice, lacking Exon 5 (Phelan et al., 2013). This mouse strain will be referred to as Trpc5-E5$^{-/-}$.

Th-tdTomato/Trpc5-E5$^{-/-}$

To visualize dopaminergic neurons in Trpc5 deficient mouse lines we crossbred Th-Cre mice and R26-tdTomato seperatly with Trpc5-E5$^{-/-}$ mice. Subsequently, we crossbred the resulting Th-Cre:Trpc5-E5$^{-/-}$ and R26-tdTomato/Trpc5-E5$^{-/-}$ to obtain Th-tdTomato/Trpc5-E5$^{-/-}$ mice, which express tdTomato in catecholaminergic cells and are deficient for Trpc5.

External breeding information:

Reproductive data about the following mice were kindly provided by Prof. Dr. V. Flockerzi and Dr. P. Weissgerber of the Center for Molecular Signaling (PZMS, Homburg, Saarland University, Germany).

Trpc1$^{-/-}$

Trpc1$^{-/-}$ mice were obtained by replacement of the gene segment downstream of *Eco*RI site in exon 8 by a PGK-Neo cassette causing a loss of the coding region for amino acids 584 - 670. As a result exon 8 is omitted due to splicing resulting in a stop codon, causing lack of Trpc1 (Dietrich et al., 2007).

Trpc4$^{-/-}$

Trpc4$^{-/-}$ mice were generated by deleting the exon encoding transmembrane segments 4 and 5 and parts of the linker between segments 5 and 6, causing a lack of Trpc4 (Freichel et al., 2001).

Trpc1/5$^{-/-}$

Trpc1/5$^{-/-}$ double knockouts were generated crossing the previous described mouse lines Trpc1$^{-/-}$ and Trpc5-E4$^{-/-}$.

Trpc4/5$^{-/-}$

Trpc4/5$^{-/-}$ double knockouts were generated crossing the previous described mouse lines Trpc4$^{-/-}$ and Trpc5-E4$^{-/-}$.

Trpc1/4/5$^{-/-}$

Trpc1/4/5$^{-/-}$ triple knockouts were generated crossing the previous described mouse lines Trpc1$^{-/-}$, Trpc4$^{-/-}$ and Trpc5-E4$^{-/-}$.

3. Methods

3.1 Evaluation of reproductive capabilities

To assess the reproductive capability, pairs of sexually mature female and male mice (if not stated otherwise of the same genotype, 8-12 weeks old) were kept in individual ventilated cages (IVC, Tecniplast) to a time period of 10 weeks. Breeding records were carefully collected by the animal facility staff. Litters remained in the parent cages until postnatal day 21-22. The following parameters were determined. A breeding was counted as a productive mating if it gave birth at least once in the time period of 70 days. The interval between the start of the forced breeding until the day of the first litter was used as latency to first litter. To calculate the relative fecundity the following equation was used:

$$Relative\ fecundity = productive\ mating * litter\ size * number\ of\ litters$$

To estimate the pup survival rate the pup count at birth (litter size) and the pup count at the day of weaning (postnatal day 21-22) was used.

3.2 Assessment of reproductive cycle stages

Before each experiment vaginal smears were obtained. A Pasteur pipette was flame-polished and filled with approximately 10 µl phosphate buffered saline (PBS) and placed gently into the vagina of the mouse. The vagina was flushed 3 times and the PBS containing the vaginal secretion was transferred onto a microscope slide and examined. According to the cell type composition the estrous cycle stage was determined (Goldman et al., 2007; Caligioni, 2009; Byers et al., 2012). High amounts of leukocytes are a determinant of diestrus (Fig. 6 B), high amount of nucleated epithelial cells imply the proestrus stage (Fig. 6 C) and cornified epithelial cells signify estrus (Fig 6 D). A mixture of those three cell types is an evidence for metestrus (Fig. 6 A). Images of each vaginal smear was tagged with an unique identifier for each mouse and digitally stored.

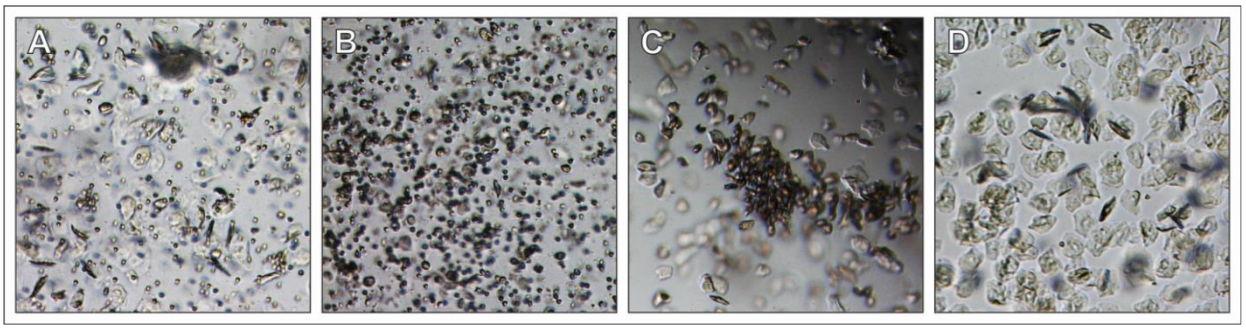

Figure 6: Vaginal cytology of different mouse estrous cycle stages.
Wet and unstained vaginal smears from female mice, in metestrus (A), diestrus (B), proestrus (C) and estrus (D).

3.3 Measurement of blood serum hormone levels

Blood was collected daily for up to 14 days from the same mouse at 1700 hours in standard light:dark cycle to obtain hormone serum levels 1 hour before lights off. Blood was collected with Minivette® POCT and transferred into blood collection microtubes without anticoagulants after bleeding puncture to the tail vein. The blood samples were allowed to clot at RT for 30 min, centrifuged (2000 x g for 10 min, 7 °C), the serum (supernatant) was carefully removed into a clean microtube and stored at -20 °C until MAGPIX measurement. Serum concentrations of ACTH, BDNF, FSH, GH, LH, TSH and PRL were determined using a MILLIPLEX MAP Mouse Pituitary Magnetic Bead Panel (5-7 Plex). The assays were performed according to the standard protocol provided by Luminex.

3.4 Sperm preparation

Adult (>8 weeks old) male mice were rapidly killed by cervical dislocation following CO_2 inhalation. Both cauda epididymis were collected, cut several times, placed into aCSF solution and incubated for 30 minutes at 37° C, 5% CO_2 and 23.7% O_2. In this time window, spermatozoa were allowed to move out of the cauda epididymis and to capacitate in the bicarbonate containing aCSF (Visconti et al., 1998). To analyze sperm motility, 100 µl of sperm containing aCSF was dropped onto a microscope slide and imaged with 5 Hz for 10 s. Individual spermatozoa were manually tracked over time using ImageJ. For sperm count, 4% PFA was added to immobilize the spermatozoa. Sperm containing solution was added to an improved Neubauer chamber and spermatozoa counted.

3.5 Preparation of acute brain slices

All experiments were performed on coronal brain slices containing the periventricular nucleus (Pe, Bregma 0.26 to -1.9) or the arcuate nucleus of the hypothalamus (ARC, Bregma -1.6 to -2.2 mm). Slices were prepared freshly every experimental day from female mice (7-12 weeks old). Previous described methods were adapted to suit the distinct experiments (Schauer and Leinders-Zufall, 2012; Schauer et al., 2015). Mice were anesthetized with isoflurane followed by decapitation. The whole mouse head was submerged in ice cold aCSF for 60 s before removal of the brain. Brains were removed quickly, submerged in ice-cold aCSF solution, and sliced (275 µm thickness) using a vibratome. In experiments using GRIC/eR26-τGFP mice to measure cells of the periventricular nucleus (Pe) slices were kept in oxygenated NMDG-substituted incubation solution at 31.5 °C for 15 minutes followed by a 30 minutes incubation in oxygenated aCSF at room temperature. Brain slices that were used for experiments in the ARC were kept in oxygenated aCSF for 15 minutes at 31.5 °C and afterwards for at least 30 minutes at room temperature prior to electrophysiological recordings.

3.6 Whole cell patch clamp recording

Whole cell patch clamp recordings from either GnRHR neurons or Th+ neurons were performed in coronal acute brain slices (275 µm) as described previously (Schauer and Leinders-Zufall, 2012; Schauer et al., 2015). GnRH was stored in stock solutions prepared in oxygenated aCSF and stored at -20 °C. On experimental days GnRH was further diluted in appropriate aCSF, containing pharmacological agents as described above, and applied via the perfusion system. Prolactin was directly prepared in aCSF in concentrations of 500 nM and stored at -20 °C in 1 ml aliquots. Prior to experiments one aliquot was equilibrated to RT and oxygenated. To stimulate with prolactin the prepared 1 ml aliquot was applied using a 1 ml syringe and a microperfusion connected to the Perfusion Mini Manifold. Patch pipettes were pulled from thick wall borosilicate glass capillaries with filament (OD 1.50mm / ID 0.86 mm). All pipettes were pulled using a vertical glass electrode puller (PP-830, Narishige International) and fire-polished using a microforge (MF-830, Narishige International) to achieve a final pipette resistance around 5-7 MΩ. Pipettes were filled with intracellular solution (IC) and to label ARC neurons for post-hoc immunostaining, 0.05‰ neurobiotin (Vector Labs) was added to the IC. The filled patch pipette is mounted on the headstage of the patch clamp amplifier (EPC-9, HEKA Elektronik) and the reference electrode connected. With motorized micromanipulators the pipette was moved towards the chosen cell. Slices were continuously superfused with oxygenated aCSF (~ 2 ml/min, gravity flow, RT), with or without additional pharmacological agents. To prevent clogging of the

pipette tip inside the recording chamber, a slight pressure was applied. After the tip approaches the tissue and especially the cell membrane, the pressure was decreased and a negative pressure applied. If it reaches the GΩ range the negative pressure was increased und the cell membrane disrupted. Now measurements of currents and voltages across the membrane were possible.

The genetically tagged neurons were visualized using a BX51WI fixed stage microscope (Olympus) equipped with infrared-optimized differential interference contrast (IR-DIC) optics. To identify and center the area of interest, the periventricular nucleus or the arcuate nucleus, the slice was first examined using a 10x magnification, whereas a 20x magnification, suitable for water immersion, was used to visualize the cells of interest, either by anatomy or expression of τGFP or tdTomato.

Spikes were analyzed as follows. For burst detection an interspike interval (ISI) was determined (Selinger et al., 2007) as a threshold for burst detection in Neuroexplorer (Nex Technologies). For dopaminergic neurons of the ARC we calculated an ISI of 2.61 s. The burst detection was then used to assist in the calculation of burst parameters such as spike frequency in burst, instantaneous burst frequency, and others. The depolarization envelope was calculated as the area under the curve of each burst detected, where the zero line was mathematically calculated between the baseline values at the beginning and end of the burst. To estimate the burst strength a linear fit was performed for each burst's rising phase und the slope used for burst strength calculation. To further analyze the oscillatory behavior of dopaminergic ARC neurons normalized and mean subtracted autocorrelation histograms (ACH) were generated for each cell recorded. To do so the spike activity was converted into a smoothed peristimulus time histogram (PSTH, bin size 1 s). The burst refractory period was estimated according to (Samonds and Bonds, 2005) as the time lag at the center of the first minimum of the ACH. The following two consecutive peaks were used to confirm the oscillatory frequency calculated from the burst detection. To further support the estimated oscillation frequency Fourier transformation of the ACH were performed and the highest Fourier energy signifying the oscillatory frequency. To identify the regularity of the oscillatory firing a rhythmicity index (RI) was calculated with two independent methods. First, the RI was defined as the amplitude of the ACH side peak (Long et al., 2004). Second, the RI was determined by fitting a linear function to the top envelope of the Hilbert transformation power function generated of each ACH from a lag of +20 s, whereby the intercept of this line to the zero lag is the RI (Zylbertal et al., 2017).

3.7 Immunohistochemistry

3.7.1 Post-hoc immunostaining of whole cell recorded cells

To identify Th+ ARC neurons, post-hoc immunostaining was performed following electrophysiological recordings. Slices were fixed in 4% PFA in PBS overnight, washed in PBS, permeabilized and incubated for 1 h in blocking solution (0.3% Triton X-100 and 4% normal donkey serum in PBS). Trpc5-deficient slices were incubated in rabbit anti-Th antibody (1:1000, polyclonal, ab112, Abcam; RRID: AB_297840) at 4 °C overnight followed by an incubation with the secondary antibody donkey anti-rabbit IgG Alexa 555 (1:1000, polyclonal, A-31572, Invitrogen; RRID: AB_297840) for anti-Th and streptavidin-Alexa 633 conjugate (1:400, S-21375, Thermo Fisher; RRID: AB_2313500) for neurobiotin at room temperature for 1 h. In Th-tdTomato mice, slices were incubated in rabbit anti-Th antibody at 4 °C overnight followed by an incubation with the secondary antibody goat anti-rabbit IgG Alexa 488 (1:1000, polyclonal, A-11034, Invitrogen; RRID: AB_2576217) for anti-Th and streptavidin-Alexa 633 conjugate for neurobiotin at RT for 1 h. Intrinsic tdTomato fluorescence could still be visualized after fixation using 555 nm laser light. Brain slices were mounted on superfrost microscope slides (VWR), covered with DAKO fluorescent mounting medium, and on the following day analyzed with a Zeiss LSM 880 confocal microscope containing a 32-channel GaAsP-PMT and 2-channel PMT QUASAR detector.

3.7.2 Immunostaining of TH and pSTAT5 in prolactin stimulated acute slices

Brain slices of both Th-tdTomato as well as Trpc5-E5$^{-/-}$ were sliced as described in 3.4. After cutting the slices were incubated in oxygenated aCSF in an O_2/CO_2 incubator supplied with 23.7% O_2 and 5% CO_2 at 37 °C for 15 minutes. Hereafter the aCSF was exchanged with prolactin stimulation solution (500 nM prolactin in oxygenated aCSF) and the slices were incubated in the O_2/CO_2 incubator for another 30 minutes. pSTAT5 staining procedure was adapted from (Munzberg et al., 2003; Frontini et al., 2008; Senzacqua et al., 2016). Slices were then fixed in 4% PFA in PBS overnight and washed in PBS. Slices then received an antigen-retrieval procedure and thereafter incubated in PBS containing 1% NaOH and 1% H_2O_2 for 20 minutes at RT, 10 minutes at RT in 0.3% glycine in PBS, and for 10 minutes in 0.03% SDS in PBS. Following the antigen-retrieval slices were permeabilized and incubated for 1 h in blocking solution (0.3% Triton X-100, 3% normal donkey serum). Brain slices were then incubated in rabbit anti-pSTAT5 antibody (1:200, monoclonal, 9314S, Cell Signaling, RRID: AB_2302702) over 2 nights at 4 °C followed by an incubation in mouse anti-Th antibody (1:1000, polyclonal, MO22941-100, Immunostar Acris, RRID: AB_1624244) for 2 h at RT. After this slices were incubated in secondary antibodies for 1 h at RT, goat anti-rabbit IgG Alexa 488 (1:500, polyclonal, A-11034, Invitrogen; RRID: AB_2576217) for anti-pSTAT5

and donkey anti-mouse Alexa 647 (1:1000, polyclonal, S-21375, Invitrogen; RRID: AB_2313500) for anti-Th. Brain slices were mounted on superfrost microscope slides (VWR), covered with DAKO fluorescent mounting medium, and on the following day analyzed with a Zeiss LSM 880 confocal microscope containing a 32-channel GaAsP-PMT and 2-channel PMT QUASAR detector.

3.8 Estimation of the influence of olfactory cues on reproductive capabilities

Olfactory cues can modulate reproductive success in mice (Bruce, 1959, 1968, 1969; Leinders-Zufall et al., 2004; Hattori et al., 2017). Previous reports indicate that forced mating may reduce reproductive deficits due to olfactory cues enhancing reproductive function in recipient female mice (Whitten et al., 1968; Oboti et al., 2014). To determine if olfactory cues can rescue Trpc5-dependent reproductive deficiency, we put pairs of sexually naïve female mice into new IVCs und started monitoring their estrous cycle for a total of 6 weeks. After 2 weeks we started blood sampling for 14 days as described in 3.3. After 2 completed cycles we added one of three stimuli. First, we prepared single housed sexually experienced males one week before and used the male scented bedding as a regularly given stimulus every morning when monitoring the estrous cycle. Second, we added a castrated C57/Bl6N male to the existing cages. Third, we added a vasectomized C57/Bl6N male. These stimuli were present until the end of the 6 week period.

3.9 Statistics

Statistical analysis was performed using Origin Pro (Origin Lab Corporation). Before statistical examination all data sets were tested for assumption of normality and uniformity of variance. In case of parametric distribution Student's t-test was used to measure the significance of the difference between two groups. Multiple data sets were compared using two-way analysis of variance (ANOVA) with either Tukey's multiple comparison test or Fisher's least significant difference test as a post-hoc comparison. Given a non-parametric distribution, the Kruskal-Wallis ANOVA and Mann-Whitney test were used. Data with a probability of error level (α) below 5% were indicated as statistical significant. If not otherwise, data are shown as mean ± sem (standard error of the mean). Box plots illustrate the interquartile (25 – 75%) ranges, median (line) and mean (squares) values with whiskers indicating standard deviation (SD) values.

4. Results

4.1 GnRH activates a depolarization in hypothalamic GnRHR neurons

In order to investigate the hypothalamic neurons involved in reproduction, I examined target neurons of the gonadotropin-releasing hormone (GnRH). It was hypothesized that GnRH could regulate reproductive physiology in the brain independent of the classical HPG axis. Neurons expressing the GnRH receptor (GnRHR) have been documented in multiple areas (Badr and Pelletier, 1987; Jennes et al., 1997; Wen et al., 2011). How GnRH acts on its target cells in the brain has not yet been investigated since it is difficult to identify the neurons between the myriad of cells in the hypothalamus. Due to the development of mice expressing a fluorescent marker in all GnRHR-expressing neurons by the team of Prof. Dr. U. Boehm (Wen et al., 2011), I could examine these neurons using electrophysiological techniques. My aim was to demonstrate that these neurons respond reliably to GnRH to indicate that the genetically-tagged neurons express a functional GnRHR. These experiments were necessary because the mice used show a historic expression pattern of GnRHR. Cre-recombinase activity is dependent on a one-time activation of the GnRHR promotor. Cre-recombinase then removes the loxP-flanked stop codon located in the Rosa26 locus. Henceforth, τGFP will be expressed in all cells that activated the GnRHR promotor at least once in their lifecycle. Here, the problem could arise that τGFP is expressed but the protein of interest – GnRHR – is no longer present. As there is no valid antibody against GnRHR, I chose the tool of functional verification.

4.1.1 GnRH stimulation induces a depolarization in GnRHR neurons causing increased activity

As an initial objective, I investigated whether hypothalamic GnRHR neurons respond to GnRH stimulation and if GnRH induces an increase in activity due to depolarization. Therefore, I first investigated the fluorescently-marked neurons using the current-clamp technique to monitor action potential activity. GnRHR neurons were spontaneously active. This activity did not depend on the input of other cells when synaptically isolated using blockers against glutamatergic and GABAergic transmission (CNQX, D-AP5, LY 341495, bicuculine methiodide, CGP-52432; Fig 7 A left). Synaptically-isolated GnRHR neurons had a resting membrane potential between -46 and -52 mV (average: -49.5 ± 2.7 mV, n = 5; 0 pA current injection). A 1s puff application of 1 nM GnRH increased excitation in GnRHR neurons, causing a depolarization in a range of 0.5 to 3.2 mV. The depolarization was dependent on the resting membrane potential, whereby higher depolarizations could be induced in cells with more negative membrane potential (Pearson's r = -0.8). The average increase in membrane potential was 1.5 ± 0.5 mV (n = 5; Fig 7 B). In unison with a

depolarization, stimulation with GnRH caused an increase in action potential frequency, confirming the results of Dr. Schauer and Dr. Tong in their loose-patch recordings (Schauer et al., 2015). The GnRH stimulation increased the mean action potential frequency in GnRHR neurons by a factor of 2.4 when comparing the first 10 s pre-stimulus and 10 s post-stimulus (Fig 4.1.1 C). This confirms that genetically-labeled GnRHR neurons indeed express a functional GnRHR, which responds to a GnRH stimulation with an increase in activity, caused by a depolarization.

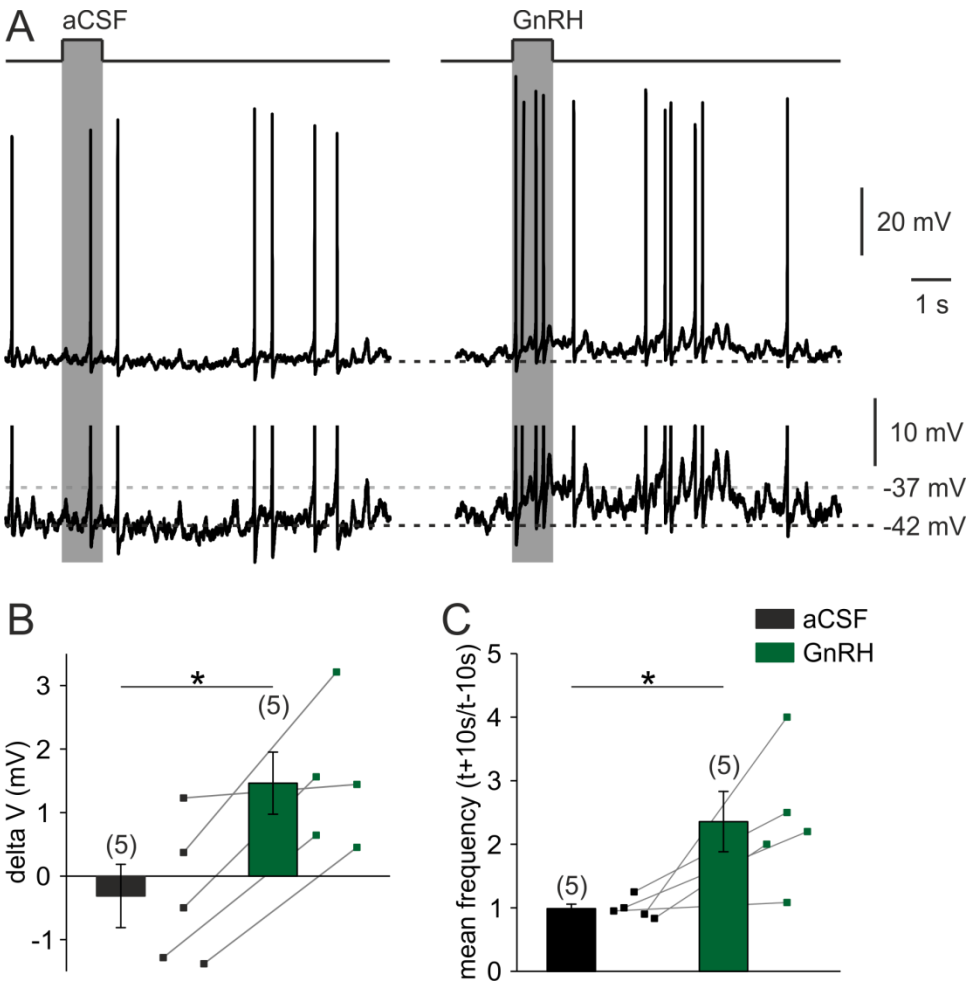

Figure 7: GnRH induces a depolarization and an increase in action potential activity in GnRHR neurons. (A) Original trace of a GnRHR neuron stimulated with a 1s pulse of either aCSF or 1 nM GnRH. GnRH induces an elevation of the membrane potential as well as an increase in action potential firing. (B) Bar histogram of the mean change in membrane potential induced by either aCSF or 1 nM GnRH in the first 10s after succeeding stimulation. Control -0.3 ± 0.5 mV; GnRH 1.5 ± 0.5 mV. Paired t-test $t(4) = -4.14$, * $p < 0.05$. (C) Relative change in mean frequency induced by either aCSF or GnRH application, comparing 10s pre- and post-stimulation. Control 0.98 ± 0.07; GnRH 2.36 ± 0.47. Paired t-test $t(4) = -2.81$, * $p < 0.05$. The numbers in brackets indicate measured cells.

4.1.2 GnRH induces an excitatory inward current in GnRHR neurons

Synaptical isolation as performed in the current-clamp recordings encourages the hypothesis that GnRH initiates the membrane depolarization in GnRHR neurons. An increase in membrane potential can be achieved by either activation of a depolarizing current or inhibition of a hyperpolarizing current. In order to further support our hypothesis and gain additional insights into GnRHR activation, we performed voltage clamp experiments were performed, adding tetrodotoxin (TTX) to the synaptic blocker cocktail to block voltage-gated sodium channels and thereby prevent action potentials and spontaneous activity of GnRHR neurons. Upon bath application of 10 nM, GnRH elicited an inward current (Fig. 4.1.2 A). Gaussian analysis as well as mean current analysis using a time frame of 50s pre- and post-stimulus indicates a GnRH-induced current amplitude of -2.4 ± 0.02 pA and -2.2 ± 0.94 pA, respectively (Fig 8 B-C). These findings provide additional proof that genetically-labeled GnRHR neurons express functional GnRHRs and that GnRH induces an inward current, causing depolarization and activity increase.

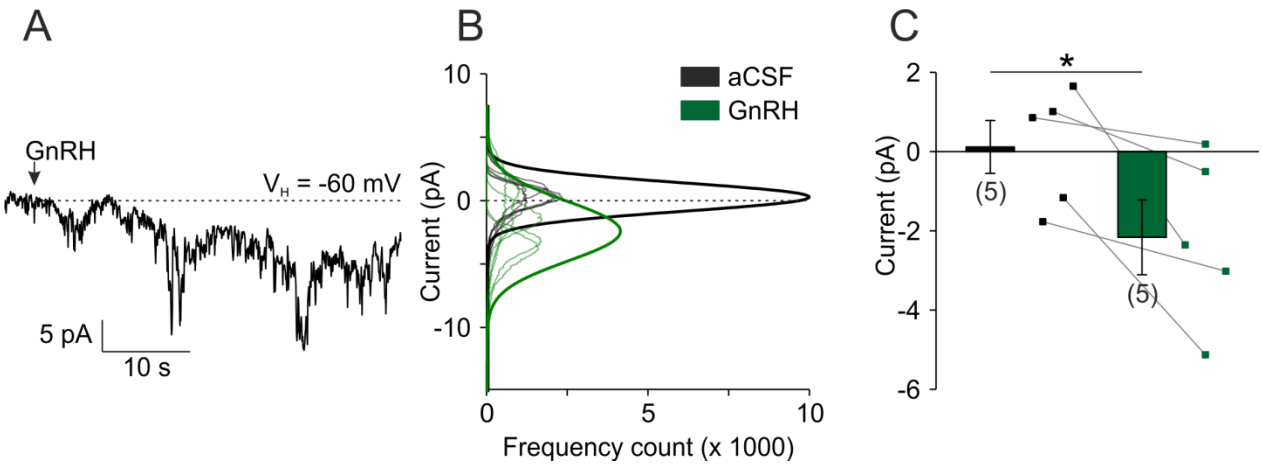

Figure 8: GnRH activates an inward current in GnRHR neurons.
(A) Example of a GnRHR neuron producing an inward current upon GnRH stimulation. (B) Gaussian fits of averaged current frequency distributions in aCSF (black, μ = 0.2 ± 0.1 pA) and a bath application of 10 nM GnRH (green, μ = -2.4 ± 0.02 pA). Raw data used (50s before and after stimulation) are shown as thin lines. (C) Mean current analysis under both aCSF and GnRH stimulation during 50s pre- and post-stimulation. Control 0.12 ± 0.67 pA; GnRH -2.16 ± 0.94 pA. Paired t-test t(4) = 3.22, * p < 0.05. The numbers in brackets indicate measured cells.

4.1.3 Discussion

The GnRHR neurons recorded in this study all responded to GnRH, providing evidence that GnRH directly acts on GnRHR neurons in the brain (Wen et al., 2011; Schauer et al., 2015) and that environmental GnRH in brain areas of the hypothalamus modulate GnRHR neuron activity and downstream targets.

GnRHR neurons respond to stimulations with GnRH with a depolarization and an increase in action potential frequency. The increase in membrane voltage could be due to either the increase in depolarizing currents or a shutdown of a hyperpolarizing current. This study demonstrates that GnRH-dependent activation of its receptor induces an inward current in GnRHR neurons that were synaptically isolated and segregated of their own action potential activity by TTX. GnRHR activation is known to trigger G-protein activation (Tsutsumi et al., 1992) and a complex intracellular signaling cascade (Naor, 1990; Ruf et al., 2003; Naor, 2009). GnRHR can be coupled with different types of G-proteins, $G_{\alpha i}$, $G_{\alpha q}$ and $G_{\alpha i}$, although GnRHR stimulation is often linked with activation of phospholipase C (PLC, (Naor and Huhtaniemi, 2013), causing the hydrolysis of phosphatidylinositol 4,5-bisphosphate (PIP_2) into inositol 1,4,5-trisphosphate (IP_3) and diacylglycerol (DAG). IP_3 binds to its receptor at the endoplasmic reticulum, releasing calcium from intracellular stores, whereas DAG is a known activator of protein kinase C (PKC). Voltage-gated calcium channels (VGCC) are supposed to contribute to the intracellular calcium rise (Kraus et al., 2001). Additionally, channels of the transient receptor potential (Trp) superfamily could also be involved in the GnRH-induced depolarizing inward current. Canonical Trp channels are known to mediate calcium entry and to be receptor operated and activated by PLC (Clapham et al., 2001; Vazquez et al., 2004; Venkatachalam and Montell, 2007; Numata et al., 2011). Trp channels and especially Trpc channel show a high expression not only in developing gonadotroph cells (Beck et al., 2017) but also in various neuroendocrine cells of the hypothalamus (Fowler et al., 2007; Gotz et al., 2017; Kelly et al., 2018). In juvenile females, Trpc5 has been proposed to be the excitatory element linking the activation of GnRHR and opening of L-type VGCCs (Beck et al., 2017; Gotz et al., 2017). As Trpc5 is also highly expressed in several hypothalamic cell types involved in reproduction (Zhang et al., 2008; Bosch et al., 2013; Zhang et al., 2013a; Zhang et al., 2013b; Qiu et al., 2014), it is reasonable to speculate that Trpc5 also mediates GnRHR signaling in the brain. Therefore, I would hypothesize that GnRHR stimulation subsequently activates G_q causing PLC-dependent PIP_2 breakdown into IP_3 and DAG, lifting the PIP_2 dependent inhibition and increasing the DAG-sensitivity of Trpc5 channels, causing cation influx and opening VGCCs.

The mutation of Trpc5 and its impact on reproductive function needs to be assessed to prove this hypothesis. Immunohistochemical stainings could be performed to show the presence of Trpc5 protein in GnRHR neurons of the brain. As functional evidence, the activity of Trpc5 deficient GnRHR neurons needs to be recorded in unstimulated conditions as well as under application of GnRH. If Trpc5 is the key element linking GnRHR to downstream elements of the second messenger cascade, loss of Trpc5 should affect the regulation of the hypothalamic-pituitary-gonadal axis (HPG axis). This would cause changes in hormonal levels of luteinizing hormone (LH) and follicle stimulation hormone (FSH), which could be measured. As an outcome of an unregulated HPG axis and altered gonadotropine levels, the reproductive capability of Trpc5 deficient mice should be affected and needs to be analyzed. For this reason, my study will continue to focus on the effects of Trpc5 mutation on reproductive function.

4.2 Loss of Trpc5 affects reproductive function in mice: Hormonal imbalance, hypoprolactinemia and subfertility

A new concept has emerged whereby Trp channels could be involved in regulating homeostatic physiological functions, including reproduction. The canonical Trp channel 5 – Trpc5 – is highly expressed in the hypothalamus (Fowler et al., 2007; Kelly et al., 2018). Thus, I aimed to determine whether Trpc5 channels are involved in the regulation of the reproductive axis. In my first objective, I examined whether the absence of Trpc channels – in particular Trpc5 – could influence the reproductive outcome of a pregnancy by analyzing the reproductive capability of wildtype versus Trpc5-deficient mice and assessing any hormonal imbalance induced by the loss of Trpc5. In particular, I determined the levels of prolactin, lutenizing hormone and follicle-stimulating hormone, which would provide information regarding the functionality of both major reproductive axes (HPG axis and lactotroph axis).

4.2.1 Loss of members of Trpc1/4/5 subfamily reduce fertility in mice

In order to determine whether mice having a loss in Trpc channels have any reproductive deficit, I first analyzed the breeding capability of global Trpc1$^{-/-}$, Trpc4$^{-/-}$, Trpc5$^{L3F1/L3F1}$, Trpc1/5$^{-/-}$ and Trpc4/5$^{-/-}$ double knockouts, and Trpc1/4/5$^{-/-}$ triple knockouts. The data of the breedings of Trpc1$^{-/-}$, Trpc4$^{-/-}$, Trpc1/5$^{-/-}$, Trpc4/5$^{-/-}$ and Trpc1/4/5$^{-/-}$ mice were kindly provided by Dr. P. Weissgerber and Prof. Dr. V. Flockerzi. Reproductive parameters were analyzed using genotype-matched breeding pairs of at least seven weeks of age, to ensure the chance to reproduce. Mated pairs were evaluated over a ten-week period.

Trpc1$^{-/-}$ and Trpc5$^{L3F1/L3F1}$ single mutants were found to have significantly reduced mating success (Fig. 9 A), i.e. 29 % (Trpc1$^{-/-}$) and 43 % (Trpc5$^{L3F1/L3F1}$) of the mated pairs did not produce offspring in the whole 70-day period. Trpc4 shows a tendency towards reduced mating success but failed to reach the significance level. In contrast to these findings, multiple deletions of Trpc1/4/5 subfamily members did not seem to have an influence on mating possibility, as is the case with single mutants. When checking for the time period between the beginning of the breeding and birth of the first litter, our wildtype controls gave birth during a time window of 25-31 days (Fig 9 B), which we would expect as pregnancies in mice take approximately 18-21 days, dependent on the strain (Murray et al., 2010). Both Trpc1$^{-/-}$ and Trpc5$^{L3F1/L3F1}$ matings displayed an increased delay of the first litter, giving birth roughly 20 days later than wildtype controls. The interval between litters was prolonged in all tested mutant mouse models compared with control animals (Fig. 9 C). This finding is in agreement with the reduced number of litters born during the test period (Fig. 9 D). Whereas

control mice gave birth to 2-3 litters, Trpc mutants in most cases produced only one litter. To complicate this reproductive deficit, Trpc5$^{L3F1/L3F1}$ mating pairs were significantly reduced in litter size (Fig. 9 E), with about 50% fewer pups born. As a measure to evaluate the reproductive potential, the relative fecundity was calculated as the product of number of litters, litter size and productive matings (Fig. 9 F). Using this measure, the analyzed single mutants display the highest reproductive limitation, whereas control mice and matings with multiple mutations reach relative fecundity values similar to those already published for the background mouse strain C57Bl/6N (Wood et al., 2009). The reproductive impairment of a mutation of Trpc5^{L3F1} shows a low fecundity value almost eight-fold lower than wildtype matings of the background strain. Strikingly reproductive deficits are absent when more than one Trpc channel is knocked out.

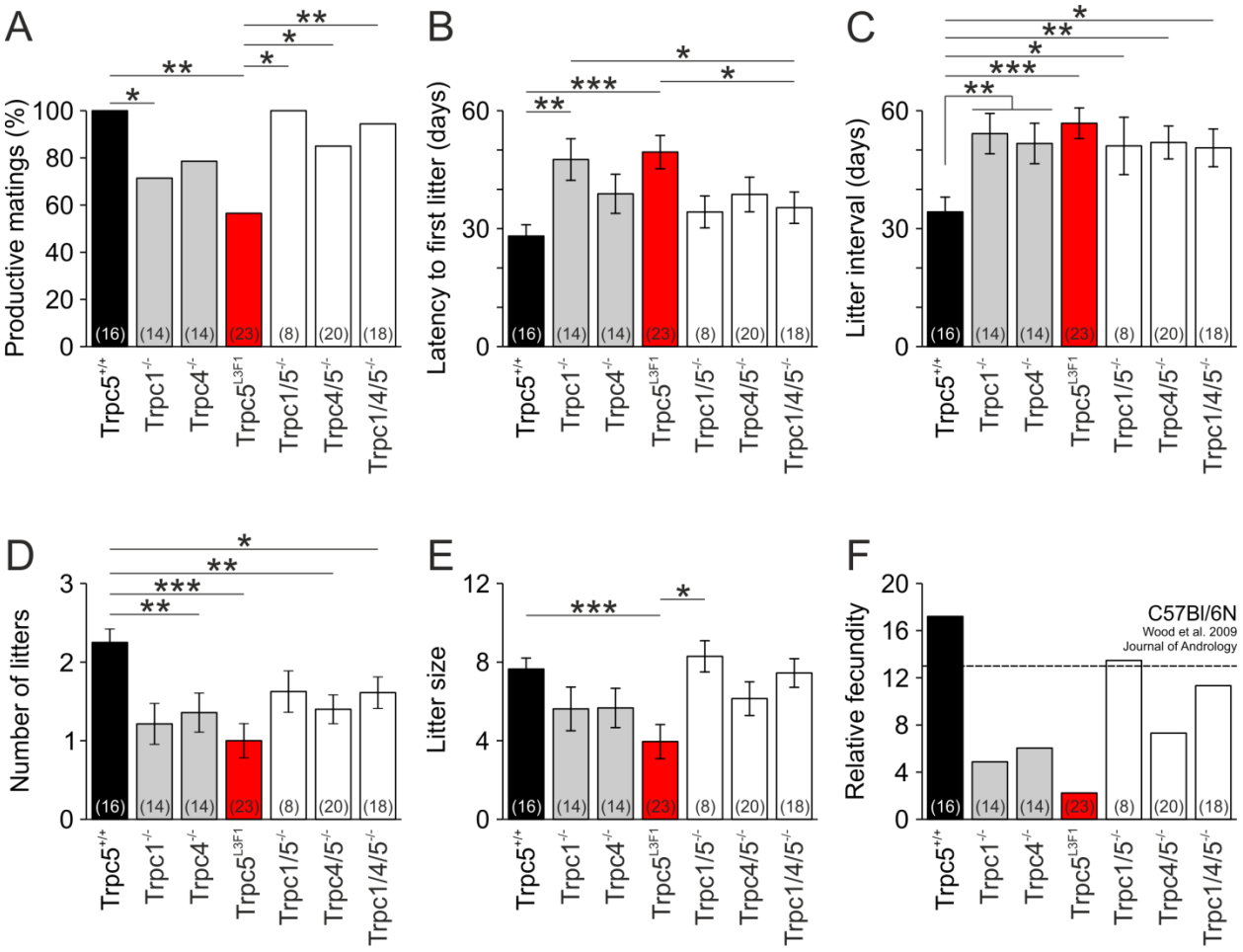

Figure 9: Reduced fertility in mice lacking members of the Trpc1/4/5 subfamily.
Sexually mature (8-15 weeks) old mice were kept in single mating pairs over a ten-week test period. (A) Loss of Trpc1 or Trpc5 causes diminished percentage of successful breeding pairs compared with $Trpc5^{+/+}$ controls, but the loss of two or even all three members did not. Productive mating: $Trpc5^{+/+}$ 16/16; $Trpc1^{-/-}$ 10/14; $Trpc4^{-/-}$ 11/14; $Trpc5^{L3F1}$ 13/23; $Trpc1/5^{-/-}$ 8/8; $Trpc4/5^{-/-}$ 17/20; $Trpc1/4/5^{-/-}$ 17/18; Chi-square = 4.11 – 9.36; * $p < 0.05$, ** $p < 0.01$. (B) Deficiency of Trpc1 and Trpc5 increase the duration until the first pregnancy. $Trpc5^{+/+}$ 28.1 ± 2.9 days; $Trpc1^{-/-}$ 47.6 ± 5.3 days; $Trpc4^{-/-}$ 38.9 ± 5.0 days; $Trpc5^{L3F1}$ 49.5 ± 4.2 days; $Trpc1/5^{-/-}$ 34.3 ± 4.1 days; $Trpc4/5^{-/-}$ 38.7 ± 4.4 days; $Trpc1/4/5^{-/-}$ 35.3 ± 4.0 days; Kruskal-Wallis ANOVA: Chi-square = 16.83, $p < 0.01$; Mann-Whitney * $p < 0.05$, ** $p < 0.01$, *** $p < 0.001$. (C) Any alteration of Trpc1/4/5 subfamily members increases the litter interval. $Trpc5^{+/+}$ 34.3 ± 3.8 days; $Trpc1^{-/-}$ 54.2 ± 5.1 days; $Trpc4^{-/-}$ 51.7 ± 5.1 days; $Trpc5^{L3F1}$ 56.8 ± 3.9 days; $Trpc1/5^{-/-}$ 51.0 ± 7.3 days; $Trpc4/5^{-/-}$ 51.9 ± 4.2 days; $Trpc1/4/5^{-/-}$ 50.6 ± 4.8 days; Kruskal-Wallis ANOVA: Chi-square = 15.59, $p < 0.05$; Mann-Whitney * $p < 0.05$, ** $p < 0.01$, *** $p < 0.001$. (D-E) Number of litters (D) and litter size (E) are reduced when lacking Trpc5 and/or Trpc4. D: $Trpc5^{+/+}$ 2.3 ± 0.2; $Trpc1^{-/-}$ 1.2 ± 0.3; $Trpc4^{-/-}$ 1.4 ± 0.2; $Trpc5^{L3F1}$ 1.0 ± 0.2; $Trpc1/5^{-/-}$ 1.6 ± 0.3; $Trpc4/5^{-/-}$ 1.4 ± 0.2; $Trpc1/4/5^{-/-}$ 1.6 ± 0.2; Kruskal-Wallis ANOVA: Chi-square = 17.66, $p < 0.01$; Mann-Whitney * $p < 0.05$, ** $p < 0.01$, *** $p < 0.001$. E: $Trpc5^{+/+}$ 7.6 ± 0.6; $Trpc1^{-/-}$ 5.6 ± 1.1; $Trpc4^{-/-}$ 5.7 ± 1.0; $Trpc5^{L3F1}$ 4.0 ± 0.9; $Trpc1/5^{-/-}$ 8.3 ± 0.8; $Trpc4/5^{-/-}$ 6.1 ± 0.9; $Trpc1/4/5^{-/-}$ 7.4 ± 0.7; Kruskal-Wallis ANOVA: Chi-square = 13.53, $p < 0.05$; Mann-Whitney * $p < 0.05$, *** $p < 0.001$. (F) Relative fecundity, as a measure for reproductive capability, is heavily reduced in Trpc1, Trpc4, Trpc5 single mutants. Relative fecundity = (productive matings) x (litter size) x (number of litters). Dashed line indicates relative fecundity levels for the background mouse strain C57Bl/6N (Wood et al., 2009). $Trpc5^{+/+}$ 17.2; $Trpc1^{-/-}$ 4.9; $Trpc4^{-/-}$ 6.0; $Trpc5^{L3F1}$ 2.2; $Trpc1/5^{-/-}$ 13.5; $Trpc4/5^{-/-}$ 7.3; $Trpc1/4/5^{-/-}$ 11.3. The numbers indicate the number of mated pairs.

4.2.2 Trpc5 deletion shows the highest impact on fertility

The lowest capability of reproduction was found to be in the $Trpc5^{L3F1/L3F1}$ mouse line. From this mutant mouse line, a global knockout was derived, namely the Trpc5-$E4^{-/-}$ mouse line. $Trpc5^{L3F1/L3F1}$ mice carry a construct containing a *loxP*-flanked Exon 4 of the *Trpc5* gene, a splice acceptor (SA)-IRES-GFP cassette, a FRT sequence, and a third *loxP* site. The Trpc5-$E4^{-/-}$ mouse line was generated in Marc Freichels and Veit Flockerzis labs by crossbreeding $Trpc5^{L3F1/L3F1}$ mice with a CMV-Cre delete mouse strain, resulting in a deletion of Exon 4 (Xue et al., 2011). In order to confirm the reproductive phenotype of the $Trpc5^{L3F1/L3F1}$ mouse line, I used the aforementioned Trpc5-$E4^{-/-}$ and an additional global mutant, lacking Exon 5 (Phelan et al., 2013), Trpc5-$E5^{-/-}$). We found that the decrease in productive matings is persistently reduced in all Trpc5 mutations (Fig. 10 A). The pronounced delay to the first litter is present only in the hypomorphic mutation $Trpc5^{L3F1}$. The global knockout strains failed to reach significant delays (Fig. 10 B). Global removal of Trpc5 consistently increased the litter interval like the $Trpc5^{L3F1}$ mutation (Fig. 10 C). Furthermore, the global knockout mice comparably decreased in terms of both the number of litters (Fig. 10 D) and the litter size (Fig. 10 E), as already described for the $Trpc5^{L3F1}$ mutation. Relative fecundity values of Trpc5 mutant mouse lines show a four- to eight-fold decrease (Fig. 10 F). This emphasizes the importance of Trpc5 for proper reproductive function.

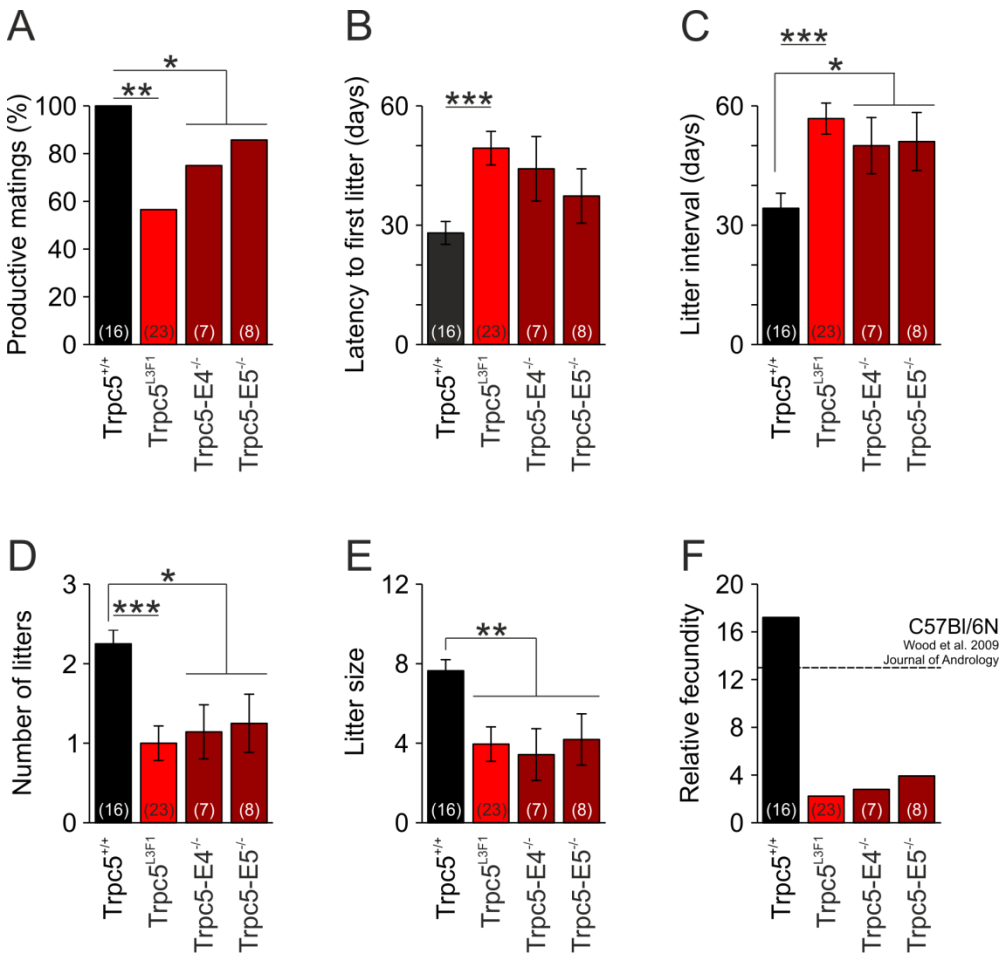

Figure 10: Mutant mice lacking Trpc5 show a forceful defect in their fertileness.
Sexually mature (8-15 weeks) old mice were kept in single mating pairs over a ten-week test period. (A) Loss of Trpc5 decreases the chance of a productive mating. $Trpc5^{+/+}$ 16/16, $Trpc5^{L3F1}$ 13/23, $Trpc5\text{-}E4^{-/-}$ 5/7, $Trpc5\text{-}E5^{-/-}$ 6/8. Chi-square = 4.36 – 9.36; * $p < 0.05$, ** $p < 0.01$. (B) Only the L3F1 mutation of Trpc5 increases the delay to the first litter. $Trpc5^{+/+}$ 28.2 ± 2.9 days, $Trpc5^{L3F1}$ 49.5 ± 4.2 days, $Trpc5\text{-}E4^{-/-}$ 44.3 ± 8.1 days, $Trpc5\text{-}E5^{-/-}$ 41.5 ± 7.2 days; Kruskal-Wallis ANOVA: Chi-square = 11.61, $p < 0.01$; Mann-Whitney *** $p < 0.001$. (C) Pregnancy intervals are prolonged if Trpc5 is mutated. $Trpc5^{+/+}$ 34.3 ± 3.8 days, $Trpc5^{L3F1}$ 56.8 ± 3.9 days, $Trpc5\text{-}E4^{-/-}$ 50.0 ± 7.1 days, $Trpc5\text{-}E5^{-/-}$ 51.0 ± 7.3 days; Kruskal-Wallis ANOVA: Chi-square = 13.17, $p < 0.01$; Mann-Whitney * $p < 0.05$, *** $p < 0.001$. (D-E) Loss of Trpc5 heavily decreases the number of offspring by decreasing the number of litters (D) and the litter size (E). D: $Trpc5^{+/+}$ 2.3 ± 0.2, $Trpc5^{L3F1}$ 1.0 ± 0.2, $Trpc5\text{-}E4^{-/-}$ 1.1 ± 0.3, $Trpc5\text{-}E5^{-/-}$ 1.3 ± 0.4; Kruskal-Wallis ANOVA: Chi-square = 14.20, $p < 0.01$; Mann-Whitney * $p < 0.05$, *** $p < 0.001$. E: $Trpc5^{+/+}$ 7.6 ± 0.6, $Trpc5^{L3F1}$ 4.0 ± 0.9, $Trpc5\text{-}E4^{-/-}$ 3.4 ± 1.3, $Trpc5\text{-}E5^{-/-}$ 4.2 ± 1.3; Kruskal-Wallis ANOVA: Chi-square = 11.06, $p < 0.05$; Mann-Whitney ** $p < 0.01$. (F) Loss of Trpc5 strongly reduces the relative fecundity. Relative fecundity = (productive matings) x (litter size) x (number of litters). Dashed line indicates relative fecundity levels for the background mouse strain C57Bl/6N (Wood et al., 2009). $Trpc5^{+/+}$ 17.2, $Trpc5^{L3F1}$ 2.2, $Trpc5\text{-}E4^{-/-}$ 2.8, $Trpc5\text{-}E5^{-/-}$ 3.9. The numbers indicate the number of mated pairs.+

4.2.3 Subfertility of Trpc5-deficient mice is most striking in forced matings of homozygote mutant mates

In order to narrow down the cause of the Trpc5-dependent subfertility to the mutation being present in the female or the male mouse, mating pairs were assembled in all possible genetic combinations of mice carrying the $Trpc5^{L3F1}$ mutation. Comparing parameters regarding mating productivity, the subfertility was most prominent only in the homozygous breeding pair (Fig. 11 A).

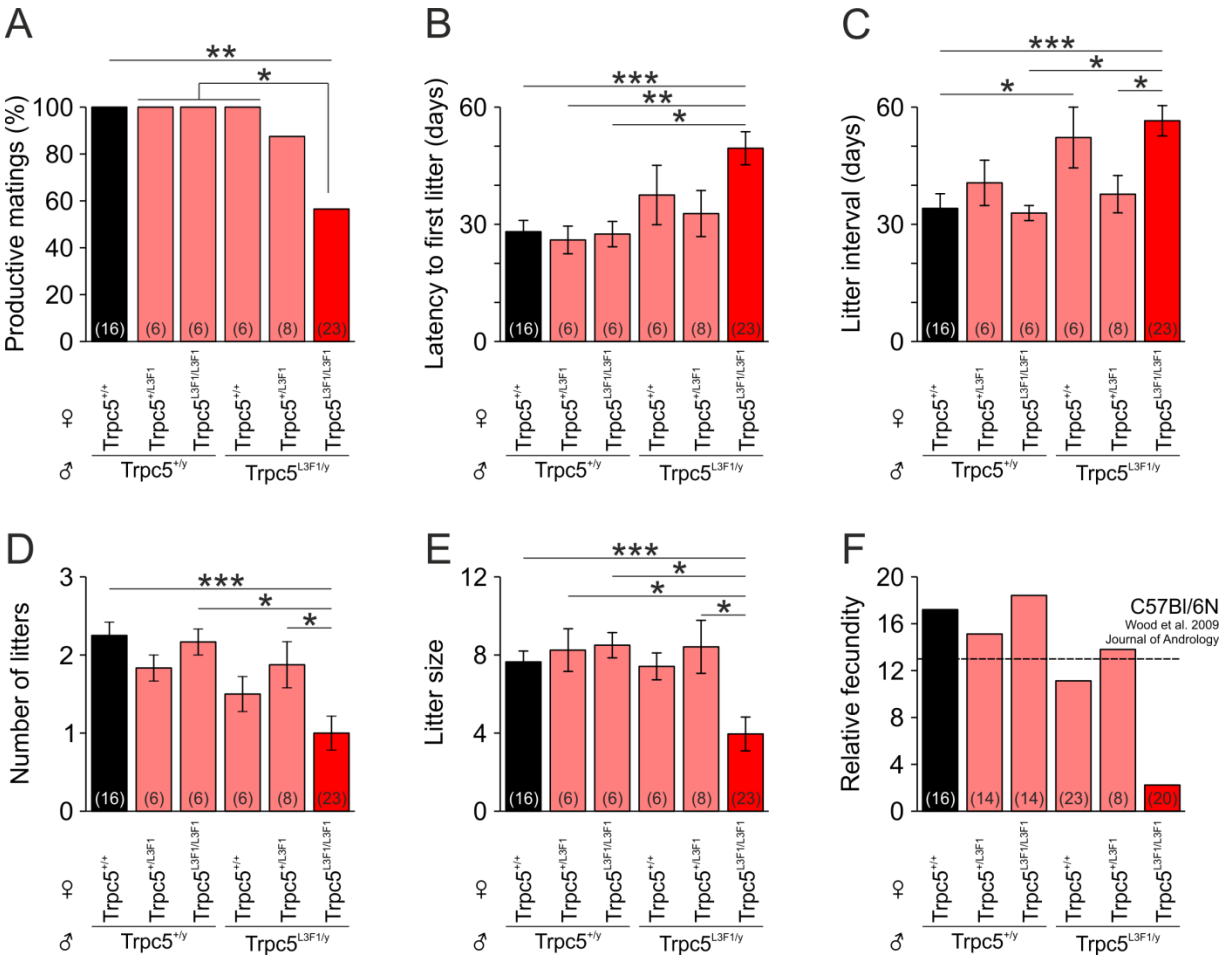

Figure 11: Inhomogeneous breeding pairs overcome the reproductive defects caused by loss of Trpc5. Sexually mature (8-15 weeks) old mice were kept in single mating pairs over a ten-week test period. (A) Varied breeding pairs of wildtype, heterozygous and homozygous Trpc5 mutants do not influence the chance of a productive mating as seen in mutant-mutant breedings. $Trpc5^{+/y}$|$Trpc5^{+/+}$ 16/16, $Trpc5^{+/y}$|$Trpc5^{+/L3F1}$ 6/6, $Trpc5^{+/y}$|$Trpc5^{L3F1/L3F1}$ 6/6, $Trpc5^{L3F1/y}$|$Trpc5^{+/+}$ 6/6, $Trpc5^{L3F1/y}$|$Trpc5^{+/L3F1}$ 7/8, $Trpc5^{L3F1/y}$|$Trpc5^{L3F1/L3F1}$ 13/23. Chi-square = 3.99 – 9.36; * $p < 0.05$, ** $p < 0.01$. (B) Only the breeding of both mutant male and homozygous mutant female increases the delay to the first litter. $Trpc5^{+/y}$|$Trpc5^{+/+}$ 28.1 ± 2.9 days, $Trpc5^{+/y}$|$Trpc5^{+/L3F1}$ 26.0 ± 3.5 days, $Trpc5^{+/y}$|$Trpc5^{L3F1/L3F1}$ 27.5 ± 3.3 days, $Trpc5^{L3F1/y}$|$Trpc5^{+/+}$ 37.5 ± 7.6 days, $Trpc5^{L3F1/y}$|$Trpc5^{+/L3F1}$ 32.8 ± 5.9 days, $Trpc5^{L3F1/y}$|$Trpc5^{L3F1/L3F1}$ 49.5 ± 4.2 days; Kruskal-Wallis ANOVA: Chi-square = 17.11, $p < 0.01$; Mann-Whitney * $p < 0.05$, ** $p < 0.01$, *** $p < 0.001$. (C) Pregnancy intervals are mainly prolonged if Trpc5 is lost in both male and female. $Trpc5^{+/y}$|$Trpc5^{+/+}$ 34.3 ± 3.8 days, $Trpc5^{+/y}$| $Trpc5^{+/L3F1}$ 40.8 ± 5.8 days, $Trpc5^{+/y}$|$Trpc5^{L3F1/L3F1}$ 33.1 ± 1.9 days, $Trpc5^{L3F1/y}$|$Trpc5^{+/+}$ 52.5 ± 7.8 days, $Trpc5^{L3F1/y}$|$Trpc5^{+/L3F1}$ 37.9 ± 4.8 days, $Trpc5^{L3F1/y}$|$Trpc5^{L3F1/L3F1}$ 56.8 ± 3.9 days; Kruskal-Wallis ANOVA: Chi-square = 18.66, $p < 0.01$; Mann-Whitney * $p < 0.05$, *** $p < 0.001$. (D-E) The number of litters (D) and the litter size (E) are only decreased when both genders have lost Trpc5. D: $Trpc5^{+/y}$|$Trpc5^{+/+}$ 2.3 ± 0.2, $Trpc5^{+/y}$|$Trpc5^{+/L3F1}$ 1.8 ± 0.2, $Trpc5^{+/y}$|$Trpc5^{L3F1/L3F1}$ 2.2 ± 0.2, $Trpc5^{L3F1/y}$|$Trpc5^{+/+}$ 1.5 ± 0.2, $Trpc5^{L3F1/y}$|$Trpc5^{+/L3F1}$ 1.9 ± 0.3, $Trpc5^{L3F1/y}$| $Trpc5^{L3F1/L3F1}$ 1.0 ± 0.2; Kruskal-Wallis ANOVA: Chi-square = 19.16, $p < 0.01$; Mann-Whitney * $p < 0.05$, *** $p < 0.001$. E: $Trpc5^{+/y}$|$Trpc5^{+/+}$ 7.6 ± 0.6, $Trpc5^{+/y}$|$Trpc5^{+/L3F1}$ 8.3 ± 1.1, $Trpc5^{+/y}$|$Trpc5^{L3F1/L3F1}$ 8.5 ± 0.6, $Trpc5^{L3F1/y}$|$Trpc5^{+/+}$ 7.4 ± 0.7, $Trpc5^{L3F1/y}$|$Trpc5^{+/L3F1}$ 8.4 ± 1.4, $Trpc5^{L3F1/y}$|$Trpc5^{L3F1/L3F1}$ 4.0 ± 0.9; Kruskal-Wallis ANOVA: Chi-square = 14.77, $p < 0.05$; Mann-Whitney * $p < 0.05$, *** $p < 0.0001$. (F) Loss of Trpc5 in both genders strongly reduces the relative fecundity, but not in mixed breedings. Relative fecundity = (productive matings) x (litter size) x (number of litters). Dashed line indicates relative fecundity levels for the background mouse strain C57Bl/6N (Wood et al., 2009). $Trpc5^{+/y}$|$Trpc5^{+/+}$ 17.2, $Trpc5^{+/y}$|$Trpc5^{+/L3F1}$ 15.1, $Trpc5^{+/y}$|$Trpc5^{L3F1/L3F1}$ 18.4, $Trpc5^{L3F1/y}$|$Trpc5^{+/+}$ 11.1, $Trpc5^{L3F1/y}$|$Trpc5^{+/L3F1}$ 13.8, $Trpc5^{L3F1/y}$|$Trpc5^{L3F1/L3F1}$ 2.2. The numbers indicate the number of mated pairs.

Any combination of mating pairs failed to reproduce the subfertility phenotype observed in breedings of Trpc5 deficient and/or mutant mates, as shown by the unaltered latency to the first litter (Fig. 11 B), unchanged litter interval (Fig. 11 C) and the unaffected number of litters (Fig. 11 D) and litter size (Fig. 11 E). Only $Trpc5^{L3F1}$ matings – deficient in both male and – show the pronounced eight-fold decrease in their relative fecundity (Fig. 11F). The Trpc5-deficient breeding pairs can be fertile but apparently 50% of the matings fail to become pregnant and do not produce any offspring, indicating that the combination of subfertility of female and male $Trpc5^{L3F1}$-deficient mice leads to a critical deficiency in reproductive capability. The results fit with a defect in nidation causing a delay in becoming pregnant and a reduced number of offspring. Nonetheless, the $Trpc5^{L3F1}$ homozygote mice avoid the fecundity phenotype when paired with mice with at least one allele being wildtype. At this moment, it is unclear why I do not observe a more severe deficit in the mixed breedings, aside from the notion that paired housing having olfactory cues and cervical stimulation may reduce a reproductive deficit in mice. Olfactory cues from a mate can reduce dopamine levels in the arcuate nucleus, thereby increasing prolactin levels and assisting the lactotroph axis in maintaining a pregnancy (Rosser et al., 1989; Matthews et al., 2013). Cervical stimulation is also able to induce prolactin surges benefiting pregnancy maintenance (Freeman et al., 2000; McKee et al., 2007; Helena et al., 2009; Helena et al., 2011). This allows the presumption that there is a summation of reproductive phenotypes that only emerge as a reproductive deficit when they coincide. Therefore, further analysis of the gender-specific restriction of their reproductive capabilities was necessary.

4.2.4 Trpc5-deficient virgin females show oligoovulation and prolonged estrous cycle length

In order to determine the consequence of a Trpc5 deletion on female reproductive performance, I evaluated the regularity of the reproductive cycle and the duration of the reproductive stages in female mice. We assessed the reproductive function in 7-12 week-old Trpc5 deficient virgin females. As a first guideline, we evaluated the regularity and the duration of the four phases of the reproductive (estrous) cycle (Fig. 12), i.e. metestrus (M), diestrus (D), proestrus (P) and estrus (E). $Trpc5^{+/+}$ mice displayed a regular estrous cycle length of 5.4 ± 0.3 days (Fig 12 A, black trace). By contrast, virgin females lacking Trpc5 had significantly prolonged cycles (Fig 12 A, red trace; Fig 12 B). Upon loss of Trpc5, estrous cycle length increased by 20-73 % ($Trpc5^{L3F1/L3F1}$ 6.5 ± 0.3 days, Trpc5-$E4^{-/-}$ 8.5 ± 1.0 days, Trpc5-$E5^{-/-}$ 9.7 ± 1.0 days). This prolongation appeared with an increased time spent in diestrus (2-4 days in $Trpc5^{+/+}$, 2-8 days in $Trpc5^{L3F1/L3F1}$) and a reduction of estrus events (Fig. 12 C). These phenotypes indicate an oligo-ovulatory phenotype in Trpc5-deficient virgin females.

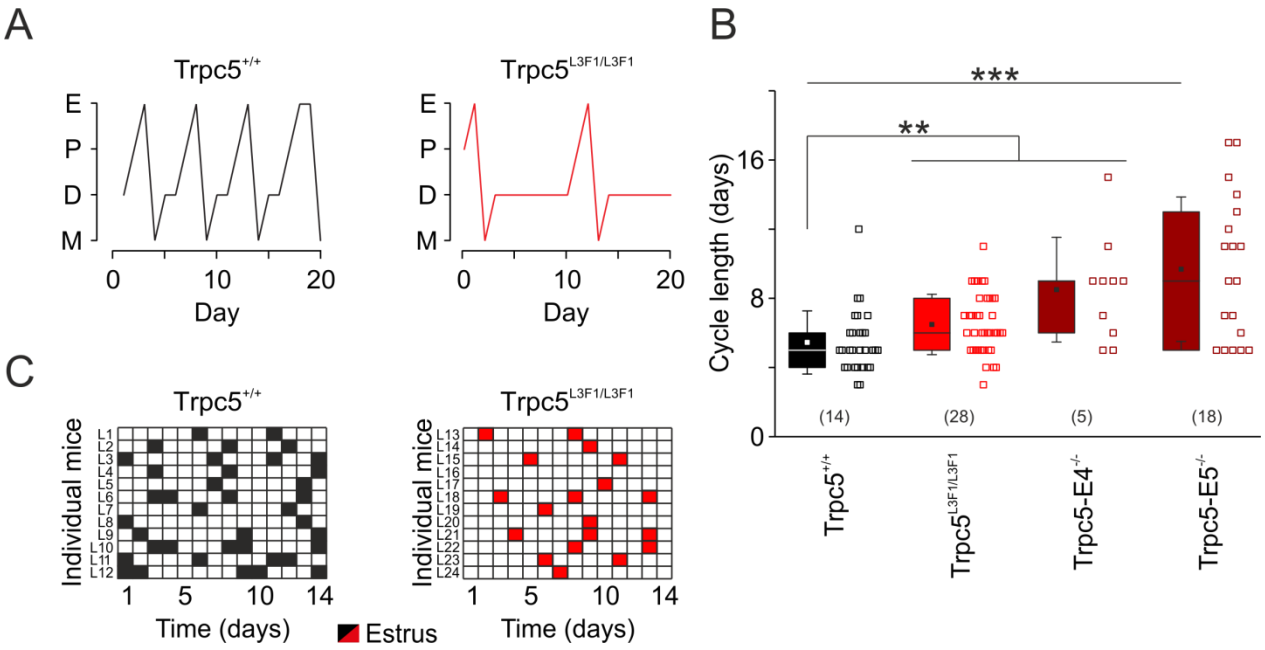

Figure 12: Prolonged estrous cycle and oligoovulation due to lack of Trpc5.
(A) Exemplary traces of the reproductive cycle from 7-12 weeks old virgin (sexually naïve) female mice. Reproductive cycle stages were evaluated by vaginal cytology on a daily basis. Trpc5$^{L3F1/L3F1}$ females display an altered estrous cycle with increased occurrence of diestrus (M, metestrus; D, diestrus; P, proestrus; E, estrus). (B) Estrous cycle length is expanded upon loss of Trpc5. Trpc5$^{+/+}$ 5.4 ± 0.3 days; Trpc5$^{L3F1/L3F1}$ 6.5 ± 0.3 days; Trpc5-E4$^{-/-}$ 8.5 ± 1.0 days; Trpc5-E5$^{-/-}$ 9.7 ± 1.0 days; Kruskal-Wallis ANOVA: Chi-Square = 27.4, $p < 0.001$; Mann-Whitney ** $p < 0.01$, *** $p < 0.001$. Box plots present interquartile ranges, median (line), and mean (squares) with whiskers indicating SD values. Squares alongside a box indicate given estrous cycle lengths. The number of mice is indicated below the boxes. (C) Checkerboard plots presenting daily evaluations of the estrous cycle stage in individual Trpc5$^{+/+}$ (black) and Trpc5$^{L3F1/L3F1}$ (red) females. The occurrence of estrus is indicated with filled squares. Trpc5$^{L3F1/L3F1}$ females exhibit less days of estrus and thus ovulation (oligoovulation).

4.2.5 Loss of Trpc5 promotes hypoprolactinemia

Extended luteal phases (metestrus and diestrus) – as found in Trpc5 deficient females – can indicate altered hormonal levels, especially indicate changes in prolactin levels. Prolonged diestrus is usually associated with hyperprolactinemia (Hansen et al., 1983). I thus examined serum prolactin levels next to other pituitary hormones in more than 60 individual mice. The other pituitary hormones investigated were LH and FSH, which are important to detect various reproductive dysfunctions (McVeigh et al., 2013), and ACTH to examine any involvement of stress. The hypothalamus-pituitary-adrenal (HPA) axis is a known factor to modify the reproductive cycle (Vermeulen, 1993; Chrousos et al., 1998; McVeigh et al., 2013; Oyola and Handa, 2017). In order to exclude the involvement of the HPA axis upon reproductive hormone levels, I also analyzed serum ACTH to estimate stress load. ACTH levels in Trpc5-deficient mice did not exceed wildtype amounts of 16.5 ± 7.5 pg/ml (mean ± SD, n = 85, 15 mice; Trpc5$^{L3F1/L3F1}$: 12.1 ± 8.6 pg/ml, n = 72, 28 mice; Trpc5-E4$^{-/-}$: 10.4 ± 5.5 pg/ml, n = 23, 5 mice; Trpc5-E5$^{-/-}$: 13.8 ± 6.8 pg/ml, n = 35, 18 mice).

My results indicate a severe hypoprolactinemia (Fig. 13 A). Prolactin levels are reduced by 42-75 % ($Trpc5^{L3F1/L3F1}$ 51 %, Trpc5-$E4^{-/-}$ 42 %, Trpc5-$E5^{-/-}$ 75 %) compared with $Trpc5^{+/+}$ females. As prolactin levels oscillate during the estrous cycle – rising to a peak in the later phase of proestrus – I also analyzed serum prolactin levels in dependence of the estrous cycle in the Trpc5-deficient females of the $Trpc5^{L3F1}$ strain (Fig. 13 B). Serum prolactin levels of $Trpc5^{+/+}$ females increased regularly during the proestrus (P) stage. Similarly, $Trpc5^{L3F1/L3F1}$ females produce prolactin peaks prior to ovulation. However, prolactin levels in these females were markedly reduced in all stages of the reproductive cycle (Fig. 13 C), indicating that estrous cycle-dependent increases of prolactin are independent of Trpc5 deficiency, whereas prolactin levels strongly depend on Trpc5. If the virgin females have a severe hypoprolactinemia, are the litters of lactating females affected? Prolactin regulates a huge set of functions in the body and plays an important role in both maternal behavior and lactation (Grattan, 2001; Grattan and Le Tissier, 2015). From my data regarding the reproductive capability of these mice, it appears that pup survival is strongly impaired in $Trpc5^{L3F1/L3F1}$ mice (Fig. 14). The other Trpc5-deficient females show also reduced pup survival rates. Thus, hypoprolactinemia caused by a loss of Trpc5 strongly affects prolactin homeostasis not only in cycling but also in pregnant/lactating females, thus presumably impairing pup care and nutrition.

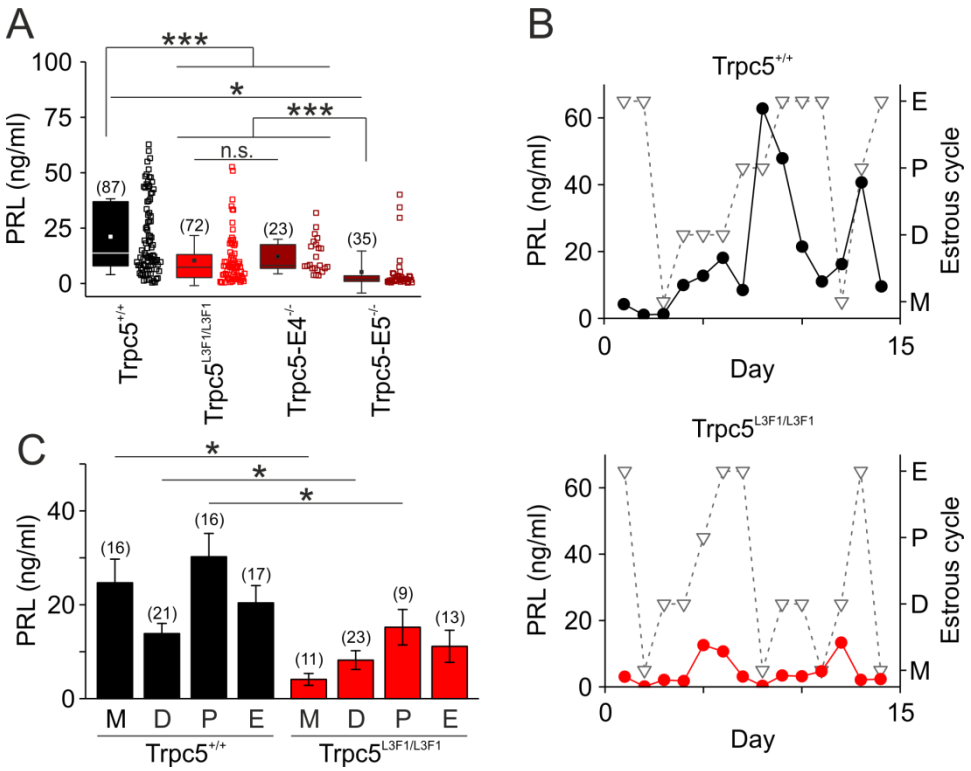

Figure 13: Hypoprolactinemia in Trpc5 deficient mice.
(A) Serum prolactin levels are lowered in naïve female mice lacking Trpc5. $Trpc5^{+/+}$ 21.1 ± 1.8 ng/ml; $Trpc5^{L3F1/L3F1}$ 10.4 ± 1.3 ng/ml; Trpc5-$E4^{-/-}$ 12.2 ± 1.6 ng/ml; Trpc5-$E5^{-/-}$ 5.2 ± 1.6 ng/ml; Kruskal-Wallis ANOVA: Chi-Square = 21.1, $p < 0.001$; Mann-Whitney * $p < 0.05$, *** $p < 0.001$, n.s. $p > 0.08$. Box plots present interquartile ranges, median (line), and mean (squares) with whiskers indicating SD values. Squares alongside a box indicate given estrous cycle lengths. The number of independent measurements from at least five mice per genotype is indicated above each box plot. (B and C) Daily analysis of prolactin levels in individual female mice during their estrous cycle. The exemplary females (B) and the mean values (C) indicate that the prolactin kinetics during the cycle remain in $Trpc5^{L3F1/L3F1}$ females, but overall levels of prolactin are reduced. $Trpc5^{+/+}$: M, PRL = 24.7 ± 5.0 ng/ml; D, PRL = 13.9 ± 2.2 ng/ml; P, PRL = 30.2 ± 5.0 ng/ml; E, PRL = 20.4 ± 3.7 ng/ml; $Trpc5^{L3F1/L3F1}$: M, PRL = 4.1 ± 1.3 ng/ml; D, PRL = 8.2 ± 2.0 ng/ml; P, PRL = 15.2 ± 3.8 ng/ml; E, PRL = 11.1 ± 3.4 ng/ml; Kruskal-Wallis ANOVA: Chi-Square = 29.12; $p < 0.001$; Mann-Whitney * $p < 0.05$. The number of independent measurements is indicated above each bar. At least five mice per genotype were used.

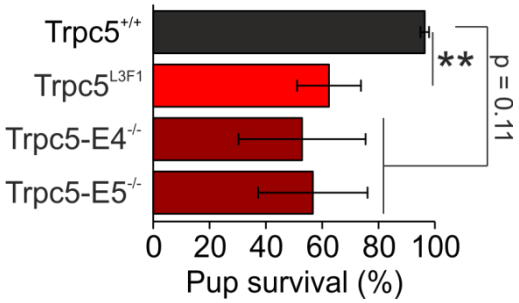

Figure 14: Pup survival is decreased in Trpc5 mutant mating pairs.
In the three week time period between birth and weaning, pups of Trpc5 deficient breeding pairs have a lower probability of survival. $Trpc5^{+/+}$ 96.4 ± 1.5, $Trpc5^{L3F1}$ 62.4 ± 11.3, Trpc5-$E4^{-/-}$ 52.9 ± 22.5, Trpc5-$E5^{-/-}$ 56.7 ±19.4; Kruskal-Wallis ANOVA: Chi-Square 7.86, $p < 0.05$; Mann-Whitney ** $p < 0.01$.

4.2.6 Trpc5 deficiency unbalances the HPG axis

Reproductive deficits can be caused by alterations of the “classical” reproductive axis (HPG axis). We analyzed serum levels of both gonadotropins FSH and LH. Serum FSH was significantly decreased in the Trpc5$^{L3F1/L3F1}$ mutant but not in the global knockouts Trpc5-E4$^{-/-}$ or Trpc5-E5$^{-/-}$ (Fig. 15 A). FSH oscillations during the reproductive cycle seem to be present in both genotypes (Fig. 15 C), although in lower amplitudes. This becomes more pronounced in a cycle stage-dependent analysis (Fig. 15 E). Serum FSH levels are decreased in Trpc5$^{L3F1/L3F1}$ females in the luteal phase and prior to ovulation. Reduced ovulatory events – as previously described – did not concur with changed LH levels (Fig. 15 B). Both Trpc5$^{+/+}$ and Trpc5$^{L3F1/L3F1}$ females showed LH surges (Fig. 15 D). Some of the LH surges seem to be missing due to the very narrow time window in which the surge occurs. Some Trpc5$^{L3F1/L3F1}$ female exhibited LH surges during the estrus phase, although in an analysis of multiple females’ serum, LH levels did not significantly alter (Fig. 15 F). Consequently, Trpc5-deficiency does not affect ovulation itself, but rather only the inter-ovulatory interval between different stages of estrus. Reduced serum levels of FSH could affect the recruitment and growth of ovarian follicles, resulting in changed numbers of follicles and thereby affecting litter size.

Figure 15: The HPG axis is unbalanced by mutation of Trpc5.
(A and B) Serum FSH (A) levels are lowered in sexually naïve female Trpc5$^{L3F1/L3F1}$ mice whereas LH (B) seems to be unchanged. A: Trpc5$^{+/+}$ 0.58 ± 0.03 ng/ml, Trpc5$^{L3F1/L3F1}$ 0.39 ± 0.03 ng/ml, Trpc5-E4$^{-/-}$ 0.91 ± 0.18, Trpc5-E5$^{-/-}$ 0.87 ± 0.26 ng/ml; Kruskal-Wallis ANOVA: Chi-Square = 6.05, $p < 0.05$; Mann-Whitney * $p < 0.05$, *** $p < 0.001$. B: Trpc5$^{+/+}$ 0.64 ± 0.33 ng/ml, Trpc5$^{L3F1/L3F1}$ 2.17 ± 0.84 ng/ml; Mann-Whitney n.s. $p > 0.48$. Box plots present interquartile ranges, median (line), and mean (squares) with whiskers indicating SD values. Squares alongside a box indicate given estrous cycle lengths. The number of independent measurements from at least five mice per genotype is indicated above each box plot. (C and D) Individual time courses of FSH (C) and LH (D) compared with the estrous cycle stage in both Trpc5$^{+/+}$ (black) and Trpc5$^{L3F1/L3F1}$ (red). (E and F) Data set comparing the entirety of mice tested for serum FSH (E) and LH (F) in Trpc5$^{+/+}$ and Trpc5$^{L3F1/L3F1}$ in dependence on their estrous cycle. FSH is decreased in the luteal phase in Trpc5$^{L3F1/L3F1}$ virgin females. E: Trpc5$^{+/+}$: M, FSH = 0.56 ± 0.05 ng/ml; D, FSH = 0.54 ± 0.04 ng/ml; P, FSH = 0.75 ± 0.10 ng/ml; E, FSH = 0.69 ± 0.10 ng/ml; Trpc5$^{L3F1/L3F1}$: M, FSH = 0.32 ± 0.03 ng/ml; D, FSH = 0.32 ± 0.03 ng/ml; P, FSH = 0.42 ± 0.09 ng/ml; E, FSH = 0.60 ± 0.08 ng/ml; Kruskal-Wallis ANOVA: Chi-Square = 36.39; $p < 0.001$; Mann-Whitney * $p < 0.05$ *** $p < 0.001$. F: Trpc5$^{+/+}$: M, LH = 0.30 ± 0.04 ng/ml; D, LH = 0.31 ± 0.03 ng/ml; P, LH = 1.84 ± 1.46 ng/ml; E, LH = 0,26 ± 0.02 ng/ml; Trpc5$^{L3F1/L3F1}$: M, LH = 0.22 ± 0.04 ng/ml; D, LH = 0.42 ± 0.06 ng/ml; P, LH = 6.36 ± 3.45 ng/ml; E, LH = 5.73 ± 2.90 ng/ml; Kruskal-Wallis ANOVA: Chi-Square = 16.62; $p < 0.05$; Mann-Whitney n.s. $p > 0.12$-0.40. The number of independent measurements is indicated above each bar, at least five mice per genotype were used.

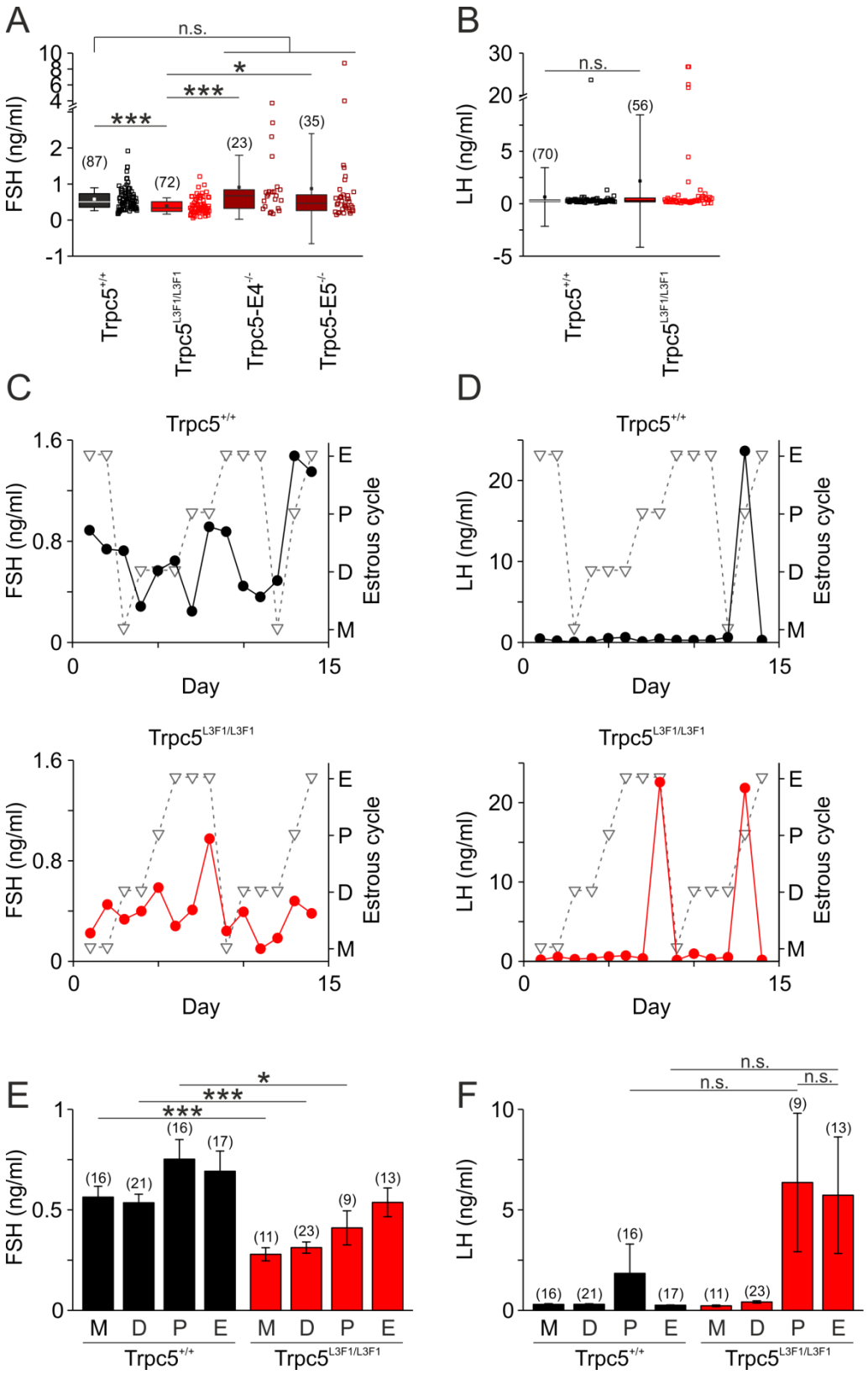
A
n.s.
*
***
***
FSH (ng/ml)
(87)
(72)
(23)
(35)
Trpc5+/+
Trpc5L3F1/L3F1
Trpc5-E4-/-
Trpc5-E5-/-
B
n.s.
LH (ng/ml)
(70)
(56)
Trpc5+/+
Trpc5L3F1/L3F1
C
Trpc5+/+
FSH (ng/ml)
Estrous cycle
E
P
D
M
Day
Trpc5L3F1/L3F1
D
Trpc5+/+
LH (ng/ml)
Trpc5L3F1/L3F1
E
*
***
***
FSH (ng/ml)
(16)
(21)
(16)
(17)
(11)
(23)
(9)
(13)
M D P E M D P E
Trpc5+/+
Trpc5L3F1/L3F1
F
n.s.
n.s.
n.s.
LH (ng/ml)
(16)
(21)
(16)
(17)
(11)
(23)
(9)
(13)
M D P E M D P E
Trpc5+/+
Trpc5L3F1/L3F1

Abnormal estrous cycle and hormonal alterations can be a sign of polycystic ovarian syndrome. As a clinical marker, the LH/FSH ratio is often used (Taylor et al., 1997). I determined the LH/FSH ratio in Trpc5$^{L3F1/L3F1}$ females and found that these females exhibit higher LH/FSH ratios than Trpc5$^{+/+}$ females (Fig. 16 A). This is mainly the case at the transition from the luteal to follicular phase (diestrus and proestrus, Fig. 16 B). Here, the mistiming of the LH peaks starts to add up to the FSH insufficiency. In order to support the hormonal imbalance phenotype and thus an additional disease like PCOS in the Trpc5$^{L3F1/L3F1}$ females, I checked – together with the Bachelor student Anela Arifovic – the ovarian morphology (Fig. 16 C). PCOS is characterized by and diagnosed if at least two of three criteria apply: oligo-/anovulation, hyperandrogenism, polycystic ovaries (Fauser et al., 2004; McVeigh et al., 2013). We could not find any increase in follicles (Fig 16 D), hinting towards the reduced serum FSH levels as a cause for the increased LH/FSH ratio.

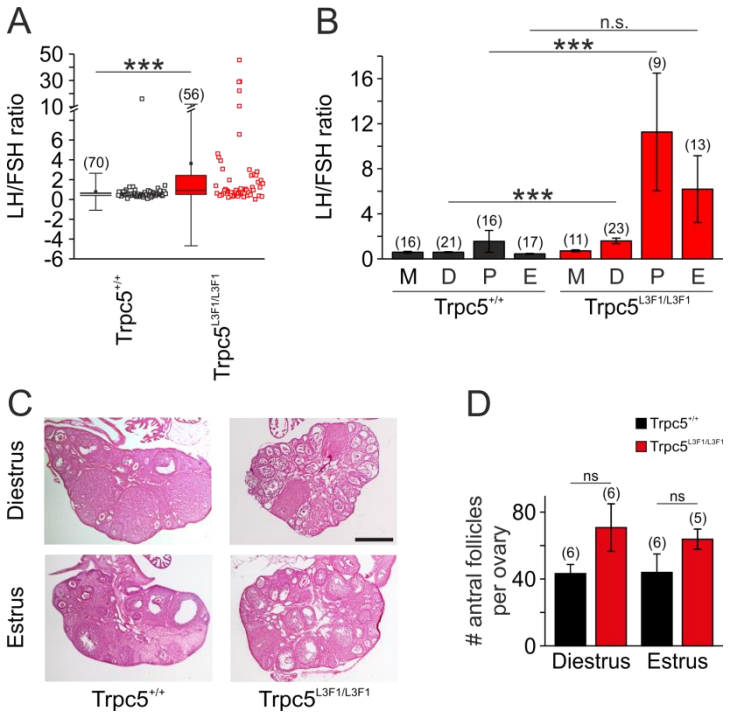

Figure 16: Increased LH/FSH ratio in Trpc5$^{L3F1/L3F1}$.
(A) Serum prolactin levels are lowered in naïve female mice lacking Trpc5. Trpc5$^{+/+}$ 0.78 ± 0.22; Trpc5$^{L3F1/L3F1}$ 3.63 ± 1.11; Mann-Whitney *** $p < 0.001$. Box plots present interquartile ranges, median (line), and mean (squares) with whiskers indicating SD values. Squares alongside a box indicate given estrous cycle lengths. The number of independent measurements from at least five mice per genotype is indicated above each box plot. (B) The LH/FSH ratio in Trpc5$^{L3F1/L3F1}$ females seems to be increased at the switch from luteal to follicular phase. Trpc5$^{+/+}$: M, LH/FSH ratio = 0.59 ± 0.08; D, LH/FSH ratio = 0.59 ± 0.05; P, LH/FSH ratio = 1.56 ± 0.97; E, LH/FSH ratio = 0.45 ± 0.04; Trpc5$^{L3F1/L3F1}$: M, LH/FSH ratio = 0.71 ± 0.09; D, LH/FSH ratio = 1.60 ± 0.25; P, LH/FSH ratio = 11.27 ± 5.22; E, LH/FSH ratio = 6.19 ± 2.96; Kruskal-Wallis ANOVA: Chi-Square = 37.73; $p < 0.001$; Mann-Whitney *** $p < 0.001$. The number of independent measurements is indicated above each bar. At least five mice per genotype were used. (C) Morphology of ovarian sections from Trpc5$^{+/+}$ and Trpc5$^{L3F1/L3F1}$ mice during diestrus and estrus stage (Anela Arifovic). (D) Trpc5$^{L3F1/L3F1}$ mice show a trend towards increased numbers of antral follicles in their ovaries. Diestrus: Trpc5$^{+/+}$ 43.7 ± 4.5; Trpc5$^{L3F1/L3F1}$ 71.2 ± 14; t-test $p = 0.11$; Estrus: Trpc5$^{+/+}$ 44.2 ± 10.7; Trpc5$^{L3F1/L3F1}$ 64.0 ±6.2; Mann-Whitney $p = 0.12$. The number of ovaries from at least three mice per genotype are indicated above each bar.

4.2.7 Lack of Trpc5 has a negative influence on sperm quality

It seems that the Trpc5-dependent subfertility is a coincidental effect. The hypoprolactinemia phenotype of Trpc5 deficient females does not appear to be sufficient to cause unfertile mating pairs. I therefore investigated pituitary hormones and sperm quality of Trpc5-deficient males. Male $Trpc5^{L3F1/y}$ have lowered prolactin levels (Fig. 17 A), although the levels were statistically not different from their wildtype littermates. The gonadotropins (LH and FSH) in $Trpc5^{L3F1/y}$ males were also unchanged compared with wildtype littermates (Fig. 17 B and C) as well as ACTH levels ($Trpc5^{+/y}$: 21.4 ± 15.1 pg/ml, 21 mice; $Trpc5^{L3F1/y}$: 21.9 ± 11.2 pg/ml, 20 mice). However, when we checked sperm quality and quantity of Trpc5-mutant males, we found striking differences. Mutants showed a two-fold increase in sperm count (Fig. 17 D), which upon first glance could be rather beneficial, although $Trpc5^{L3F1/y}$-derived sperm were severely limited in their motility. Observing the movement of wildtype sperm, we found spermatozoa to move in a directed, effective kind of way (Fig. 17 E). On the other hand, $Trpc5^{L3F1/y}$ spermatozoa traveled shorter distances or even failed to progress, showing only flagellar movement (Fig. 17 F). When summarized, we found that the total traveling distance of $Trpc5^{L3F1/y}$ spermatozoa was significantly decreased (Fig. 17 G). As for reproductive success, the effective traveling distance is more important because it also includes a targeted component, whereby we could show that the motility defect becomes even more obvious (Fig. 17 H). To make matters worse, $Trpc5^{L3F1/y}$ spermatozoa are 40% slower than those of wildtype littermates (Fig. 17 I). Trpc5 renders male mice subfertile, causing asthenozoospermia and thus reducing the chance of oocyte fertilization. In combination with diminished ovulatory events and hypoprolactinemia in female mice, the likelihood of infertile breeding pairs is strongly increased.

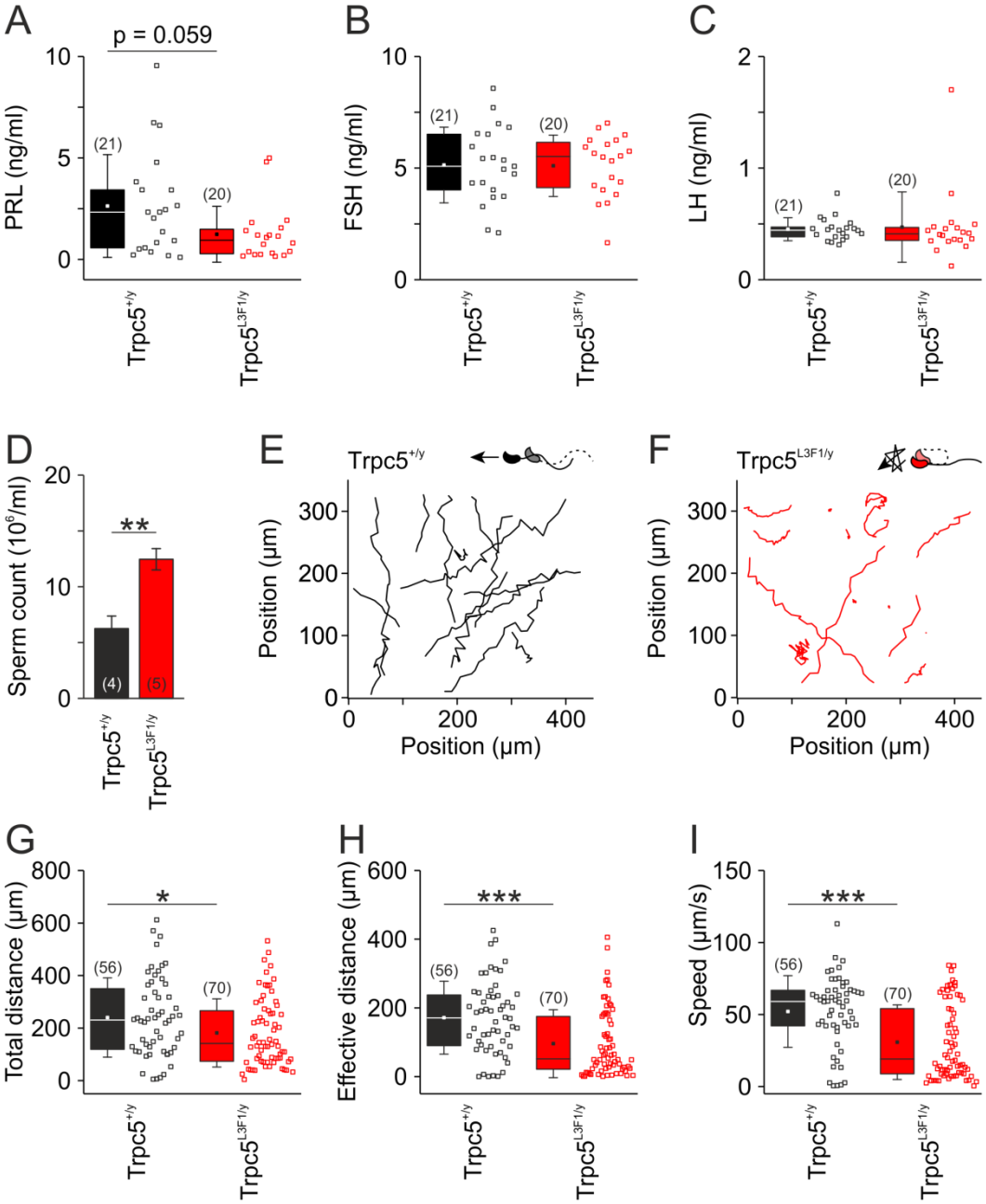

Figure 17: Increased sperm quantity and severely limited motility.
(A - C) Trpc5$^{L3F1/y}$ males show no obvious changes in either prolactin (A) or FSH (B) nor LH (C), but a tendency to hypoprolactinemia. A: Trpc5$^{+/y}$ 2.6 ± 0.6 ng/ml; Trpc5$^{L3F1/y}$ 1.2 ± 0.3 ng/ml; Mann-Whitney n.s. p = 0.059. B: Trpc5$^{+/y}$ 0.5 ± 0.02 ng/ml; Trpc5$^{L3F1/y}$ 0.5 ± 0.07 ng/ml; Mann-Whitney n.s. p = 0.35. C: Trpc5$^{+/y}$ 5.1 ± 0.4 ng/ml; Trpc5$^{L3F1/y}$ 5.1 ± 0.3 ng/ml; Mann-Whitney n.s. p = 0.94. Box plots present interquartile ranges, median (line), and mean (squares) with whiskers indicating SD values. Squares alongside a box indicate given estrous cycle lengths. The number of independent measurements from at least five mice per genotype is indicated above each box plot. (D) Sperm count in mutant males increased two fold. Trpc5$^{+/y}$ 6.3 ± 1.1 10^6/ml; Trpc5$^{L3F1/y}$ 12.5 ± 1.0 10^6/ml; Student's t-test t(7) = -4.2, ** p < 0.01. Number of animals is indicated above each bar. (E-F) Examples of sperm tracking, comparing the motility of Trpc5$^{+/y}$ (E) and Trpc5$^{L3F1/y}$ males (F). (G – I) Trpc5$^{L3F1/y}$ sperm motility is strongly reduced. G: Trpc5$^{+/y}$ 240.2 ± 20.2 µm; Trpc5$^{L3F1/y}$ 181.5 ± 15.5 µm; Mann-Whitney * p < 0.05. H: Trpc5$^{+/y}$ 171.4 ± 14.2 µm; Trpc5$^{L3F1/y}$ 95.8 ± 11.8 µm; Mann-Whitney *** p < 0.001. I: Trpc5$^{+/y}$ 52.1 ± 3.3 µm/s; Trpc5$^{L3F1/y}$ 30.8 ± 3.1 µm/s; Mann-Whitney *** p < 0.001. Box plots present interquartile ranges, median (line), and mean (squares) with whiskers indicating SD values. Squares alongside a box indicate given estrous cycle lengths. The number of independent measurements from at least five mice per genotype is indicated above each box plot.

4.2.8 Olfactory inputs as a rescue for Trpc5-deficiency-caused hypoprolactinemia

As indicated in the introduction (Chapter 1.4), olfactory cues can influence reproductive physiology. Olfactory cues from a mate can reduce dopamine levels in the arcuate nucleus, thereby increasing prolactin levels and assisting the lactotroph axis (Rosser et al., 1989; Matthews et al., 2013). Paired housing and thus a constant presence of a mate could help to prevent severe hypoprolactinemia. I thus examined prolactin levels in various habitation schemes. In a first attempt to examine whether a combination of olfactory cues and vaginal stimulation present in a paired housing can influence prolactin levels, I presented three different types of "stimuli" to Trpc5$^{L3F1/L3F1}$ females. As an olfactory cue, the bedding of a sexually-experienced C57Bl/6N male was presented on a daily basis. A castrated C57Bl/6N male was used as non-sexual male stimulus and a vasectomized C57Bl/6N male as a sexually-active male stimulus. Thus far, preliminary experiments suggest that olfactory stimuli (male bedding, Fig. 18 A) and the sexually-active male stimulus (vasectomized male, Fig. 18 C) have a chance to improve the hypoprolactinemia phenotype, whereas a non-sexual male stimulus (castrated male, Fig. 18 B) does not. These preliminary results suggest that olfactory stimuli already have the capability to improve prolactin levels in Trpc5$^{L3F1/L3F1}$ females. In addition, sexual activity is also highly beneficial for serum prolactin levels. In females, pseudopregnancy – induced by mating with a vasectomized male – is known to induce diurnal prolactin peaks (Butcher et al., 1972; Smith and Neill, 1976; Yang et al., 2009). Orgasm-induced peripheral prolactin secretion is also known in humans (Egli et al., 2010), possibly indicating that copulation itself benefits prolactin levels.

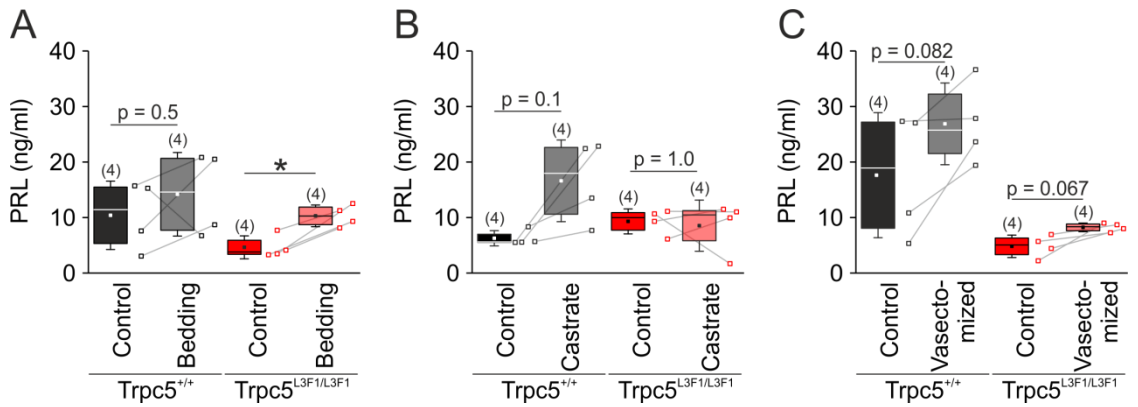

Figure 18: Olfactory inputs could serve as a rescue for Trpc5 dependent hypoprolactinemia.
(A-C) Box plots showing serum prolactin levels before and after receiving a stimulus. Bedding of a sexually-experienced C57Bl/6N given daily (A), a castrated C57Bl/6N male (B), or a vasectomized C57Bl/6N male (C). A: Trpc5$^{+/+}$: Control, PRL = 10.4 ± 3.1 ng/ml; Bedding, PRL = 14.2 ± 3.8 ng/ml; Trpc5$^{L3F1/L3F1}$: Control, PRL = 4.6 ± 1.0 ng/ml; Bedding, PRL = 10.3 ± 1.0 ng/ml; paired t-test: t(3) = -4.53, * p < 0.05. B: Trpc5$^{+/+}$: Control, PRL = 6.3 ± 0.7 ng/ml; Castrate, PRL = 16.6 ± 3.7 ng/ml; Trpc5$^{L3F1/L3F1}$: Control, PRL = 9.3 ± 1.1 ng/ml; Castrate, PRL = 8.5 ± 2.3 ng/ml; Wilcoxon signed rank test for paired data Z = -1.64317, p = 0.1. C: Trpc5$^{+/+}$: Control, PRL = 17.6 ± 5.6 ng/ml; Vasectomized, PRL = 26.9 ± 3.7 ng/ml; Trpc5$^{L3F1/L3F1}$: Control = 4.8 ± 1.0 ng/ml; Vasectomized, PRL = 8.2 ± 0.4 ng/ml; paired t-test Trpc5$^{+/+}$: t(3) = -2.6, p = 0.08; paired t-test Trpc5$^{L3F1/L3F1}$: t(3) = -2.8, p = 0.07. Box plots present interquartile ranges, median (line), and mean (squares) with whiskers indicating SD values. Squares alongside a box indicate given estrous cycle lengths. The number of animals is indicated above each box plot.

4.2.9 Discussion

A deficiency in serum levels of the hypothalamic-pituitary hormone prolactin is poorly understood (Arbogast and Voogt, 1991; Rehm et al., 2007; Grattan, 2015; Grattan and Le Tissier, 2015; Rastrelli et al., 2015). To date, no gene defects in any ion channel have been described that cause this medical condition. Therefore, the aim of this part of my thesis was to assess whether the absence of Trpc5 channels could influence the reproductive outcome of a pregnancy (Bruce effect) by analyzing the reproductive capability of wildtype versus Trpc5-deficient mice and assessing any hormonal imbalance induced by the loss of Trpc5.
My findings demonstrate that Trpc5 mutant females display severe impairments in their reproductive capabilities. In case of productive matings, a temporal delay in the occurrence of pregnancy and a reduced number of offspring is observed, consistent with low prolactin levels and defects in nidation. Reduced prolactin levels suggest an increase in dopamine release (Lyons et al., 2012; Romano et al., 2013). In order to counterbalance raised dopamine levels in the arcuate nucleus, I investigated the effect whereby olfactory cues from a mate can decrease dopamine levels in the arcuate nucleus in rodents, thereby increasing prolactin levels and assisting the lactotroph axis (Rosser et al., 1989; Matthews et al., 2013). In my preliminary data, it appears that prolactin levels increased in the Trpc5-deficient females when exposed to olfactory cues from bedding material of an intact male mouse or to a vasectomized male mouse.

Proteins of the Trpc family can form many homo- and heterotetrameric cation channels, each with their own characteristics and functions (Minard et al., 2018). Within a Trpc subgroup, it seems that Trpc1, c4 and c5 are prone to formation of heteromeric channels. Single mutations of Trpc1, c4 and c5 in mating pairs caused infertility in 20-50% and subfertility in those that mated successfully. Interestingly, if more than one member of Trpc1, c4 and c5 is deleted, the subfertility seen in single channel knockouts is absent. The reproductive phenotype is most noticeable in Trpc5-deficient mice and became manifest in a temporal delay of pregnancies and reduced number of offspring, in terms of both the quantity of litters and number of pups per litter. A reduced number of pups could be caused by a reduced supply of ovulated oocytes (Cacioppo et al., 2017), pregnancy failure (Hattori et al., 2017), or pup mortality, due to a lack of maternal behavior or infanticide (Grattan, 2001; Larsen and Grattan, 2012; Weber et al., 2013a; Weber et al., 2013b).

In order to narrow down the cause of the reproductive phenotype, assorted breeding pairs of the $Trpc5^{L3F1/L3F1}$ mouse line were generated. Mixed breeding pairs did not expose a striking defect in reproductive capability. This suggests a combinatorial pattern that causes striking subfertility only when both sexes are deficient for Trpc5. This can be induced by either slight subfertility of the single sex that is unrecognized when the mating partner is fully capable, or

by secondary pathways activated during breeding, which improves the subfertility of the Trpc5 deficient mouse. Further investigations of sex specific phenotypes of Trpc5 deficient mice reveal that both sexes show reproductive impairments.

Female Trpc5-deficient mice show prolonged estrous cycle and increased time spent in diestrus. Prolonged diestrus is often linked with changed levels of prolactin (Hansen et al., 1983). In accordance with this, I found Trpc5 mutant females to suffer from hypoprolactinemia. Hypoprolactinemia is a poorly-described syndrome compared with hyperprolactinemia, which is the more common and better diagnosable prolactin dysfunction. In humans, hypoprolactinemia is associated with systemic disorders like hypopituitarism, hypothyroidism, autoimmune disease or growth hormone deficiency (Davis, 2011; Strauss et al., 2014). Moreover, drug-induced hypoprolactinemia is described, causing changes in dopamine levels (Kauppila et al., 1988; Stone, 1996). In females, hypoprolactinemia is associated with ovarian dysfunction (Kauppila et al., 1988). Clinical symptoms in males are more diverse. Metabolic syndrome, anxiety, erectile dysfunction, premature ejaculation, sperm defects – in terms of both number and motility – hypofunction of seminal vesicles as well as hypoandrogenism can be recognized in hypoprolactinemia (Gonzales et al., 1989b; Gonzales et al., 1989a; Corona et al., 2009). In a first step to assess ovarian function, I analyzed serum levels of the gonadotropins LH and FSH, as markers for the activity of the classical reproductive axis. LH levels were unchanged, although FSH levels were decreased in $Trpc5^{L3F1/L3F1}$ females. Reduced serum levels of FSH could affect the recruitment and growth of ovarian follicles (Kumar et al., 1997), resulting in changed numbers of follicles and thereby restricted ovarian function. Diminished levels of FSH and increased LH/FSH ratios are an indicator of another form of ovarian dysfunction, namely polycystic ovary syndrome (PCOS, Taylor et al., 1997; Lewandowski et al., 2011). Trpc5-deficient females show increased LH/FSH ratios. In our case, we did not find any defects in ovary morphology (performed by Anela Arifovic). Furthermore, I could not find increased levels or alterations of LH, but a shortage of FSH. Given that the increased LH/FSH ratio is most likely caused by reduced FSH levels, I conclude that the reduced prolactin levels causes the prolonged cycle and oligoovulation. An additional consequence of the hypoprolactinemia phenotype is the loss of pups between birth and weaning (P21). Prolactin is essential for lactation (Freeman et al., 2000; Grattan, 2015; Grattan and Le Tissier, 2015; Le Tissier et al., 2015). Prolactin regulates not only mammogenesis (Bern and Nicoll, 1968; Freeman et al., 2000; Larsen and Grattan, 2012; Le Tissier et al., 2015) but also milk production (lactogenesis) and its upkeep (galactopoiesis, Nelson and Gaunt, 1936; Lyons, 1942; Cowie et al., 1969). In addition, prolactin also controls milk composition (Barber et al., 1992; Anderson et al., 2014). A reduction in prolactin will very likely affect the quality and quantity of milk production and thus influence pup survival.

Trpc5-deficient male mice show a trend towards hypoprolactinemia, narrowly failing to reach significance. In human males, hypoprolactinemia is associated with fertility defects, such as erectile dysfunction, premature ejaculation, sperm defects and hypoandrogenism (Gonzales et al., 1989b; Gonzales et al., 1989a; Corona et al., 2009; Rastrelli et al., 2015). I found that sperm count is considerably increased. By contrast, sperm motility is dramatically reduced in terms of traveled distance and sperm movement speed. In males, gonadotropins stimulate cells in the testis, regulating testosterone secretion and sperm development (Attia et al., 2013). Changed levels of LH and FSH are a diagnostic tool in human medicine when evaluating androgen deficiency (Bhasin et al., 2018). $Trpc5^{L3F1/y}$ males did not show any alterations in either LH or FSH, indicating that the HPG axis functions regularly and that changes in sperm count and motility are most likely changed by reduced prolactin levels. This phenomenon is already known in humans, where prolactin is positively correlated with sperm motility and in a negative relationship with sperm count, meaning that low prolactin levels occur with increased sperm count and reduced motility (Gonzales et al., 1989b).

Taken together, both sexes of Trpc5-deficient mice show profound defects in their reproductive capabilities. By contrast, when bred with wildtype litter mates, the reproductive phenotype is rescued. Accordingly, the suggestion that there are some secondary pathways improving the reproductive condition of Trpc5 deficient mice seems more likely. In rodents, olfactory cues from a mate can reduce dopamine levels in the arcuate nucleus, to enable increased prolactin secretion (Rosser et al., 1989; Matthews et al., 2013). Furthermore, copulation or copulomimetic stimulation is known to increase prolactin levels in female rodents (Butcher et al., 1972; Smith and Neill, 1976; Freeman et al., 2000; Bachelot and Binart, 2005; Yang et al., 2009). Preliminary results of this thesis indicate that olfactory stimuli already benefit prolactin secretion in hypoprolactinemic $Trpc5^{L3F1/L3F1}$ female mice. Likewise, presenting a vasectomized mate, giving both olfactory as well as copulatory stimuli, female mice of all tested genotypes showed a tendency to higher prolactin levels.

My results conclude that Trpc5-deficency causes hypoprolactinemia, which is most likely induced by a dysregulation of the lactotroph axis. In male mice, Trpc5-deficiency causes asthenozoospermia and increased sperm count. In female mice, a lack of Trpc5 causes subfertility due to hypoprolactinemia itself, increased estrous cycle length, oligoovulation, and unbalanced gonadotropin secretion. Olfactory stimuli – which are known to change dopamine levels in the arcuate nucleus – are able to rescue the hypoprolactinemia phenotype. This suggests that Trpc5-deficiency affects dopaminergic neurons in the arcuate nucleus of the hypothalamus that regulate prolactin secretion.

4.3 Trpc5 channels are essential for the infraslow oscillatory activity of hypothalamic dopaminergic neurons

In an attempt to determine the cause of hypoprolactinemia and resulting subfertility, I investigated dopaminergic neurons of the arcuate hypothalamic nucleus (ARC) in female mice at the cellular level. Dopaminergic neurons of the hypothalamus and especially the ARC maintain the regulation of prolactin release from lactotroph cells of the anterior pituitary (Freeman et al., 2000; Ben-Jonathan and Hnasko, 2001). I focused on dopaminergic neurons located in the dorsomedial ARC, which are thought to be the main source of dopamine released into the median eminence. In addition, Trpc channels have been proposed to be involved in the prolactin feedback loop (Lyons et al., 2012; Lyons and Broberger, 2014). These findings together with our hypoprolactinemia phenotype in Trpc5 deficient female mice suggest that an increase in dopamine release – which inhibits the secretion of prolactin from the lactotroph cells – might be the cause of the hypoprolactinemia. A change in dopamine release could be visible in an altered cellular performance of dopaminergic ARC neurons. My aim was thus to demonstrate that dopaminergic neurons of the dorsomedial ARC change their pattern of activity and their responsivity to prolactin stimulation.

4.3.1 Trpc5 stabilizes infraslow oscillatory activity in ARC dopaminergic neurons

In order to assess the cellular activity of dopaminergic ARC neurons, I first performed whole-cell current-clamp recordings in genetically-labeled Th+ neurons using the Th-tdTomato mouse line. Th+ cells in these mice are labeled with tdTomato, enabling targeted patch clamp recordings in acute brain slices. I focused on labeled cells in the dorsomedial (dm) ARC, which are known to express dopamine (Zhang and van den Pol, 2015). I could confirm that Th+ ARC neurons show spontaneous oscillatory burst firing (Fig. 19 A, Lyons et al., 2010; Lyons et al., 2012; Lyons and Broberger, 2014; Zhang and van den Pol, 2015). A prominent feature of these oscillations is that they show clear periods of quiescence (down state (V_D); V_D = -61.7 ± 1.3 mV) and periods of action potential discharges (up state (V_U); V_U = -49.1 ± 2.2 mV; Fig. 19 B). V_D and V_U alternate in regular intervals, respectively 15 s in V_D and 6 s in V_U (n= 17 neurons from fourteen mice). This is in agreement with previous results (Lyons et al., 2010; Lyons et al., 2012; Lyons and Broberger, 2014; Zhang and van den Pol, 2015). Normalized autocorrelation histograms (ACH) demonstrated a distinct peak, which indicates a predominance of bursting intervals in the cellular activity (Fig. 19 C). The burst refractory period (indicating the period of silence following a burst) was 10.5 ± 1.3 s. In addition, subsequent peaks indicate oscillatory burst activity at frequencies between 0.02 and 0.05 Hz, which can be classified as infraslow (Gorin et al., 2016; Zylbertal et al., 2017).

In order to confirm that the recorded neurons are indeed Th+, recorded cells were filled with neurobiotin and *post-hoc* labeled with an antibody direct against Th (Fig. 20 A). Contrary to recordings in Th-tdTomato females, Trpc5-deficient Th+ ARC neurons showed drastically altered oscillatory burst firing activity (Fig 19 D-L). This holds true for female Trpc5$^{L3F1/L3F1}$ (n = 6 neurons from five mice), Trpc5-E4$^{-/-}$ (n = 8 neurons from eight mice) and Trpc5-E5$^{-/-}$ mice (n = 10 neurons from eight mice). Here, the necessity arose for all recorded cells to be labeled with neurobiotin and *post-hoc* stained for Th (exemplary picture of a Trpc5$^{L3F1/L3F1}$ recorded neuron, Fig. 20 B). Trpc5-deficient Th+ ARC neurons showed increased bursting activity, which features in strikingly decreased interburst intervals (Fig. 20 C) as well as increased instantaneous burst frequency (Fig. 20 E). In addition to the increased occurrence of burst action potential discharges, loss of Trpc5 changes additional burst parameters. Trpc5-deficient Th+ ARC neurons showed reduced burst strength (steepness of burst slope, Fig. 20 D), decreased amounts of voltage conduction over the membrane (voltage envelope, Fig. 20 G) and limited spike frequency within a burst (Fig. 20 F). In order to further evaluate the regularity of bursting, I calculated a rhythmicity index (RI, Zylbertal et al., 2017) and found a two-fold reduction in Trpc5$^{L3F1/L3F1}$ (RI = 0.16 ± 0.05) compared with Th-tdTomato Th+ ARC neurons (RI = 0.32 ± 0.05). The global Trpc5 mutants Trpc5-E4$^{-/-}$ and Trpc5-E5$^{-/-}$ showed an even higher (2.5-fold) reduction (Trpc5-E4$^{-/-}$: RI = 0.14 ± 0.05; Trpc5-E5$^{-/-}$: RI = 0.13 ± 0.03). These findings indicate that Trpc5 is important to stabilize the regularity of the rhythmic oscillatory burst activity in Th+ ARC neurons and their bias to oscillate in an infraslow manner. If the Trpc5-dependent perpetuation of burst stability is lost, Th+ ARC neurons demonstrate reduced interburst intervals and thereby increased activity.

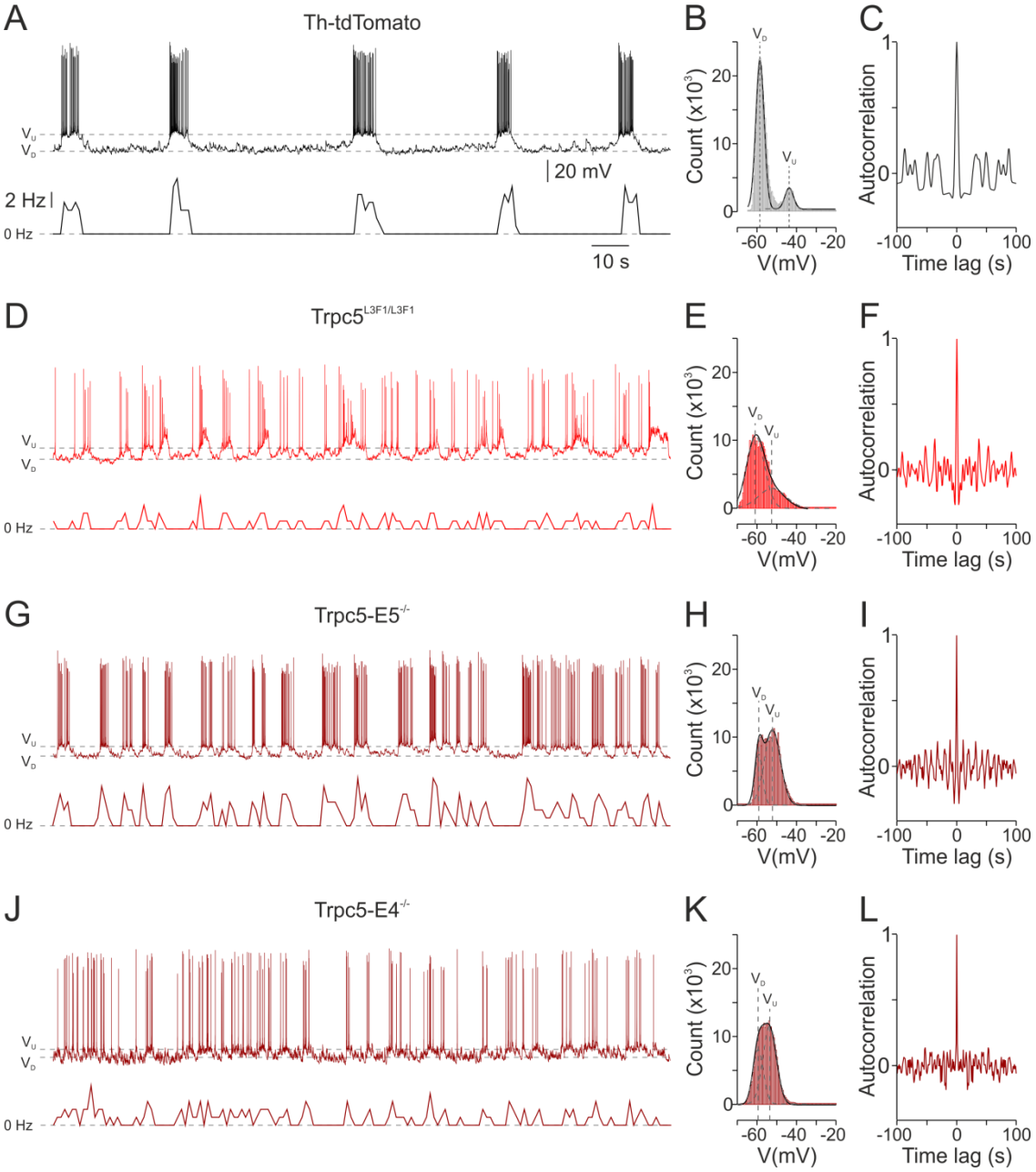

Figure 19: Loss of Trpc5 disrupts infraslow oscillations in dopaminergic neurons of the arcuate nucleus. (A) Representative current-clamp recording (I_H = 0 pA) of a Th+ (dopaminergic) ARC neuron displaying rhythmic burst activity (upper trace). The infraslow oscillations can be observed in the time histogram (lower trace). (B) Plot of frequency distribution (5 min recording of the cell shown in A). V_D = -58.3 ± 0.03 mV; V_U = -43.4 ± 0.03 mV (mean ± SD). (C) Normalized autocorrelation histogram (ACH, 5-min recording period) generated from the cell shown in A. (D) Representative current-clamp recording showing altered burst activity in Trpc5$^{L3F1/L3F1}$ females (upper trace, I_H = 0 pA). Increased burst activity can be seen in the time histogram (lower trace). (E) Plot of frequency distribution (5 min recording of the cell shown in D). V_D = -60.9 ± 0.3 mV; V_U = -53.4 ± 4.4 mV (mean ± SD). (F) Normalized ACH (5-min recording period) generated from the cell shown in D. (G) Representative current-clamp recording (I_H = 0 pA) of a Th+ ARC neuron from Trpc5-E5$^{-/-}$ females displaying higher burst frequency (upper trace). This can also be observed in the time histogram (lower trace). (H) Plot of frequency distribution (5 min recording of the cell shown in G). V_D = -59.2 ± 0.05 mV; V_U = -52.3 ± 0.08 mV (mean ± SD). (I) Normalized ACH (5-min recording period) generated from the cell shown in G. (J) Representative current-clamp recording showing disorganized burst activity in Trpc5-E4$^{-/-}$ females (upper trace, I_H = 0 pA). Irregular burst activity can be seen in the time histogram (lower trace). (K) Plot of frequency distribution (5 min recording of the cell shown in J). V_D = -59.5 ± 0.11 mV; V_U = -53.6 ± 0.12 mV ± 4.4 mV (mean ± SD). (L) Normalized ACH (5-min recording period) generated from the cell shown in J.

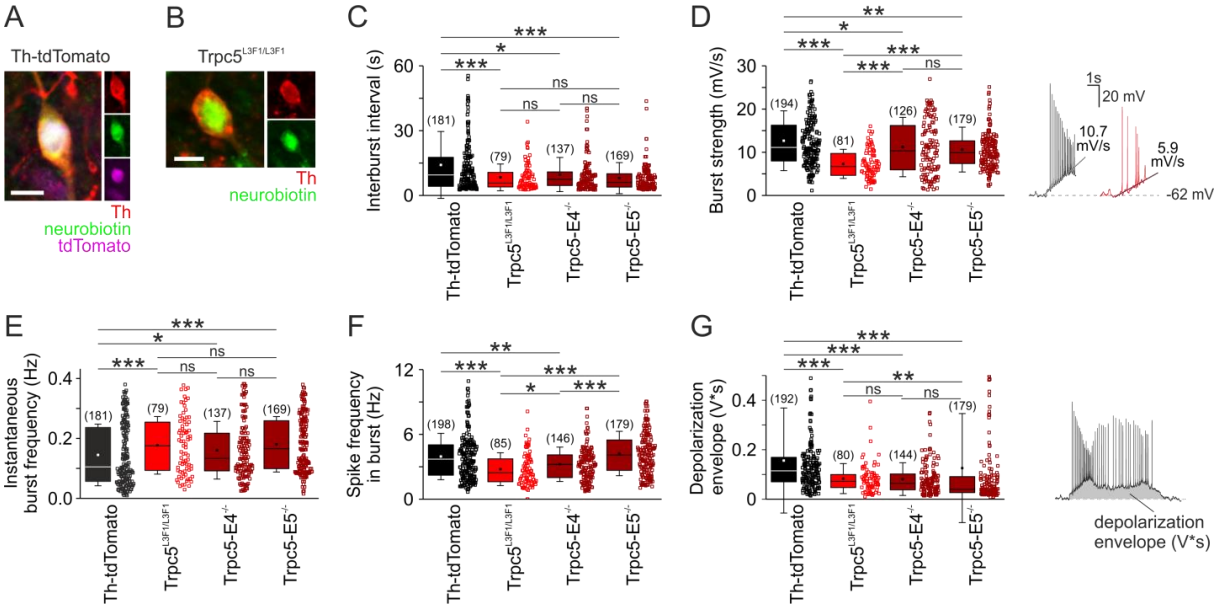

Figure 20: Altered oscillatory activity in Trpc5 deficient dopaminergic ARC neurons.
(A) Example of a recorded and neurobiotin-filled (green) tdTomato labeled (magenta) neuron of the dorsomedial ARC from a Th-tdTomato female that was additionally identified using *post-hoc* immunolabeling for Th (red). Scale bar, 10 µm. (B) *Post-hoc* immunofluorescence classifies a neurobiotin-filled dorsomedial ARC neuron (green) as Th positive (red). Scale bar, 10 µm. (C) The interburst interval (IBI) shortened from 14.1 ± 1.2 s (n = 17 cells, Th-tdTomato) to 8.4 ± 0.7 s (n = 6 cells) in Trpc5$^{L3F1/L3F1}$, 9.7 ± 0.7 s (n = 8 cells) in Trpc5-E4$^{-/-}$, and 8.0 ± 0.6 s in Trpc5-E5$^{-/-}$ Th+ ARC neurons. Kruskal-Wallis ANOVA: Chi-Square = 17.9, p < 0.001, Mann-Whitney ns p = 0.06 - 0.67, * p < 0.05, *** p < 0.001. (D) Declining burst strength in Trpc5-deficient female mice. Th-tdTomato: 12.7 ± 0.5 mV/s; Trpc5$^{L3F1/L3F1}$: 7.3 ± 0.4 mV/s; Trpc5-E4$^{-/-}$: 11.2 ± 0.6 mV/s; Trpc5-E5$^{-/-}$: 10.6 ± 0.4 mV/s; Kruskal-Wallis ANOVA: Chi-Square = 51.6, p < 0.001; Mann-Whitney: * p < 0.05, ** p < 0.01, *** p < 0.001, ns p < 0.89. (E) Loss of Trpc5 raises the instantaneous burst frequency in Th+ ARC neurons. Th-tdTomato: 0.14 ± 0.01 Hz; Trpc5$^{L3F1/L3F1}$: 0.18 ± 0.01 Hz; Trpc5-E4$^{-/-}$: 0.16 ± 0.01 Hz; Trpc5-E5$^{-/-}$: 0.18 ± 0.01 Hz; Kruskal-Wallis ANOVA: Chi-Square = 17.9, p < 0.001; Mann-Whitney: ns p = 0.06 - 0.67, * p < 0.05, *** p < 0.001. (F) Reduced spike frequency during the upstate of Trpc5$^{L3F1/L3F1}$ and Trpc5-E4$^{-/-}$ Th+ ARC neurons. Th-tdTomato: 4.0 ± 0.2 Hz; Trpc5$^{L3F1/L3F1}$: 2.8 ± 0.2 Hz; Trpc5-E4$^{-/-}$: 3.2 ± 0.1 Hz; Trpc5-E5$^{-/-}$: 4.2 ± 0.2 Hz; Kruskal-Wallis ANOVA: Chi-Square = 42.0. p < 0.001; Mann-Whitney: * p < 0.05, ** p < 0.01, *** p < 0.001. (G) Deficiency of Trpc5 diminishes the depolarization envelope, a measure for the amount of voltage conduction across the cell membrane. Th-tdTomato: 0.16 ± 0.02 Vs; Trpc5$^{L3F1/L3F1}$: 0.08 ± 0.01 Vs; Trpc5-E4$^{-/-}$: 0.08 ± 0.01 Vs; Trpc5-E5$^{-/-}$: 0.13 ± 0.02; Kruskal-Wallis ANOVA: Chi-Square = 73.7, p < 0.001; Mann-Whitney: ns = 0.06 - 0.28, ** p < 0.01, *** p< 0.001. Box plots display the interquartile ranges, median (line) and mean (square) values with whiskers indicating SD values. The total number of bursts analyzed (from at least three mice per genotype) is indicated in brackets and plotted as individual data points next to each box.

4.3.2 Trpc5 is necessary for the excitatory component of the prolactin feedback mechanism at the level of the hypothalamus

Any neuroendocrine regulation of hormonal release is adjusted by a feedback mechanism, whereby the product controls its own production. As part of a short-loop feedback, prolactin itself stimulates the secretion of inhibitory dopamine (Freeman et al., 2000; Ben-Jonathan and Hnasko, 2001; Grattan, 2001; Kokay and Grattan, 2005; Lyons et al., 2012; Romano et al., 2013; Lyons and Broberger, 2014; Grattan, 2015).

A depolarizing conductance that has been suggested to be Trpc-like is considered to play a role in this prolactin-dependent excitation (Lyons et al., 2012). In my electrophysiological recordings of Th+ ARC neurons in acute slices of female Th-tdTomato mice, I could confirm this change in activity upon prolactin stimulation. Upon prolactin stimulation (500 nM, ten mice), Th+ ARC neurons switch from their infraslow oscillatory burst firing to a tonic depolarization, causing enhanced action potential firing (Fig 21 A-C). Th+ ARC neurons of Trpc5-deficient neurons of $Trpc5^{L3F1/L3F1}$ mice seemed to be unresponsive to prolactin stimulation, showing the complete absence of a tonic depolarization or an increased action potential frequency (n = 5, Fig. 21 D-F). These cells simply continue to produce rhythmic burst activity. Global knockout of Trpc5 produced similar results in both Trpc5-$E4^{-/-}$ (n = 3) and Trpc5-$E5^{-/-}$ (n = 7) Th+ ARC neurons (Fig. 21 G-J). In order to quantify this lack of activity switch, I calculated a ratio comparing the time spent in the up state (V_U) potential during aCSF and prolactin application. Trpc5-deficient Th+ ARC neurons did not alter the time spent in V_U, in contrast to Trpc5-positive Th+ ARC neurons, which demonstrate a 1.7-fold increase the time spent in V_U (Fig. 21 K). This increased time spent in the up state is associated with an increase in action potential frequency, which is absent in Trpc5- deficient Th+ ARC neurons (Fig. 21 L). Thus Trpc5 is essential for the prolactin-induced long-lasting plateau potentials in these neurons.

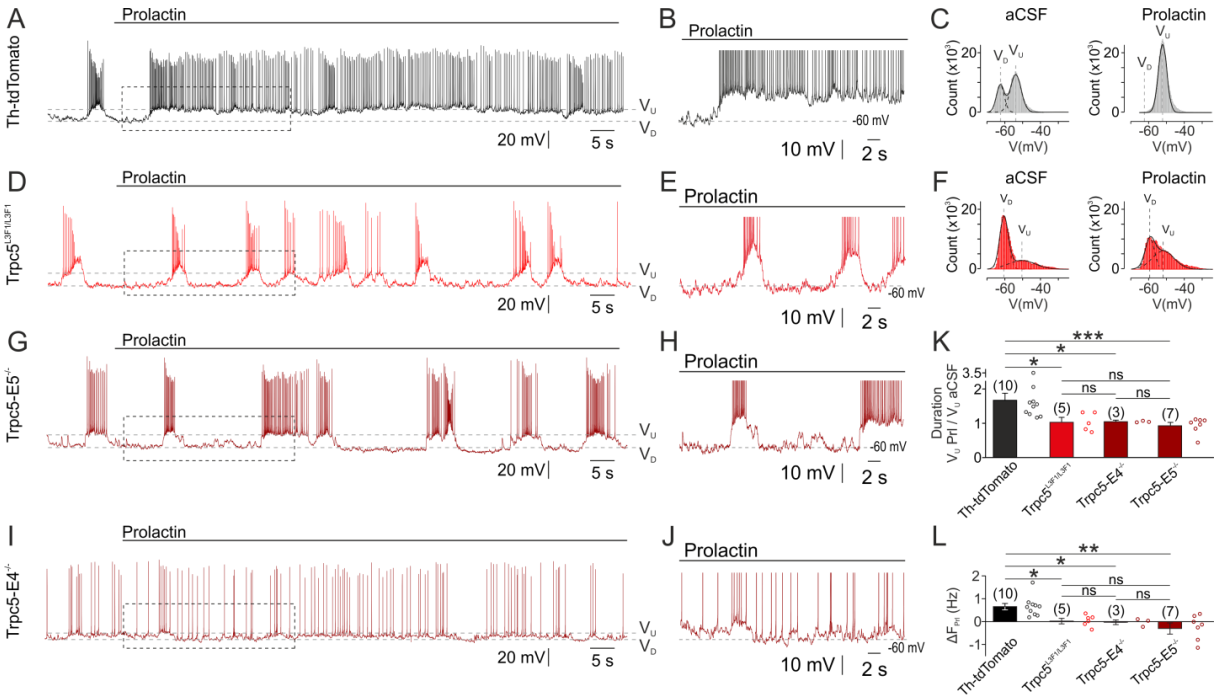

Figure 21: Trpc5 is crucial for prolactin-evoked excitation of Th+ ARC neurons.
(A and B) Stimulation of Th+ ARC neurons from female Th-tdTomato mice with Prolactin (Prl, 500 nM) induces a tonic, long-lasting depolarization. Representative current-clamp recording (I_H = 0 pA). Dashed box represents the section magnified in B. (C) Frequency distribution plot (10 min recording period) of the cell shown in A before (aCSF) and upon Prl stimulation. aCSF: V_D = -62.4 ± 0.1 mV; V_U = -53.9 ± 0.1 mV; Prl: V_U = -52.1 ± 0.04 mV (mean ± SD). (D and E) Prl stimulation of Th+ ARC neurons of $Trpc5^{L3F1/L3F1}$ female mice causes no change of the oscillatory. Representative current-clamp recording (I_H = 0 pA). Dashed box represents the section magnified in E. (F) Frequency distribution plot (10 min recording) of the cell shown in D prior (aCSF) and upon Prl stimulation. aCSF: V_D = -60.5 ± 0.03 mV; V_U = -50.1 ± 0.7 mV; Prl: V_D = -59.4 ± 0.1 mV; V_U = -51.9 ± 0.8 mV (mean ± SD). (G-J) Global knockout of Trpc5 prevents Prl-evoked excitation in Th+ ARC neurons of both Trpc5-$E4^{-/-}$ and Trpc5-$E5^{-/-}$ female mice. Representative current-clamp recordings (I_H = 0 pA; G and I). Dashed boxes represent the sections magnified in H and J respectively. (K) Treatment with prolactin induces a 1.7-fold increase in the duration and thus occurrence of V_U in Th+ ARC neurons of Th-tdTomato mice (n = 10), which cannot be triggered in Trpc5-deficient Th+ ARC neurons of $Trpc5^{L3F1/L3F1}$ (n = 5), Trpc5-$E4^{-/-}$ (n = 3) or Trpc5-$E5^{-/-}$ (n = 7) mice. Duration ratio of V_U Prl / V_U aCSF: Th-tdTomato: 1.67 ± 0.21; $Trpc5^{L3F1/L3F1}$: 1.04 ± 0.12; Trpc5-$E4^{-/-}$: 1.04 ± 0.01; Trpc5-$E5^{-/-}$: 0.94 ± 0.09, Kruskal-Wallis ANOVA: Chi-Square = 14.8, $p < 0.01$; Mann-Whitney: ns p = 0.82 - 0.97, * $p < 0.05$, *** $p < 0.001$. (L) In Th+ ARC neurons of Trpc5-deficient mice, prolactin fails to modify the mean frequency, in contrast to Th+ ARC neurons of Th-tdTomato mice. Th-tdTomato: 0.65 ± 0.15 Hz; $Trpc5^{L3F1/L3F1}$: 0.02 ± 0.12 Hz; Trpc5-$E4^{-/-}$: -0.03 ± 0.1 Hz; Trpc5-$E5^{-/-}$: -0.29 ± 0.24 Hz; ANOVA: F = 5.71, $p < 0.01$; Tukey: ns p = 0.66 - 0.99, * $p < 0.05$, ** $p < 0.01$. Indicated above each bar are the number of cells from at least three mice per genotype.

4.3.3 Loss of Trpc5 does not alter phosphorylation of Signal Transducer and Activator of Transcription 5 (STAT5) upon prolactin receptor activation

The feedback of prolactin upon dopaminergic neurons of the hypothalamus involves the activation of prolactin receptors (PrlR). Loss of Trpc5 causes a loss of the electrical excitation in Th+ ARC neurons. This could be caused by either the loss of Trpc5 itself or the loss of PrlR on the plasma membrane. Activation of PrlR causes not only electrical changes but also increases the phosphorylation of signal transducer and activator of transcription 5 (STAT5), which dimerizes, translocates to the nucleus and increases the amount of TH mRNA (Grattan, 2001; Grattan and Le Tissier, 2015).

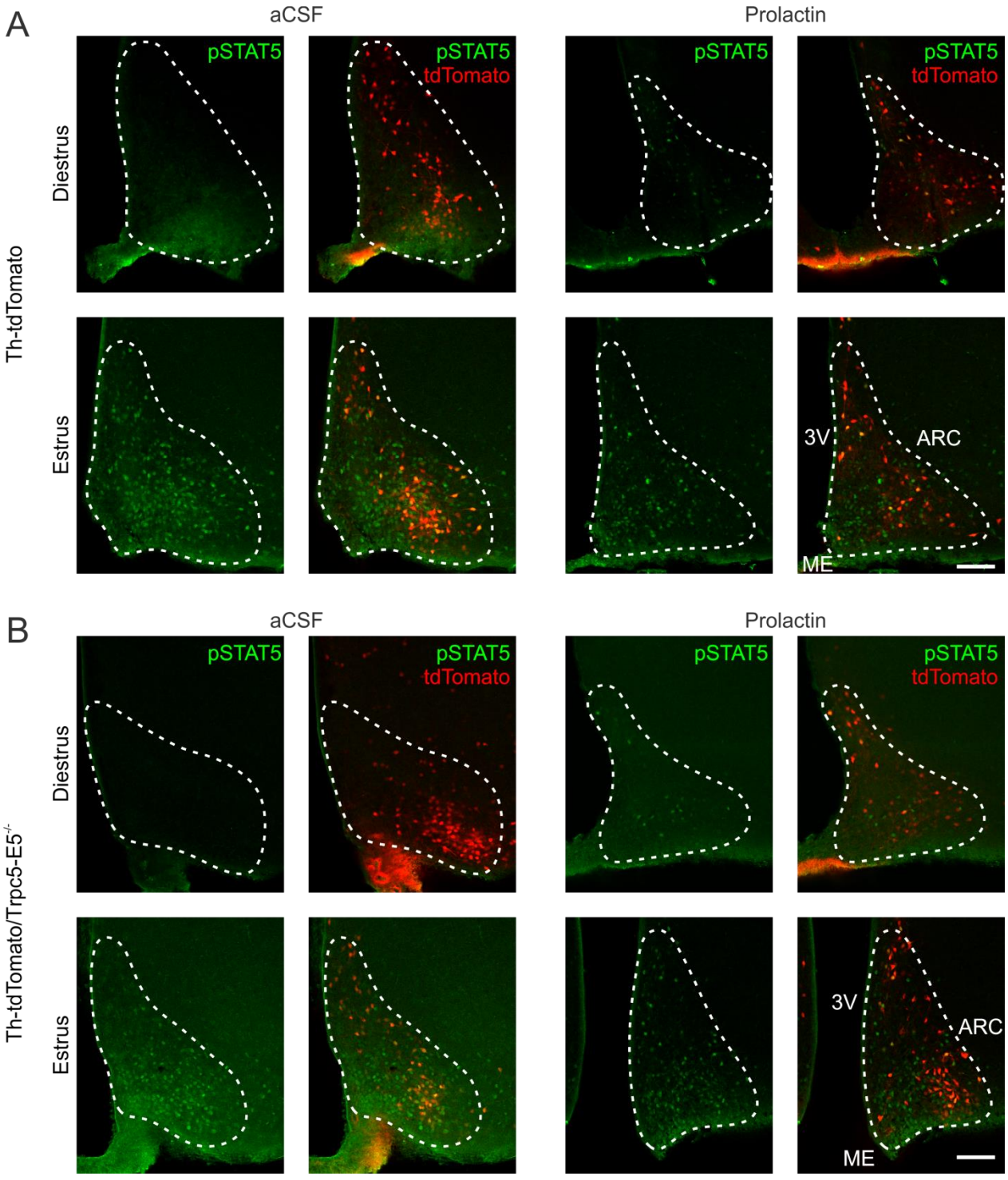

Figure 22: Endogenous and external prolactin activate prolactin receptor dependent phosphorylation of Signal Transducer and Activator of Translation 5 (STAT5).
(A and B) Immunostainings of either Th-tdTomato (A) or Th-tdTomato/Trpc5-E5$^{-/-}$ (B) females showing pSTAT5 (green) and tdTomato (red) expression in the arcuate nucleus (ARC). Slices from both estrus and diestrus females were either kept in aCSF or stimulated with 500 nM prolactin. 3V, third ventricle; ME, median eminence; scale bar, 100 µm.

In order to ensure that the Trpc5 dependent lack of prolactin-induced increase in electrical activity is indeed caused by loss of Trpc5 and not PrlR, I performed *post-hoc* immunostaining of either stimulated or unstimulated acute brain slices of Th-tdTomato mice as well as Th-tdTomato/Trpc5-E5$^{-/-}$ mice. In order to also investigate endogenous PrlR activation due to the estrous cycle, I analyzed female mice in diestrus and estrus. Th-tdTomato mice show PrlR activation, and subsequent phosphorylation of STAT5, upon both endogenous (estrus phase) and exogenous prolactin (500 nM, Fig. 4.3.4 A). Trpc5 deficient Th-tdTomato/Trpc5-E5$^{-/-}$ females also produced phosphorylated STAT5 upon both exogenous and endogenous prolactin (Fig 4.3.4 B), indicating that even though Trpc5 is lost PrlR is still expressed and functional.

4.3.4 Discussion

Th+ ARC neurons that are positive for Trpc5 (data produced by Ana Moreno-Pérez) show oscillatory infraslow burst activity and increase their activity upon prolactin stimulation, in conformation with previous reports (Lyons et al., 2010; Lyons et al., 2012; Romano et al., 2013; Lyons and Broberger, 2014; Grattan and Le Tissier, 2015).

I could show that Trpc5 is a determining factor in the physiological activity of Th+ dmARC neurons. These neurons play an important role in the regulation of prolactin release from lactotroph cells in the anterior pituitary and linking the release of dopamine to prolactin secretion from the pituitary (Freeman et al., 2000; Ben-Jonathan and Hnasko, 2001; Grattan and Le Tissier, 2015). My data provides evidence that Trpc5 has a strong influence on the firing activity of Th+ ARC neurons. Trpc5 is highly important to maintain the spontaneous infraslow rhythmic oscillatory burst activity. My data indicates that Trpc5 positively affects the onset of a burst, the burst duration and the voltage conducted during a burst. This suggests that Trpc5 is a limiting factor for burst frequency and the interval between bursts. Loss of Trpc5 therefore increases the overall activity of Th+ dmARC neurons, which in turn should increase the amounts of dopamine released into the median eminence. In order to elaborate this, further experiments should determine the amount of dopamine at the level of the median eminence by using either carbon fiber amperometry (Bruns and Jahn, 1995; Staal et al., 2007) or newly-developed fluorescent dopamine indicators (Patriarchi et al., 2018).

Besides the general role of Trpc5 in the upkeep of membrane oscillations, Trpc5 is an essential component of the prolactin feedback loop. Prolactin stimulation of Th+ dmARC neurons causes the phosphorylation of STAT5, as well as an increase in electrical activity (Arbogast and Voogt, 1991; Freeman et al., 2000; Ma et al., 2005b; Ma et al., 2005a; Lyons et al., 2012; Lyons and Broberger, 2014; Grattan and Le Tissier, 2015). As I could show, loss

of Trpc5 affects only the electrical component of prolactin stimulation in Th+ dmARC neurons. Therefore, a deficiency of Trpc5 renders Th+ dmARC neurons uncapable of fully responding to prolactin feedback. Activation of the PrlR in Trpc5 deficient Th+ dmARC neurons is still able to produce pSTAT5, suggesting that the JAK/STAT pathway remains intact and should still raise the dopamine content of Th+ dmARC neurons, which remains to be tested, e.g. using high-performance liquid chromatography (HPLC) of labeled Th+ cells in different estrous cycle stages and in unstimulated and prolactin stimulated conditions. Moreover, the phosphorylation of Th – which increases the catecholamine synthesis – should be unaffected. This could be confirmed using phosphorylation site-specific antibodies against Th (Ma et al., 2005a). Prolactin stimulation of Trpc5-deficient Th+ dmARC neurons would then lose its “fast” electrical response and reside on the slower increase of cellular dopamine content and thereby potentially increased vesicular load and dopamine release.

Taken together, the loss of Trpc5 has the potential to increase the dopamine release of Th+ dmARC neurons in a dual manner. Under unstimulated conditions, the oscillatory frequency of burst activity is significantly increased and upon prolactin stimulation dopamine contents can be raised, further increasing the amount of dopamine released.

5. General discussion

Transient receptor potential (Trp) channels – especially the canonical Trp channels – emerge as important key components at multiple stages of neuronal circuits of the hypothalamus that are in control of the endocrine system and regulate reproduction, body homeostasis, stress, defensive and aggressive behavior (Riccio et al., 2002; Fowler et al., 2007; Riccio et al., 2009; Kelly et al., 2018). This thesis yields new insights into the involvement of Trpc5 channels in reproductive pathways. The classical hypothalamic-pituitary-gonadal axis (HPG) relies on gonadotropin-releasing hormone (GnRH), the so-called “master molecule of reproduction” (Gore, 2002). In order to investigate the role of hypothalamic neurons involved in reproduction, I first aimed to verify whether genetically-tagged GnRH receptor (GnRHR) neurons that express GFP (Wen et al., 2011) express a functional GnRHR. The nature of this kind of mice is that the fluorescent marker is continuously expressed once the GnRHR promotor is activated. This could result in a historical labeling with no functional GnRHR present.

All GnRHR neurons recorded in this study responded to GnRH, providing evidence that GnRH directly acts on GnRHR neurons in the brain, and that environmental GnRH in brain areas of the hypothalamus is able to modulate GnRHR neuron activity (Wen et al., 2011; Schauer et al., 2015). GnRH stimulation induces a depolarization and an increase in action potential activity in GnRH neurons. This depolarization could be triggered by either an increased depolarizing conductance or a reduction of the hyperpolarizing current. Upon GnRH stimulation, synaptically-isolated GnRHR neurons that have been segregated of their own action potential activity using TTX produce an inward current.
GnRHR activation is known to be linked to G-protein activation (Tsutsumi et al., 1992), leading to a complex intracellular signaling cascade (Naor, 1990; Ruf et al., 2003; Naor, 2009). GnRHR stimulation is repeatedly linked to the activity of phospholipase C (PLC, Naor and Huhtaniemi, 2013), inducing the conversion of phosphatidylinositol 4,5-bisphosphate (PIP_2) into in inositol 1,4,5-trisphosphate (IP_3) and diacylglycerol (DAG). IP_3 causes calcium release from intracellular stores, whereas DAG activates PKC. Voltage-gated calcium channels (VGCC) are supposed to take part in the intracellular calcium increase (Kraus et al., 2001).

An additional component conducting depolarizing currents could arise from the Trpc channel sub-family. These channels are known to mediate calcium entry, to be receptor operated and PLC activated (Clapham et al., 2001; Clapham, 2003; Vazquez et al., 2004; Venkatachalam and Montell, 2007; Numata et al., 2011). Supporting this hypothesis, Trpc channels show a high expression in neuroendocrine cells of the hypothalamus and developing gonadotroph cells (Fowler et al., 2007; Beck et al., 2017; Gotz et al., 2017; Kelly et al., 2018). Trpc5 has

been proposed to be the link between GnRHR and L-type VGCCs in juvenile gonadotrophs. In addition, Trpc5 is highly expressed in various hypothalamic cell types involved in reproduction (Zhang et al., 2008; Bosch et al., 2013; Zhang et al., 2013a; Zhang et al., 2013b; Qiu et al., 2014). Resulting from this, Trpc5 also emerges as a candidate to mediate GnRHR signaling in the brain. The GnRHR signaling cascade could include GnRH-induced G_q-activation, followed by PLC-dependent breakdown of PIP_2 into IP_3 and DAG, lifting the PIP_2-dependent inhibition and increasing the DAG-sensitivity of Trpc5 channels, causing cation influx and the opening of VGCCs.

There are various ways to provide proof for this hypothesis. Newly-emerging pharmacological tools like HC-070 (Just et al., 2018) or Clemizole hydrochloride (Richter et al., 2014) could be used to block Trpc5 activity in labeled GnRHR neurons stimulated with GnRH. A main disadvantage of these compounds is the possible cross reactivity upon other channel conductances or upon cell viability. In addition to a pharmacological approach, a Trpc5 knockout mouse model should be investigated. This would support the results obtained with pharmacology and provide the possibility to also analyze the consequences of Trpc5-defeciency not only on cellular levels but also in the living organism. If Trpc5 is the key element linking GnRHR to downstream elements of the second messenger cascade, knockout of Trpc5 should affect the regulation of the HPG axis and thereby reproductive capabilities. This would become apparent in changed hormonal levels of luteinizing hormone (LH) and follicle-stimulating hormone (FSH), which could be measured. An unregulated HPG axis and altered gonadotropin levels would strongly affect the reproductive capabilities of Trpc5-deficient mice and is necessary to be analyzed. For this reason, my study focused on the effects of Trpc5 mutation on reproductive function.

With a new concept of Trpc channels as important key molecules in regulation of various homeostatic physiological functions, including reproductive functions, emerging (Kelly et al., 2018), systematic investigation of the effect of mutation of Trpc5 channels on reproductive capabilities was inevitable. In the sub-family of Trpc1, c4 and c5, Trpc5 deletion shows the strongest impact on fertility. I could show that this subfertility is caused by a profound hypoprolactinemia in females associated with irregular reproductive cyclicity, oligoovulation and gonadotropin imbalance, and in males with increased sperm count and asthenozoospermia.

A deficiency in serum levels of prolactin is poorly understood (Arbogast and Voogt, 1991; Rehm et al., 2007; Grattan, 2015; Grattan and Le Tissier, 2015; Rastrelli et al., 2015). To date, no gene defects in any ion channel have been described that cause this medical condition. The pleiotropic hormone prolactin executes a broad spectrum of biological

functions, ranging up to roughly 300 different actions (Larsen and Grattan, 2012; Grattan and Le Tissier, 2015).

In rodents, prolactin is the major luteotropic factor, maintaining the corpus luteum and subsequently progesterone secretion (Grattan and Le Tissier, 2015). In addition to preparing the ovaries and reproductive tract for a pregnancy, prolactin also adapts the body homeostasis to enable successful reproduction. Lack of prolactin – as is common in the postovulatory period – causes luteolysis, the degredation of the corpus luteum (Bachelot and Binart, 2005). Female mice suffering from hypoprolactinemia could display a reduced supply of ovulated oocytes (Cacioppo et al., 2017) and they might not be able to fully maintain corpus luteum function, thus further increasing the chance of nidation deficits or pregnancy failure (Hattori et al., 2017), and thereby reducing the chance of successful pregnancy, the number of pups born and thus also subfertility.

Furthermore, hypoprolactinemia might be able to interfere with proper mammogenesis, lactogenesis and galactopoiesis (Nelson and Gaunt, 1936; Lyons, 1942; Bern and Nicoll, 1968; Cowie et al., 1969; Barber et al., 1992; Anderson et al., 2014). Insufficient milk production and milk nutrition could be the cause of the high lethality of Trpc5-deficient pups that are raised by Trpc5 deficient parents, while reduced prolactin-dependent maternal behavior could also strongly influence pup survival (Grattan, 2001; Larsen and Grattan, 2012; Weber et al., 2013a; Weber et al., 2013b).

Prolactin secretion is uniquely regulated. Spontaneous release of prolactin from lactotroph cells of the anterior pituitary is predominantly inhibited by dopaminergic neurons of the hypothalamus (Fuxe, 1963; MacLeod et al., 1970; Bjorklund et al., 1973; Mansour et al., 1990; Goudreau et al., 1992; Ben-Jonathan and Hnasko, 2001). Dysregulation of prolactin secretion could have its cause in hypothalamic neurons and/or lactotroph cells of the pituitary. Our lab could show that Trpc5 protein is present in Th+ neurons of the dorsomedial ARC but not in prolactin-positive cells of the pituitary (data produced by Ana Moreno-Pérez).
I could show that Trpc5 is a determining factor in the physiological activity of Th+ dmARC neurons. Dopaminergic neurons of the dmARC have been shown to oscillate and release dopamine in a pulsatile fashion (Lyons et al., 2012; Romano et al., 2013). These cells increase their activity upon prolactin stimulation, forming a short feedback loop by switching from oscillatory bursting to long-lasting tonic activity (Lyons et al., 2010; Lyons et al., 2012; Romano et al., 2013; Lyons and Broberger, 2014; Grattan and Le Tissier, 2015). I could confirm these results and show that these neurons show infraslow oscillations (0.02 - 0.05 Hz) and they switch their action potential activity to tonic firing upon prolactin stimulation. Trpc5 actively influences the rhythmic oscillatory burst activity of Th+ dmARC neurons. Trpc5 positively affects burst onset, burst duration and voltage conductance during a burst.

Therefore oscillatory activity in Trpc5-deficient Th+ dmARC neurons is distinctly increased. This suggests that dopamine levels at the median eminence are increased. Elevated amounts of dopamine are transported to lactotroph cells in the anterior pituitary and prolactin secretion is subdued. This is presumably the cause of hypoprolactinemia found in Trpc5 deficient females. Further experiments are needed to confirm this hypothesis. Therefore, dopamine levels at the level of the median eminence should be determined by using either carbon fiber amperometry (Bruns and Jahn, 1995; Staal et al., 2007) or newly-developed fluorescent dopamine indicators (Patriarchi et al., 2018)

Besides the general role of Trpc5 in the upkeep of membrane oscillations, Trpc5 is a key component of the prolactin feedback loop. Prolactin stimulation of Th+ dmARC neurons causes the phosphorylation of STAT5, as well as an increase in electrical activity, with a prominent switch from oscillatory bursting to long-lasting tonic activity (Arbogast and Voogt, 1991; Freeman et al., 2000; Ma et al., 2005b; Ma et al., 2005a; Lyons et al., 2012; Lyons and Broberger, 2014; Grattan and Le Tissier, 2015). Trpc5 is essential to convert the change of burst firing to tonic firing, as Trpc5-deficient Th+ dmARC neurons lack this electrical feature. Therefore, Trpc5 manifests itself as a downstream target of prolactin receptor (PrlR) activation. As the lack of change in firing activity could also be due to a lack or internalization of PrlR itself, I could show that prolactin stimulated phosphorylation of STAT5 is still possible in Trpc5-deficient Th+ dmARC neurons, in both endogenous stimulation occurring in the estrus stage of the reproductive cycle as well as exogenous stimulation with recombinant prolactin. This proves that Trpc5-deficient Th+ dmARC neurons still express a functional PrlR and have the possibility to increase dopamine synthesis but not to change electrical activity. Loss of Trpc5 therefore has the potential to increase the oscillatory frequency of Th+ dmARC neurons, thereby increasing dopamine secretion at the median eminence. In addition, Trpc5-deficiency partially uncouples the prolactin short feedback loop.

In order to counterbalance raised dopamine levels in the arcuate nucleus, I investigated the effect that olfactory cues from a mate reduce dopamine levels in the arcuate nucleus in rodents, thereby increasing prolactin levels and assisting the lactotroph axis (Rosser et al., 1989; Matthews et al., 2013). Assorted breeding pairs of the $Trpc5^{L3F1}$ mouse line did not show the subfertility phenotype that is present in breedings, when both sexes were Trpc5-deficient. On the one hand, this suggests that Trpc5-dependent subfertility is a combinatorial pattern of male and female phenotypes, or on the other hand that olfactory or other cues of mates indeed improve the hypoprolactinemic condition. Other stimuli known to increase prolactin levels are copulation or copulomimetic stimulation (Butcher et al., 1972; Smith and Neill, 1976; Freeman et al., 2000; Bachelot and Binart, 2005; Yang et al., 2009). Preliminary results of this thesis strongly suggest that olfactory stimuli can already counteract the Trpc5-

dependent hypoprolactinemia. Moreover, the presence of a sexually-active mate – in this case a vasectomized male – is able to increase prolactin levels in Trpc5$^{L3F1/L3F1}$ females. Here olfactory as well as copulatory stimuli trend to correct the hypoprolacinemia phenotype.

In addition to the subfertility phenotype in Trpc5-deficient females, mutant males show a trend towards hypoprolactinemia. In humans, male cases of hypoprolactinemia are associated with fertility defects, such as erectile dysfunction, premature ejaculation, sperm defects and hypoandrogenism (Gonzales et al., 1989b; Gonzales et al., 1989a; Corona et al., 2009; Rastrelli et al., 2015). In accordance, I found that Trpc5-deficient males indeed show sperm defects, whereby sperm count was about two-fold higher than in wildtype littermates. However, a more striking phenotype was severe asthenozoospermia. In males, gonadotropins stimulate cells in the testis, regulating testosterone secretion and sperm development (Attia et al., 2013). Blood serum levels of the gonadotropins LH and FSH are a diagnostic tool in human medicine when evaluating androgen deficiency (Bhasin et al., 2018). In Trpc5$^{L3F1/y}$ mice, neither LH nor FSH were altered, indicating a functional HPG axis and subsequently normal testosterone secretion and sperm development. Other causes of sperm defects could arise from the direct involvement of Trpc5 in sperm development, independent of gonadotropin action, as Trpc5 has often been reported in testis tissue preparations (Okada et al., 1998; Philipp et al., 1998; Riccio et al., 2002; Beech, 2007b), but also from the direct function of Trpc5 in spermatozoa themselves, as Trpc5 is reported to be localized at the head and flagellum of human sperm (Kumar et al., 2018; Zhu et al., 2018). In mice the close homologue Trpc4 is localized at the flagellum of spermatozoa, whereas the expression of Trpc5 in sperm and its localization remains controversial (Trevino et al., 2001; Castellano et al., 2003). Nonetheless, the common opinion is that Trpc channels are implicated in sperm motility (Trevino et al., 2001; Castellano et al., 2003; Kumar et al., 2018; Zhu et al., 2018). Altered sperm motility could also be caused by reduced prolactin levels. In human sperm, prolactin is positively correlated with sperm motility and in a negative correlation with sperm count. Therefore in hypoprolactinemic males sperm count would be increased and sperm motility limited, as I could show to be the case in Trpc5$^{L3F1/y}$ male mice.

This thesis provides conclusive evidence that Trpc5 in dopaminergic neurons of the arcuate nucleus directly influences prolactin regulation in the pituitary gland. In further detail, I hypothesize that the altered oscillatory pattern of Trpc5-deficient dmARC neurons influences the release of dopamine into the hypothalamo-hypophyseal tract. This altered dopamine release further causes a hypoprolactinemic phenotype and subsequent subfertility. As this thesis has only examined global mutations of Trpc5 and the impact of Trpc5 deletion in other areas of the brain and/or body cannot be excluded. This renders further investigations of

conditional Trpc5 only in dopaminergic ARC neurons indispensable, although we could not find Trpc5 in lactotroph cells. Trpc5 might at least influence juvenile murine gonadotrop function (Beck et al., 2017) but seems to lose its impact in adulthood. This thesis is a start towards studying Trpc5 channelopathies as a cause for prolactin dysregulation or other dysfunctions or disease in humans. In addition to progress in pharmacological modulation of Trpc5 (Just et al., 2018) and further fundamental research on Trpc channels, such research initiatives could explore new treatment possibilities, improving prolactin dysregulation, reproductive disorders and other dysfunctions associated with Trpc5.

6. References

Akbulut Y, Gaunt HJ, Muraki K, Ludlow MJ, Amer MS, Bruns A, Vasudev NS, Radtke L, Willot M, Hahn S, Seitz T, Ziegler S, Christmann M, Beech DJ, Waldmann H (2015) (-)-Englerin A is a Potent and Selective Activator of TRPC4 and TRPC5 Calcium Channels. Angewandte Chemie.

Anderson SM, MacLean PS, McManaman JL, Neville MC (2014) Lactation and its Hormonal Control. In: Knobil and Neill's Physiology of Reproduction, 4th Edition (Plant TM, Zeleznik AJ, eds), pp 2055-2092: Elsevier.

Andrews ZB, Kokay IC, Grattan DR (2001) Dissociation of prolactin secretion from tuberoinfundibular dopamine activity in late pregnant rats. Endocrinology 142:2719-2724.

Arbogast LA, Voogt JL (1991) Hyperprolactinemia increases and hypoprolactinemia decreases tyrosine hydroxylase messenger ribonucleic acid levels in the arcuate nuclei, but not the substantia nigra or zona incerta. Endocrinology 128:997-1005.

Arbogast LA, Soares MJ, Tomogane H, Voogt JL (1992) A trophoblast-specific factor(s) suppresses circulating prolactin levels and increases tyrosine hydroxylase activity in tuberoinfundibular dopaminergic neurons. Endocrinology 131:105-113.

Arimura A, Dunn JD, Schally AV (1972) Effect of infusion of hypothalamic extracts on serum prolactin levels in rats treated with nembutal, CNS depressants or bearing hypothalamic lesions. Endocrinology 90:378-383.

Attia AM, Abou-Setta AM, Al-Inany HG (2013) Gonadotrophins for idiopathic male factor subfertility. Cochrane Database Syst Rev:CD005071.

Bachelot A, Binart N (2005) Corpus luteum development: lessons from genetic models in mice. Curr Top Dev Biol 68:49-84.

Badr M, Pelletier G (1987) Characterization and autoradiographic localization of LHRH receptors in the rat brain. Synapse 1:567-571.

Barber MC, Clegg RA, Finley E, Vernon RG, Flint DJ (1992) The role of growth hormone, prolactin and insulin-like growth factors in the regulation of rat mammary gland and adipose tissue metabolism during lactation. The Journal of endocrinology 135:195-202.

Beck A, Gotz V, Qiao S, Weissgerber P, Flockerzi V, Freichel M, Boehm U (2017) Functional Characterization of Transient Receptor Potential (TRP) Channel C5 in Female Murine Gonadotropes. Endocrinology 158:887-902.

Beech DJ (2007a) Bipolar phospholipid sensing by TRPC5 calcium channel. Biochemical Society transactions 35:101-104.

Beech DJ (2007b) Canonical transient receptor potential 5. Handbook of experimental pharmacology:109-123.

Beech DJ (2012) Integration of transient receptor potential canonical channels with lipids. Acta Physiol (Oxf) 204:227-237.

Bellringer JF, Pratt HP, Keverne EB (1980) Involvement of the vomeronasal organ and prolactin in pheromonal induction of delayed implantation in mice. J Reprod Fertil 59:223-228.

Ben-Jonathan N, Hnasko R (2001) Dopamine as a prolactin (PRL) inhibitor. Endocrine reviews 22:724-763.

Berg AP, Sen N, Bayliss DA (2007) TrpC3/C7 and Slo2.1 are molecular targets for metabotropic glutamate receptor signaling in rat striatal cholinergic interneurons. The Journal of neuroscience : the official journal of the Society for Neuroscience 27:8845-8856.

Bern HA, Nicoll CS (1968) The comparative endocrinology of prolactin. Recent Prog Horm Res 24:681-720.

Bhasin S, Brito JP, Cunningham GR, Hayes FJ, Hodis HN, Matsumoto AM, Snyder PJ, Swerdloff RS, Wu FC, Yialamas MA (2018) Testosterone Therapy in Men With Hypogonadism: An Endocrine Society Clinical Practice Guideline. J Clin Endocrinol Metab 103:1715-1744.

Binart N, Melaine N, Pineau C, Kercret H, Touzalin AM, Imbert-Bollore P, Kelly PA, Jegou B (2003) Male reproductive function is not affected in prolactin receptor-deficient mice. Endocrinology 144:3779-3782.

Bjorklund A, Moore RY, Nobin A, Stenevi U (1973) The organization of tubero-hypophyseal and reticulo-infundibular catecholamine neuron systems in the rat brain. Brain research 51:171-191.

Bosch MA, Tonsfeldt KJ, Ronnekleiv OK (2013) mRNA expression of ion channels in GnRH neurons: subtype-specific regulation by 17beta-estradiol. Mol Cell Endocrinol 367:85-97.

Brennan PA (2009) Outstanding issues surrounding vomeronasal mechanisms of pregnancy block and individual recognition in mice. Behav Brain Res 200:287-294.

Broker-Lai J, Kollewe A, Schindeldecker B, Pohle J, Nguyen Chi V, Mathar I, Guzman R, Schwarz Y, Lai A, Weissgerber P, Schwegler H, Dietrich A, Both M, Sprengel R, Draguhn A, Kohr G, Fakler B, Flockerzi V, Bruns D, Freichel M (2017) Heteromeric channels formed by TRPC1, TRPC4 and TRPC5 define hippocampal synaptic transmission and working memory. The EMBO journal 36:2770-2789.

Brown RS, Piet R, Herbison AE, Grattan DR (2012) Differential actions of prolactin on electrical activity and intracellular signal transduction in hypothalamic neurons. Endocrinology 153:2375-2384.

Brown RSE, Khant Aung Z, Phillipps HR, Barad Z, Lein HJ, Boehm U, Szawka RE, Grattan DR (2019) Acute suppression of LH secretion by prolactin in female mice is mediated by kisspeptin neurons in the arcuate nucleus. Endocrinology.

Bruce HM (1959) An exteroceptive block to pregnancy in the mouse. Nature 184:105.

Bruce HM (1968) Absence of pregnancy-block in mice when stud and test males belong to an inbred strain. J Reprod Fertil 17:407-408.

Bruce HM (1969) Pheromones and behavior in mice. Acta Neurol Psychiatr Belg 69:529-538.

Bruns D, Jahn R (1995) Real-time measurement of transmitter release from single synaptic vesicles. Nature 377:62-65.

Butcher RL, Fugo NW, Collins WE (1972) Semicircadian rhythm in plasma levels of prolactin during early gestation in the rat. Endocrinology 90:1125-1127.

Butcher RL, Collins WE, Fugo NW (1974) Plasma concentration of LH, FSH, prolactin, progesterone and estradiol-17beta throughout the 4-day estrous cycle of the rat. Endocrinology 94:1704-1708.

Byers SL, Wiles MV, Dunn SL, Taft RA (2012) Mouse estrous cycle identification tool and images. PloS one 7:e35538.

Cacioppo JA, Lin PP, Hannon PR, McDougle DR, Gal A, Ko C (2017) Granulosa cell endothelin-2 expression is fundamental for ovulatory follicle rupture. Sci Rep 7:817.

Caligioni CS (2009) Assessing reproductive status/stages in mice. Curr Protoc Neurosci Appendix 4:Appendix 4I.

Castellano LE, Trevino CL, Rodriguez D, Serrano CJ, Pacheco J, Tsutsumi V, Felix R, Darszon A (2003) Transient receptor potential (TRPC) channels in human sperm: expression, cellular localization and involvement in the regulation of flagellar motility. FEBS letters 541:69-74.

Cheung CY (1983) Prolactin suppresses luteinizing hormone secretion and pituitary responsiveness to luteinizing hormone-releasing hormone by a direct action at the anterior pituitary. Endocrinology 113:632-638.

Chrousos GP, Torpy DJ, Gold PW (1998) Interactions between the hypothalamic-pituitary-adrenal axis and the female reproductive system: clinical implications. Ann Intern Med 129:229-240.

Clapham DE (2003) TRP channels as cellular sensors. Nature 426:517-524.

Clapham DE, Runnels LW, Strubing C (2001) The TRP ion channel family. Nature reviews Neuroscience 2:387-396.

Clarke IJ (1987) GnRH and ovarian hormone feedback. Oxf Rev Reprod Biol 9:54-95.

Clarke IJ, Cummins JT (1982) The temporal relationship between gonadotropin releasing hormone (GnRH) and luteinizing hormone (LH) secretion in ovariectomized ewes. Endocrinology 111:1737-1739.

Clarke IJ, Campbell R, Smith JT, Prevot V, Wray S (2012) Neuroendocrine Control of Reproduction. In: Handbook of Neuroendocrinology (Fink G, Pfaff D, Levine JE, eds), pp 197-235: Elsevier.

Cohen-Becker IR, Selmanoff M, Wise PM (1986) Hyperprolactinemia alters the frequency and amplitude of pulsatile luteinizing hormone secretion in the ovariectomized rat. Neuroendocrinology 42:328-333.

Colby DR, Vandenberg JG (1974) Regulatory effects of urinary pheromones on puberty in the mouse. Biology of reproduction 11:268-279.

Corona G, Mannucci E, Jannini EA, Lotti F, Ricca V, Monami M, Boddi V, Bandini E, Balercia G, Forti G, Maggi M (2009) Hypoprolactinemia: a new clinical syndrome in patients with sexual dysfunction. J Sex Med 6:1457-1466.

Cowie AT, Hartmann PE, Turvey A (1969) The maintenance of lactation in the rabbit after hypophysectomy. The Journal of endocrinology 43:651-662.

Davis AS (2011) The handbook of pediatric neuropsychology. New York: Springer.

De Rosa M, Zarrilli S, Di Sarno A, Milano N, Gaccione M, Boggia B, Lombardi G, Colao A (2003) Hyperprolactinemia in men: clinical and biochemical features and response to treatment. Endocrine 20:75-82.

Dietrich A, Kalwa H, Storch U, Mederos y Schnitzler M, Salanova B, Pinkenburg O, Dubrovska G, Essin K, Gollasch M, Birnbaumer L, Gudermann T (2007) Pressure-induced and store-operated cation influx in vascular smooth muscle cells is independent of TRPC1. Pflugers Archiv : European journal of physiology 455:465-477.

Egli M, Leeners B, Kruger TH (2010) Prolactin secretion patterns: basic mechanisms and clinical implications for reproduction. Reproduction 140:643-654.

Fauser B, Tarlatzis B, Chang J, Group TREA-SPCW (2004) Revised 2003 consensus on diagnostic criteria and long-term health risks related to polycystic ovary syndrome. Fertil Steril 81:19-25.

Fink G, Jamieson MG (1976) Immunoreactive luteinizing hormone releasing factor in rat pituitary stalk blood: effects of electrical stimulation of the medial preoptic area. The Journal of endocrinology 68:71-87.

Fowler MA, Sidiropoulou K, Ozkan ED, Phillips CW, Cooper DC (2007) Corticolimbic expression of TRPC4 and TRPC5 channels in the rodent brain. PloS one 2:e573.

Freeman ME, Kanyicska B, Lerant A, Nagy G (2000) Prolactin: structure, function, and regulation of secretion. Physiological reviews 80:1523-1631.

Freichel M, Suh SH, Pfeifer A, Schweig U, Trost C, Weissgerber P, Biel M, Philipp S, Freise D, Droogmans G, Hofmann F, Flockerzi V, Nilius B (2001) Lack of an endothelial store-operated Ca2+ current impairs agonist-dependent vasorelaxation in TRP4-/- mice. Nature cell biology 3:121-127.

Frontini A, Bertolotti P, Tonello C, Valerio A, Nisoli E, Cinti S, Giordano A (2008) Leptin-dependent STAT3 phosphorylation in postnatal mouse hypothalamus. Brain research 1215:105-115.

Fuxe K (1963) Cellular Localization of Monoamines in the Median Eminence and in the Infundibular Stem of Some Mammals. Acta Physiol Scand 58:383-384.

Goldman JM, Murr AS, Cooper RL (2007) The rodent estrous cycle: characterization of vaginal cytology and its utility in toxicological studies. Birth Defects Res B Dev Reprod Toxicol 80:84-97.

Gomis A, Soriano S, Belmonte C, Viana F (2008) Hypoosmotic- and pressure-induced membrane stretch activate TRPC5 channels. The Journal of physiology 586:5633-5649.

Gonzales GF, Velasquez G, Garcia-Hjarles M (1989a) Hypoprolactinemia as related to seminal quality and serum testosterone. Arch Androl 23:259-265.

Gonzales GF, Garcia-Hjarles M, Velazquez G, Coyotupa J (1989b) Seminal prolactin and its relationship to sperm motility in men. Fertil Steril 51:498-503.

Gore AC (2002) GnRH: The Master Molecule of Reproduction: Kluwer Academic Publishers.

Gorin M, Tsitoura C, Kahan A, Watznauer K, Drose DR, Arts M, Mathar R, O'Connor S, Hanganu-Opatz IL, Ben-Shaul Y, Spehr M (2016) Interdependent Conductances Drive Infraslow Intrinsic Rhythmogenesis in a Subset of Accessory Olfactory Bulb Projection Neurons. The Journal of neuroscience : the official journal of the Society for Neuroscience 36:3127-3144.

Gorospe WC, Freeman ME (1985) Effects of placenta and maternal serum on prolactin secretion in vitro. Biology of reproduction 32:279-283.

Gotz V, Qiao S, Beck A, Boehm U (2017) Transient receptor potential (TRP) channel function in the reproductive axis. Cell calcium.

Goudreau JL, Lindley SE, Lookingland KJ, Moore KE (1992) Evidence that hypothalamic periventricular dopamine neurons innervate the intermediate lobe of the rat pituitary. Neuroendocrinology 56:100-105.

Grattan DR (2001) The actions of prolactin in the brain during pregnancy and lactation. Prog Brain Res 133:153-171.

Grattan DR (2015) 60 YEARS OF NEUROENDOCRINOLOGY: The hypothalamo-prolactin axis. The Journal of endocrinology 226:T101-122.

Grattan DR, Le Tissier P (2015) Hypothalamic Control of Prolactin Secretion, and the Multiple Reproductive Functions of Prolactin. Physiology of Reproduction:469-526.

Grattan DR, Jasoni CL, Liu X, Anderson GM, Herbison AE (2007) Prolactin regulation of gonadotropin-releasing hormone neurons to suppress luteinizing hormone secretion in mice. Endocrinology 148:4344-4351.

Grattan DR, Xu J, McLachlan MJ, Kokay IC, Bunn SJ, Hovey RC, Davey HW (2001) Feedback regulation of PRL secretion is mediated by the transcription factor, signal transducer, and activator of transcription 5b. Endocrinology 142:3935-3940.

Guillaumot P, Tabone E, Benahmed M (1996) Sertoli cells as potential targets of prolactin action in the testis. Mol Cell Endocrinol 122:199-206.

Hansen S, Sodersten P, Eneroth P (1983) Mechanisms regulating hormone release and the duration of dioestrus in the lactating rat. The Journal of endocrinology 99:173-180.

Hattori T, Osakada T, Masaoka T, Ooyama R, Horio N, Mogi K, Nagasawa M, Haga-Yamanaka S, Touhara K, Kikusui T (2017) Exocrine Gland-Secreting Peptide 1 Is a Key Chemosensory Signal Responsible for the Bruce Effect in Mice. Current biology : CB 27:3197-3201 e3193.

Helena CV, McKee DT, Bertram R, Walker AM, Freeman ME (2009) The rhythmic secretion of mating-induced prolactin secretion is controlled by prolactin acting centrally. Endocrinology 150:3245-3251.

Helena CV, Cristancho-Gordo R, Gonzalez-Iglesias AE, Tabak J, Bertram R, Freeman ME (2011) Systemic oxytocin induces a prolactin secretory rhythm via the pelvic nerve in ovariectomized rats. Am J Physiol Regul Integr Comp Physiol 301:R676-681.

Hofmann T, Schaefer M, Schultz G, Gudermann T (2002) Subunit composition of mammalian transient receptor potential channels in living cells. Proceedings of the National Academy of Sciences of the United States of America 99:7461-7466.

Hofmann T, Obukhov AG, Schaefer M, Harteneck C, Gudermann T, Schultz G (1999) Direct activation of human TRPC6 and TRPC3 channels by diacylglycerol. Nature 397:259-263.

Holzbauer M, Racke K (1985) The dopaminergic innervation of the intermediate lobe and of the neural lobe of the pituitary gland. Med Biol 63:97-116.

Horseman ND, Zhao W, Montecino-Rodriguez E, Tanaka M, Nakashima K, Engle SJ, Smith F, Markoff E, Dorshkind K (1997) Defective mammopoiesis, but normal hematopoiesis, in mice with a targeted disruption of the prolactin gene. The EMBO journal 16:6926-6935.

Jemal I, Soriano S, Conte AL, Morenilla C, Gomis A (2014) G protein-coupled receptor signalling potentiates the osmo-mechanical activation of TRPC5 channels. Pflugers Archiv : European journal of physiology 466:1635-1646.

Jemiolo B, Novotny M (1994) Inhibition of sexual maturation in juvenile female and male mice by a chemosignal of female origin. Physiol Behav 55:519-522.

Jennes L, Eyigor O, Janovick JA, Conn PM (1997) Brain gonadotropin releasing hormone receptors: localization and regulation. Recent Prog Horm Res 52:475-490; discussion 490-471.

Jeon JP, Hong C, Park EJ, Jeon JH, Cho NH, Kim IG, Choe H, Muallem S, Kim HJ, So I (2012) Selective Galphai subunits as novel direct activators of transient receptor potential canonical (TRPC)4 and TRPC5 channels. The Journal of biological chemistry 287:17029-17039.

Just S et al. (2018) Treatment with HC-070, a potent inhibitor of TRPC4 and TRPC5, leads to anxiolytic and antidepressant effects in mice. PloS one 13:e0191225.

Kanematsu S, Sawyer CH (1973) Elevation of plasma prolactin after hypophysial stalk section in the rat. Endocrinology 93:238-241.

Kanki H, Kinoshita M, Akaike A, Satoh M, Mori Y, Kaneko S (2001) Activation of inositol 1,4,5-trisphosphate receptor is essential for the opening of mouse TRP5 channels. Molecular pharmacology 60:989-998.

Kauppila A, Martikainen H, Puistola U, Reinila M, Ronnberg L (1988) Hypoprolactinemia and ovarian function. Fertil Steril 49:437-441.

Kelly MJ, Qiu J, Ronnekleiv OK (2018) TRPCing around the hypothalamus. Frontiers in neuroendocrinology.

Kimchi T, Xu J, Dulac C (2007) A functional circuit underlying male sexual behaviour in the female mouse brain. Nature 448:1009-1014.

Kokay IC, Grattan DR (2005) Expression of mRNA for prolactin receptor (long form) in dopamine and pro-opiomelanocortin neurones in the arcuate nucleus of non-pregnant and lactating rats. Journal of neuroendocrinology 17:827-835.

Kokay IC, Petersen SL, Grattan DR (2011) Identification of prolactin-sensitive GABA and kisspeptin neurons in regions of the rat hypothalamus involved in the control of fertility. Endocrinology 152:526-535.

Kong L, Tang M, Zhang T, Wang D, Hu K, Lu W, Wei C, Liang G, Pu Y (2014) Nickel nanoparticles exposure and reproductive toxicity in healthy adult rats. Int J Mol Sci 15:21253-21269.

Koyama S, Kamimura S (2000) Influence of social dominance and female odor on the sperm activity of male mice. Physiol Behav 71:415-422.

Kraus S, Naor Z, Seger R (2001) Intracellular signaling pathways mediated by the gonadotropin-releasing hormone (GnRH) receptor. Archives of medical research 32:499-509.

Kucka M, Kretschmannova K, Stojilkovic SS, Zemkova H, Tomic M (2012) Dependence of spontaneous electrical activity and basal prolactin release on nonselective cation channels in pituitary lactotrophs. Physiol Res 61:267-275.

Kumar A, Mishra AK, Swain DK, Singh V, Yadav S, Saxena A (2018) Role of transient receptor potential channels in regulating spermatozoa functions: A mini-review. Vet World 11:1618-1623.

Kumar TR, Wang Y, Lu N, Matzuk MM (1997) Follicle stimulating hormone is required for ovarian follicle maturation but not male fertility. Nature genetics 15:201-204.

Larsen CM, Grattan DR (2010) Prolactin-induced mitogenesis in the subventricular zone of the maternal brain during early pregnancy is essential for normal postpartum behavioral responses in the mother. Endocrinology 151:3805-3814.

Larsen CM, Grattan DR (2012) Prolactin, neurogenesis, and maternal behaviors. Brain Behav Immun 26:201-209.

Le Tissier PR, Hodson DJ, Martin AO, Romano N, Mollard P (2015) Plasticity of the prolactin (PRL) axis: mechanisms underlying regulation of output in female mice. Advances in experimental medicine and biology 846:139-162.

Lee YM, Kim BJ, Kim HJ, Yang DK, Zhu MH, Lee KP, So I, Kim KW (2003) TRPC5 as a candidate for the nonselective cation channel activated by muscarinic stimulation in murine stomach. American journal of physiology Gastrointestinal and liver physiology 284:G604-616.

Leinders-Zufall T, Brennan P, Widmayer P, S PC, Maul-Pavicic A, Jager M, Li XH, Breer H, Zufall F, Boehm T (2004) MHC class I peptides as chemosensory signals in the vomeronasal organ. Science 306:1033-1037.

Lerant A, Freeman ME (1998) Ovarian steroids differentially regulate the expression of PRL-R in neuroendocrine dopaminergic neuron populations: a double label confocal microscopic study. Brain research 802:141-154.

Lerant A, Herman ME, Freeman ME (1996) Dopaminergic neurons of periventricular and arcuate nuclei of pseudopregnant rats: semicircadian rhythm in Fos-related antigens immunoreactivities and in dopamine concentration. Endocrinology 137:3621-3628.

Lerant A, Kanyicska B, Freeman ME (2001) Nuclear translocation of STAT5 and increased expression of Fos related antigens (FRAs) in hypothalamic dopaminergic neurons after prolactin administration. Brain research 904:259-269.

Lewandowski KC, Cajdler-Luba A, Salata I, Bienkiewicz M, Lewinski A (2011) The utility of the gonadotrophin releasing hormone (GnRH) test in the diagnosis of polycystic ovary syndrome (PCOS). Endokrynol Pol 62:120-128.

Leypold BG, Yu CR, Leinders-Zufall T, Kim MM, Zufall F, Axel R (2002) Altered sexual and social behaviors in trp2 mutant mice. Proceedings of the National Academy of Sciences of the United States of America 99:6376-6381.

Liman ER, Corey DP, Dulac C (1999) TRP2: a candidate transduction channel for mammalian pheromone sensory signaling. Proceedings of the National Academy of Sciences of the United States of America 96:5791-5796.

Liu X, Lee K, Herbison AE (2008) Kisspeptin excites gonadotropin-releasing hormone neurons through a phospholipase C/calcium-dependent pathway regulating multiple ion channels. Endocrinology 149:4605-4614.

Long MA, Landisman CE, Connors BW (2004) Small clusters of electrically coupled neurons generate synchronous rhythms in the thalamic reticular nucleus. The Journal of neuroscience : the official journal of the Society for Neuroscience 24:341-349.

Lyons DJ, Broberger C (2014) TIDAL WAVES: Network mechanisms in the neuroendocrine control of prolactin release. Frontiers in neuroendocrinology 35:420-438.

Lyons DJ, Horjales-Araujo E, Broberger C (2010) Synchronized network oscillations in rat tuberoinfundibular dopamine neurons: switch to tonic discharge by thyrotropin-releasing hormone. Neuron 65:217-229.

Lyons DJ, Hellysaz A, Broberger C (2012) Prolactin regulates tuberoinfundibular dopamine neuron discharge pattern: novel feedback control mechanisms in the lactotrophic axis. The Journal of neuroscience : the official journal of the Society for Neuroscience 32:8074-8083.

Lyons WR (1942) The direct mammotrophic action of lactogenic hormone. Proc Soc Exp Biol Med 51:308-311.

Ma FY, Grattan DR, Goffin V, Bunn SJ (2005a) Prolactin-regulated tyrosine hydroxylase activity and messenger ribonucleic acid expression in mediobasal hypothalamic cultures: the differential role of specific protein kinases. Endocrinology 146:93-102.

Ma FY, Anderson GM, Gunn TD, Goffin V, Grattan DR, Bunn SJ (2005b) Prolactin specifically activates signal transducer and activator of transcription 5b in neuroendocrine dopaminergic neurons. Endocrinology 146:5112-5119.

MacLeod RM, Fontham EH, Lehmeyer JE (1970) Prolactin and growth hormone production as influenced by catecholamines and agents that affect brain catecholamines. Neuroendocrinology 6:283-294.

Macrides F, Bartke A, Dalterio S (1975) Strange females increase plasma testosterone levels in male mice. Science 189:1104-1106.

Madisen L, Zwingman TA, Sunkin SM, Oh SW, Zariwala HA, Gu H, Ng LL, Palmiter RD, Hawrylycz MJ, Jones AR, Lein ES, Zeng H (2010) A robust and high-throughput Cre reporting and characterization system for the whole mouse brain. Nature neuroscience 13:133-140.

Mansour A, Meador-Woodruff JH, Bunzow JR, Civelli O, Akil H, Watson SJ (1990) Localization of dopamine D2 receptor mRNA and D1 and D2 receptor binding in the rat brain and pituitary: an in situ hybridization-receptor autoradiographic analysis. The Journal of neuroscience : the official journal of the Society for Neuroscience 10:2587-2600.

Matthews GA, Patel R, Walsh A, Davies O, Martinez-Ricos J, Brennan PA (2013) Mating increases neuronal tyrosine hydroxylase expression and selectively gates transmission of male chemosensory information in female mice. PloS one 8:e69943.

McClintock MK (1984) Estrous synchrony: modulation of ovarian cycle length by female pheromones. Physiol Behav 32:701-705.

McKee DT, Poletini MO, Bertram R, Freeman ME (2007) Oxytocin action at the lactotroph is required for prolactin surges in cervically stimulated ovariectomized rats. Endocrinology 148:4649-4657.

McVeigh E, Guillebaud J, Homburg R (2013) Reproductive Medicine and Family Planning, 2 Edition: Oxford University Press.

Mederos YSM, Gudermann T, Storch U (2018) Emerging Roles of Diacylglycerol-Sensitive TRPC4/5 Channels. Cells 7.

Miller BH, Takahashi JS (2013) Central circadian control of female reproductive function. Front Endocrinol (Lausanne) 4:195.

Minard A, Bauer CC, Wright DJ, Rubaiy HN, Muraki K, Beech DJ, Bon RS (2018) Remarkable Progress with Small-Molecule Modulation of TRPC1/4/5 Channels: Implications for Understanding the Channels in Health and Disease. Cells 7.

Montell C, Birnbaumer L, Flockerzi V, Bindels RJ, Bruford EA, Caterina MJ, Clapham DE, Harteneck C, Heller S, Julius D, Kojima I, Mori Y, Penner R, Prawitt D, Scharenberg AM, Schultz G, Shimizu N, Zhu MX (2002) A unified nomenclature for the superfamily of TRP cation channels. Mol Cell 9:229-231.

Munger SD, Leinders-Zufall T, Zufall F (2009) Subsystem organization of the mammalian sense of smell. Annual review of physiology 71:115-140.

Munzberg H, Huo L, Nillni EA, Hollenberg AN, Bjorbaek C (2003) Role of signal transducer and activator of transcription 3 in regulation of hypothalamic proopiomelanocortin gene expression by leptin. Endocrinology 144:2121-2131.

Murray SA, Morgan JL, Kane C, Sharma Y, Heffner CS, Lake J, Donahue LR (2010) Mouse gestation length is genetically determined. PloS one 5:e12418.

Naor Z (1990) Signal transduction mechanisms of Ca2+ mobilizing hormones: the case of gonadotropin-releasing hormone. Endocrine reviews 11:326-353.

Naor Z (2009) Signaling by G-protein-coupled receptor (GPCR): studies on the GnRH receptor. Frontiers in neuroendocrinology 30:10-29.

Naor Z, Huhtaniemi I (2013) Interactions of the GnRH receptor with heterotrimeric G proteins. Frontiers in neuroendocrinology 34:88-94.

Neill JD, Reichert LE, Jr. (1971) Development of a radioimmunoassay for rat prolactin and evaluation of the NIAMD rat prolactin radioimmunoassay. Endocrinology 88:548-555.

Nelson WO, Gaunt R (1936) Initiation of lactation in the hypophysectomized guinea pig. Proc Soc Exp Biol Med 33:488-526.

Nesin V, Tsiokas L (2014) Trpc1. Handbook of experimental pharmacology 222:15-51.

Numata T, Kiyonaka S, Kato K, Takahashi N, Mori Y (2011) Activation of TRP Channels in Mammalian Systems. In: TRP Channels (Zhu MX, ed). Boca Raton (FL).

Oboti L, Perez-Gomez A, Keller M, Jacobi E, Birnbaumer L, Leinders-Zufall T, Zufall F, Chamero P (2014) A wide range of pheromone-stimulated sexual and reproductive behaviors in female mice depend on G protein Galphao. BMC Biol 12:31.

Okada T, Shimizu S, Wakamori M, Maeda A, Kurosaki T, Takada N, Imoto K, Mori Y (1998) Molecular cloning and functional characterization of a novel receptor-activated TRP Ca2+ channel from mouse brain. The Journal of biological chemistry 273:10279-10287.

Ormandy CJ, Camus A, Barra J, Damotte D, Lucas B, Buteau H, Edery M, Brousse N, Babinet C, Binart N, Kelly PA (1997) Null mutation of the prolactin receptor gene produces multiple reproductive defects in the mouse. Genes & development 11:167-178.

Owsianik G, Talavera K, Voets T, Nilius B (2006) Permeation and selectivity of TRP channels. Annual review of physiology 68:685-717.

Oyola MG, Handa RJ (2017) Hypothalamic-pituitary-adrenal and hypothalamic-pituitary-gonadal axes: sex differences in regulation of stress responsivity. Stress 20:476-494.

Patriarchi T, Cho JR, Merten K, Howe MW, Marley A, Xiong WH, Folk RW, Broussard GJ, Liang R, Jang MJ, Zhong H, Dombeck D, von Zastrow M, Nimmerjahn A, Gradinaru V, Williams JT, Tian L (2018) Ultrafast neuronal imaging of dopamine dynamics with designed genetically encoded sensors. Science 360.

Phelan KD, Shwe UT, Abramowitz J, Wu H, Rhee SW, Howell MD, Gottschall PE, Freichel M, Flockerzi V, Birnbaumer L, Zheng F (2013) Canonical transient receptor channel 5 (TRPC5) and TRPC1/4 contribute to seizure and excitotoxicity by distinct cellular mechanisms. Molecular pharmacology 83:429-438.

Philipp S, Hambrecht J, Braslavski L, Schroth G, Freichel M, Murakami M, Cavalie A, Flockerzi V (1998) A novel capacitative calcium entry channel expressed in excitable cells. The EMBO journal 17:4274-4282.

Piet R, Boehm U, Herbison AE (2013) Estrous cycle plasticity in the hyperpolarization-activated current ih is mediated by circulating 17beta-estradiol in preoptic area kisspeptin neurons. The Journal of neuroscience : the official journal of the Society for Neuroscience 33:10828-10839.

Plant TD, Schaefer M (2003) TRPC4 and TRPC5: receptor-operated Ca2+-permeable nonselective cation channels. Cell calcium 33:441-450.

Purvis K, Clausen OP, Olsen A, Haug E, Hansson V (1979) Prolactin and Leydig cell responsiveness to LH/hCG in the rat. Arch Androl 3:219-230.

Qiu J, Fang Y, Ronnekleiv OK, Kelly MJ (2010) Leptin excites proopiomelanocortin neurons via activation of TRPC channels. The Journal of neuroscience : the official journal of the Society for Neuroscience 30:1560-1565.

Qiu J, Wagner EJ, Ronnekleiv OK, Kelly MJ (2018) Insulin and leptin excite anorexigenic pro-opiomelanocortin neurones via activation of TRPC5 channels. Journal of neuroendocrinology 30.

Qiu J, Zhang C, Borgquist A, Nestor CC, Smith AW, Bosch MA, Ku S, Wagner EJ, Ronnekleiv OK, Kelly MJ (2014) Insulin excites anorexigenic proopiomelanocortin neurons via activation of canonical transient receptor potential channels. Cell Metab 19:682-693.

Radovick S, Levine JE, Wolfe A (2012) Estrogenic regulation of the GnRH neuron. Front Endocrinol (Lausanne) 3:52.

Rastrelli G, Corona G, Maggi M (2015) The role of prolactin in andrology: what is new? Rev Endocr Metab Disord 16:233-248.

Rehm S, Stanislaus DJ, Wier PJ (2007) Identification of drug-induced hyper- or hypoprolactinemia in the female rat based on general and reproductive toxicity study parameters. Birth Defects Res B Dev Reprod Toxicol 80:253-257.

Riccio A, Medhurst AD, Mattei C, Kelsell RE, Calver AR, Randall AD, Benham CD, Pangalos MN (2002) mRNA distribution analysis of human TRPC family in CNS and peripheral tissues. Brain research Molecular brain research 109:95-104.

Riccio A, Li Y, Moon J, Kim KS, Smith KS, Rudolph U, Gapon S, Yao GL, Tsvetkov E, Rodig SJ, Van't Veer A, Meloni EG, Carlezon WA, Jr., Bolshakov VY, Clapham DE (2009) Essential role for TRPC5 in amygdala function and fear-related behavior. Cell 137:761-772.

Richter JM, Schaefer M, Hill K (2014) Clemizole Hydrochloride is a Novel and Potent Inhibitor of Transient Receptor Potential Channel TRPC5. Molecular pharmacology.

Romano N, Yip SH, Hodson DJ, Guillou A, Parnaudeau S, Kirk S, Tronche F, Bonnefont X, Le Tissier P, Bunn SJ, Grattan DR, Mollard P, Martin AO (2013) Plasticity of hypothalamic dopamine neurons during lactation results in dissociation of electrical activity and release. The Journal of neuroscience : the official journal of the Society for Neuroscience 33:4424-4433.

Ronnekleiv OK, Kelly MJ (2013) Kisspeptin excitation of GnRH neurons. Advances in experimental medicine and biology 784:113-131.

Ronnekleiv OK, Zhang C, Bosch MA, Kelly MJ (2015) Kisspeptin and Gonadotropin-Releasing Hormone Neuronal Excitability: Molecular Mechanisms Driven by 17beta-Estradiol. Neuroendocrinology 102:184-193.

Rosser AE, Remfry CJ, Keverne EB (1989) Restricted exposure of mice to primer pheromones coincident with prolactin surges blocks pregnancy by changing hypothalamic dopamine release. J Reprod Fertil 87:553-559.

Ruf F, Fink MY, Sealfon SC (2003) Structure of the GnRH receptor-stimulated signaling network: insights from genomics. Frontiers in neuroendocrinology 24:181-199.

Samonds JM, Bonds AB (2005) Gamma oscillation maintains stimulus structure-dependent synchronization in cat visual cortex. Journal of neurophysiology 93:223-236.

Sarkar DK, Chiappa SA, Fink G, Sherwood NM (1976) Gonadotropin-releasing hormone surge in pro-oestrous rats. Nature 264:461-463.

Savitt JM, Jang SS, Mu W, Dawson VL, Dawson TM (2005) Bcl-x is required for proper development of the mouse substantia nigra. The Journal of neuroscience : the official journal of the Society for Neuroscience 25:6721-6728.

Schaefer M, Plant TD, Obukhov AG, Hofmann T, Gudermann T, Schultz G (2000) Receptor-mediated regulation of the nonselective cation channels TRPC4 and TRPC5. The Journal of biological chemistry 275:17517-17526.

Schauer C, Leinders-Zufall T (2012) Imaging calcium responses in GFP-tagged neurons of hypothalamic mouse brain slices. Journal of visualized experiments : JoVE:e4213.

Schauer C, Tong T, Petitjean H, Blum T, Peron S, Mai O, Schmitz F, Boehm U, Leinders-Zufall T (2015) Hypothalamic gonadotropin releasing hormone (GnRH) receptor neurons fire in synchrony with the female reproductive cycle. Journal of neurophysiology:jn 00357 02015.

Schradin C, Anzenberger G (1999) Prolactin, the Hormone of Paternity. News Physiol Sci 14:223-231.

Schulz KM, Molenda-Figueira HA, Sisk CL (2009) Back to the future: The organizational-activational hypothesis adapted to puberty and adolescence. Horm Behav 55:597-604.

Selinger JV, Kulagina NV, O'Shaughnessy TJ, Ma W, Pancrazio JJ (2007) Methods for characterizing interspike intervals and identifying bursts in neuronal activity. Journal of neuroscience methods 162:64-71.

Senzacqua M, Severi I, Perugini J, Acciarini S, Cinti S, Giordano A (2016) Action of Administered Ciliary Neurotrophic Factor on the Mouse Dorsal Vagal Complex. Front Neurosci 10:289.

Sisk CL, Richardson HN, Chappell PE, Levine JE (2001) In vivo gonadotropin-releasing hormone secretion in female rats during peripubertal development and on proestrus. Endocrinology 142:2929-2936.

Smith MS, Neill JD (1976) Termination at midpregnancy of the two daily surges of plasma prolactin initiated by mating in the rat. Endocrinology 98:696-701.

Staal RGW, Rayport S, Sulzer D (2007) Amperometric Detection of Dopamine Exocytosis from Synaptic Terminals. In: Electrochemical Methods for Neuroscience (Michael AC, Borland LM, eds). Boca Raton (FL).

Stone TW (1996) CNS neurotransmitters and neuromodulators: dopamine. Boca Raton, Fla. ; London: CRC.

Storch U, Forst AL, Pardatscher F, Erdogmus S, Philipp M, Gregoritza M, Mederos YSM, Gudermann T (2017) Dynamic NHERF interaction with TRPC4/5 proteins is required for channel gating by diacylglycerol. Proceedings of the National Academy of Sciences of the United States of America 114:E37-E46.

Stowers L, Holy TE, Meister M, Dulac C, Koentges G (2002) Loss of sex discrimination and male-male aggression in mice deficient for TRP2. Science 295:1493-1500.

Strauss JF, III, Barbieri RL, Yen SSCRe (2014) Yen and Jaffe's reproductive endocrinology : physiology, pathophysiology, and clinical management, 7th ed. Edition. Philadelphia, PA: Elsevier/Saunders.

Strubing C, Krapivinsky G, Krapivinsky L, Clapham DE (2001) TRPC1 and TRPC5 form a novel cation channel in mammalian brain. Neuron 29:645-655.

Strubing C, Krapivinsky G, Krapivinsky L, Clapham DE (2003) Formation of novel TRPC channels by complex subunit interactions in embryonic brain. The Journal of biological chemistry 278:39014-39019.

Taylor AE, McCourt B, Martin KA, Anderson EJ, Adams JM, Schoenfeld D, Hall JE (1997) Determinants of abnormal gonadotropin secretion in clinically defined women with polycystic ovary syndrome. J Clin Endocrinol Metab 82:2248-2256.

Tomic M, Kucka M, Kretschmannova K, Li S, Nesterova M, Stratakis CA, Stojilkovic SS (2011) Role of nonselective cation channels in spontaneous and protein kinase A-stimulated calcium signaling in pituitary cells. Am J Physiol Endocrinol Metab 301:E370-379.

Tomogane H, Mistry AM, Voogt JL (1992) Late pregnancy and rat choriocarcinoma cells inhibit nocturnal prolactin surges and serotonin-induced prolactin release. Endocrinology 130:23-28.

Tomogane H, Arbogast LA, Soares MJ, Robertson MC, Voogt JL (1993) A factor(s) from a rat trophoblast cell line inhibits prolactin secretion in vitro and in vivo. Biology of reproduction 48:325-332.

Tonkowicz P, Robertson M, Voogt J (1983) Secretion of rat placental lactogen by the fetal placenta and its inhibitory effect on prolactin surges. Biology of reproduction 28:707-716.

Tonkowicz PA, Voogt JL (1983a) Examination of rat placental lactogen and prolactin at 6-hr intervals during midpregnancy. Proc Soc Exp Biol Med 173:583-587.

Tonkowicz PA, Voogt JL (1983b) Termination of prolactin surges with development of placental lactogen secretion in the pregnant rat. Endocrinology 113:1314-1318.

Tortonese DJ, Brooks J, Ingleton PM, McNeilly AS (1998) Detection of prolactin receptor gene expression in the sheep pituitary gland and visualization of the specific translation of the signal in gonadotrophs. Endocrinology 139:5215-5223.

Trebak M, Vazquez G, Bird GS, Putney JW, Jr. (2003) The TRPC3/6/7 subfamily of cation channels. Cell calcium 33:451-461.

Trebak M, Lemonnier L, DeHaven WI, Wedel BJ, Bird GS, Putney JW, Jr. (2009) Complex functions of phosphatidylinositol 4,5-bisphosphate in regulation of TRPC5 cation channels. Pflugers Archiv : European journal of physiology 457:757-769.

Trevino CL, Serrano CJ, Beltran C, Felix R, Darszon A (2001) Identification of mouse trp homologs and lipid rafts from spermatogenic cells and sperm. FEBS letters 509:119-125.

Tsutsumi M, Zhou W, Millar RP, Mellon PL, Roberts JL, Flanagan CA, Dong K, Gillo B, Sealfon SC (1992) Cloning and functional expression of a mouse gonadotropin-releasing hormone receptor. Molecular endocrinology 6:1163-1169.

Van Der Lee S, Boot LM (1955) Spontaneous pseudopregnancy in mice. Acta Physiol Pharmacol Neerl 4:442-444.

Vandenbergh JG (1969) Male odor accelerates female sexual maturation in mice. Endocrinology 84:658-660.

Vannier B, Peyton M, Boulay G, Brown D, Qin N, Jiang M, Zhu X, Birnbaumer L (1999) Mouse trp2, the homologue of the human trpc2 pseudogene, encodes mTrp2, a store depletion-activated capacitative Ca2+ entry channel. Proceedings of the National Academy of Sciences of the United States of America 96:2060-2064.

Vazquez G, Wedel BJ, Aziz O, Trebak M, Putney JW, Jr. (2004) The mammalian TRPC cation channels. Biochimica et biophysica acta 1742:21-36.

Venkatachalam K, Montell C (2007) TRP channels. Annual review of biochemistry 76:387-417.

Venkatachalam K, Zheng F, Gill DL (2003) Regulation of canonical transient receptor potential (TRPC) channel function by diacylglycerol and protein kinase C. The Journal of biological chemistry 278:29031-29040.

Vermeulen A (1993) Environment, human reproduction, menopause, and andropause. Environ Health Perspect 101 Suppl 2:91-100.

Visconti PE, Galantino-Homer H, Moore GD, Bailey JL, Ning X, Fornes M, Kopf GS (1998) The molecular basis of sperm capacitation. J Androl 19:242-248.

Weber EM, Algers B, Hultgren J, Olsson IA (2013a) Pup mortality in laboratory mice--infanticide or not? Acta Vet Scand 55:83.

Weber EM, Algers B, Wurbel H, Hultgren J, Olsson IA (2013b) Influence of strain and parity on the risk of litter loss in laboratory mice. Reprod Domest Anim 48:292-296.

Weber RF, de Greef WJ, de Koning J, Vreeburg JT (1983) LH-RH and dopamine levels in hypophysial stalk plasma and their relationship to plasma gonadotrophins and prolactin levels in male rats bearing a prolactin- and adrenocorticotrophin-secreting pituitary tumor. Neuroendocrinology 36:205-210.

Wen S, Gotze IN, Mai O, Schauer C, Leinders-Zufall T, Boehm U (2011) Genetic identification of GnRH receptor neurons: a new model for studying neural circuits underlying reproductive physiology in the mouse brain. Endocrinology 152:1515-1526.

Wen S, Schwarz JR, Niculescu D, Dinu C, Bauer CK, Hirdes W, Boehm U (2008) Functional characterization of genetically labeled gonadotropes. Endocrinology 149:2701-2711.

Wes PD, Chevesich J, Jeromin A, Rosenberg C, Stetten G, Montell C (1995) TRPC1, a human homolog of a Drosophila store-operated channel. Proceedings of the National Academy of Sciences of the United States of America 92:9652-9656.

Whitten WK, Bronson FH, Greenstein JA (1968) Estrus-inducing pheromone of male mice: transport by movement of air. Science 161:584-585.

Williams KW, Sohn JW, Donato J, Jr., Lee CE, Zhao JJ, Elmquist JK, Elias CF (2011) The acute effects of leptin require PI3K signaling in the hypothalamic ventral premammillary nucleus. The Journal of neuroscience : the official journal of the Society for Neuroscience 31:13147-13156.

Wood HM, Lee UJ, Vurbic D, Sabanegh E, Ross JH, Li T, Damaser MS (2009) Sexual development and fertility of Loxl1-/- male mice. J Androl 30:452-459.

Wu LJ, Sweet TB, Clapham DE (2010) International Union of Basic and Clinical Pharmacology. LXXVI. Current progress in the mammalian TRP ion channel family. Pharmacological reviews 62:381-404.

Xu SZ, Zeng F, Boulay G, Grimm C, Harteneck C, Beech DJ (2005) Block of TRPC5 channels by 2-aminoethoxydiphenyl borate: a differential, extracellular and voltage-dependent effect. British journal of pharmacology 145:405-414.

Xue T, Do MT, Riccio A, Jiang Z, Hsieh J, Wang HC, Merbs SL, Welsbie DS, Yoshioka T, Weissgerber P, Stolz S, Flockerzi V, Freichel M, Simon MI, Clapham DE, Yau KW (2011) Melanopsin signalling in mammalian iris and retina. Nature 479:67-73.

Yang JJ, Larsen CM, Grattan DR, Erskine MS (2009) Mating-induced neuroendocrine responses during pseudopregnancy in the female mouse. Journal of neuroendocrinology 21:30-39.

Zeng F, Xu SZ, Jackson PK, McHugh D, Kumar B, Fountain SJ, Beech DJ (2004) Human TRPC5 channel activated by a multiplicity of signals in a single cell. The Journal of physiology 559:739-750.

Zhang C, Roepke TA, Kelly MJ, Ronnekleiv OK (2008) Kisspeptin depolarizes gonadotropin-releasing hormone neurons through activation of TRPC-like cationic channels. The Journal of neuroscience : the official journal of the Society for Neuroscience 28:4423-4434.

Zhang C, Bosch MA, Ronnekleiv OK, Kelly MJ (2013a) Kisspeptin activation of TRPC4 channels in female GnRH neurons requires PIP2 depletion and cSrc kinase activation. Endocrinology 154:2772-2783.

Zhang C, Tonsfeldt KJ, Qiu J, Bosch MA, Kobayashi K, Steiner RA, Kelly MJ, Ronnekleiv OK (2013b) Molecular mechanisms that drive estradiol-dependent burst firing of Kiss1 neurons in the rostral periventricular preoptic area. Am J Physiol Endocrinol Metab 305:E1384-1397.

Zhang X, van den Pol AN (2012) Thyrotropin-releasing hormone (TRH) inhibits melanin-concentrating hormone neurons: implications for TRH-mediated anorexic and arousal actions. The Journal of neuroscience : the official journal of the Society for Neuroscience 32:3032-3043.

Zhang X, van den Pol AN (2015) Dopamine/Tyrosine Hydroxylase Neurons of the Hypothalamic Arcuate Nucleus Release GABA, Communicate with Dopaminergic and Other Arcuate Neurons, and Respond to Dynorphin, Met-Enkephalin, and Oxytocin. The Journal of neuroscience : the official journal of the Society for Neuroscience 35:14966-14982.

Zhu G, Xie C, Yang Z, Wang Y, Chen D, Wang X (2018) Expression of TRPC5 is decreased in the sperm of patients with varicocele-associated asthenozoospermia. Biomed Rep 8:529-534.

Zhu MH, Chae M, Kim HJ, Lee YM, Kim MJ, Jin NG, Yang DK, So I, Kim KW (2005) Desensitization of canonical transient receptor potential channel 5 by protein kinase C. American journal of physiology Cell physiology 289:C591-600.

Zufall F (2014) TRPs in olfaction. Handbook of experimental pharmacology 223:917-933.

Zylbertal A, Yarom Y, Wagner S (2017) Synchronous Infra-Slow Bursting in the Mouse Accessory Olfactory Bulb Emerge from Interplay between Intrinsic Neuronal Dynamics and Network Connectivity. The Journal of neuroscience : the official journal of the Society for Neuroscience 37:2656-2672.

7. Publications

Schauer C, Tong T, Petitjean H, **Blum T**, Peron S, Mai O, Schmitz F, Boehm U, Leinders-Zufall T (2015) Hypothalamic gonadotropin releasing hormone (GnRH) receptor neurons fire in synchrony with the female reproductive cycle. Journal of neurophysiology:jn 00357 02015.

Blum T, Moreno-Pérez A, Bufe B, Pyrski M, Arifovic A, Weissgerber P, Freichel M, Zufall F, Leinders-Zufall T (**in press**) Trpc5 deficiency causes hypoprolactinemia and altered function of oscillatory dopamine neurons in the arcuate nucleus. Proceedings of the National Academy of Sciences of the United States of America.

8. Acknowledgments

I would like to thank my family and friends, my colleagues and all those that supported and encouraged me, which made it possible for me to succeed in my work and in finishing this thesis.

Special thanks are due to the following persons:

First of all, I like to thank **Prof. Dr. Trese Leinders-Zufall**. She gave me the opportunity to initiate this project in her laboratory. This gave me the chance to develop my scientific commitment in a highly professional environment that guided me without being too restrictive. She encouraged me to become an independent scientist, to use my ideas in order to design strategies and to tackle complications. Along with **Prof. Dr. Dr. Frank Zufall** they excelled themselves in pushing my scientific career, giving me the opportunities to present my work at several big scientific meetings, e.g. the AChemS Meeting in Florida as well as the ECRO Meeting in Würzburg, and to get in touch with renown scientists.

I want to thank **Prof. Dr. Veit Flockerzi**, **Prof. Dr. Marc Freichel**, **Prof. Dr. Ulrich Boehm** and **Dr. Petra Weissgerber** for their scientific input and kind provision of mouse models and breeding related information and therefore enabling me to follow this fascinating project.

I am grateful for all the **Lab Members of the Zufall- and Leinders-Zufall-Labs**. The supportive and pleasant atmosphere created by the excellent people in the lab. Once in a while this was more supportive than one would think. The following outstanding people I want to thank in person:
First of all I want to thank **Lisa Knieriemen**, who was at my side for most of my thesis and luckily still is. Thank you for all the support and love you showed me during all the ups and downs of this thesis and for all the kind words and the occasional motivational kick in the butt. Thank you for your help in all our animal protocol related procedures.
I also want to thank **Michael Konzmann** for all the lab-related organizational matters, technical support, acute slice preparations, and most importantly for all the laughs, kind words and your friendship.
I would also like to thank **Ana Moreno-Pérez** for the excellent teamwork in the Trpc5-project, the great office partnership and all the fun discussions and the nice time.
Additional thanks go to **Christian Schauer**, **Katherin Bleymehl** and **Eugenia Eckstein**, who strongly influenced the happy and positive atmosphere in the lab.
Thanks go out to **Dr. Martina Pyrski** and **Prof. Dr. Bernd Bufe** for the constructive discussions and criticism.

I also want to thank **Petra Hammes** and **Monika Vorndran** for their help in genotyping, technical questions and ordering of compounds/antibodies.
Also, thanks go to **Gabriele Mörschbächer** for her help in all the organizational work I stumbled upon.
In addition I want to thank the people of the animal facility, especially **Kerstin Becker** and **Angelika Stroer**.

Last but not least, special thanks go to my family and my parents – **Marion** and **Michael Blum** – for giving me the opportunity to study and all their loving support during my entire academic career.